CHARACTERIZATION OF A MYCOBACTERIUM TUBERCULOSIS DELETION MUTANT, ΔRV3351C

by

MEGAN PRESCOTT

(Under the Direction of FREDERICK QUINN)

ABSTRACT

Mycobacterium tuberculosis, the causative agent of the lung disease tuberculosis (TB), is the world's leading cause of death by a single infectious agent. The BCG vaccine for tuberculosis has been in use for almost 100 years, making it the oldest and currently the most widely distributed vaccine, but it fails to protect against pulmonary disease in adults. Because of the limitations of the BCG vaccine and an increase in multidrug-resistant and extensively drug-resistant *M. tuberculosis*, development of new vaccines is a cornerstone of the World Health Organization "End TB Strategy". The inability to decrease the burden of *M. tuberculosis* infection in the human population also reinforces the need for a better understanding of the host/pathogen interactions. Until recently, the efforts to understand these dynamics have primarily focused on interactions of *M. tuberculosis* with host alveolar macrophages, but previous work by our laboratory and others have shown that epithelial pneumocytes, the most numerous cell type in the lung alveolus, play a role during *M. tuberculosis* infection. Our laboratory has identified *Rv3351c* as a gene important in epithelial cell infection. The goal of the research described in this dissertation was to characterize interactions and trafficking of a *M. tuberculosis* deletion mutant ΔRv3351c within alveolar epithelial cells. Our data suggest that ΔRv3351c bacilli, once internalized, are less able to

survive and multiply intracellularly, and are thus less cytotoxic compared with the parent strain. The survival in alveolar epithelial cells was dependent on the formation of lipid rafts on the host cell plasma membrane and inhibition of fusion of the mycobacterial containing compartment with the host cell lysosome. Thus, the role of Rv3351c in trafficking and survival of *M. tuberculosis* bacilli through epithelial cells may begin with modifications to the plasma membrane prior to attachment. We found that the localization of the Rv3351c protein to the membrane of *M. tuberculosis*, its ability to elicit antibodies in patients with active tuberculosis, and its ability to reduce *M. tuberculosis* killing of A549 cells, makes it an attractive candidate for a mucosal subunit vaccine with other proteins that target alveolar epithelial cells.

INDEX WORDS: *Mycobacterium tuberculosis*, Alveolar Epithelial Cells, ΔRv3351, Mucosal Vaccination, Lipid Rafts, Trafficking

CHARACTERIZATION OF A MYCOBACTERIUM TUBERCULOSIS DELETION MUTANT, ΔRV3351C

by

MEGAN PRESCOTT

BS, GEORGIA SOUTHERN UNIVERSITY, 2012

A Dissertation Submitted to the Graduate Faculty of The University of Georgia in Partial Fulfillment of the Requirements for the Degree

DOCTOR OF PHILOSOPHY

ATHENS, GEORGIA

2020

CHARACTERIZATION OF A MYCOBACTERIUM TUBERCULOSIS DELETION MUTANT, ΔRV3351C

by

MEGAN PRESCOTT

Major Professor:	Frederick Quinn
Committee:	Vincent Starai
	Timothy Hoover
	Tuhina Gupta
	Russel Karls

Electronic Version Approved:

Ron Walcott
Interim Dean of the Graduate School
The University of Georgia
August 2020

DEDICATION

This thesis is dedicated to all the people who helped me make it through the past 8 years. Everyone I've shared a drink with or cried with, everyone who gave me a place to stay while I pursued my goals across multiple states and countries, everyone who entertained and supported my ideas and dreams, and to those who were lights in the darkest times.

ACKNOWLEDGEMENTS

I would like to acknowledge the members of the Quinn/Karls Lab who provided invaluable help and support over the past 8 years, and pushed me to be a better (and neater) scientist.

TABLE OF CONTENTS

Page

CHAPTER 1

INTRODUCTION

*Mycobacterium tuberculosi*s has been associated with human disease for millennia, and yet tuberculosis (TB) is again the leading cause of death from a single infectious organism[1]. The success of *M. tuberculosis* as a pathogen can be attributed to its ability to spread easily from person to person through the air in aerosol droplets, its ability to cause acute active disease with symptoms including severe cough, spiking fever and weight loss, and its ability to cause latent infections in which viable bacteria can persist for decades without causing active disease[2–4]. It is only when an infected person's immune defenses decline due to various factors such as HIV co-infection or advanced age, do the latent bacteria reactivate to cause disease[3,4]. Despite rigorous public health campaigns that significantly reduced the case rate in the United States, Canada and much of western Europe, it is estimated that a quarter of the world's population is infected with the organism[5]. Albert Calmette and Camille Guérin developed the Bacille Calmette-Guérin (BCG) vaccine and first used it on humans in the 1920s[6]. The vaccine remains the oldest and the most widely distributed vaccine in the world due to its success at preventing TB meningitis in young children[7]. However, the vaccine's ability to prevent pulmonary tuberculosis ranges anywhere from 0-80% depending on a number of different factors, including pre-exposure to environmental mycobacteria, route of administration, time frame of vaccination, and even geographical location[8–10]. Long courses of harsh antibiotics and a lack of quick and specific diagnostic tools further exacerbate the epidemic: failure to properly complete the course of antibiotics has led to the rise of multi-drug resistant and extensively-drug resistant

forms of *M. tuberculosis*, while inaccurate and lengthy diagnoses can prevent patients from receiving treatment, thus allowing the continued spread of the bacteria to others or eventual reactivation of latent TB[3,5,9,11,12]. In addition to the need for new antibiotics and better diagnostics in the fight against TB, a new vaccine is needed that can prevent the pulmonary form of TB in children and adults. One of the main drawbacks of the BCG vaccine is its subcutaneous delivery into a patient's arm[13]. This mode of delivery does not complement the aerosol mode of transmission. A better option for a TB vaccine may be one that mimics the natural route of transmission to prevent the initial *M. tuberculosis* infection at the mucosal surface of the lungs.[14] The respiratory mucosal route of immunization is superior to the parenteral route in because of its ability to induce anti-TB T-cell immunity in the lung airways in addition to inducing T-cell responses in the lung interstitium. In contrast, parenteral immunization fails to elicit T-cell responses in the airway lumen although it induces T-cells to populate the lung interstitium that may or may not be protective[15].

Our inability to control and decrease the burden of *M. tuberculosis* infection in the human population also reinforces the need for a better understanding of the host/pathogen relationship. Much of the research examining *M. tuberculosis* interactions with host cells is specific to alveolar macrophages[16–18]. The continued high prevalence of *M. tuberculosis* infections worldwide demonstrates that limiting research to this single cell type limits understanding of *M. tuberculosis* and its complex relationship with the host. Macrophages make up a small percentage of the total cell population in the lung alveolus. Most of the alveolar surface is made up of Type I and Type II alveolar epithelial cells, and interaction with these cells is an important part of the infection process for other bacterial pathogens such as *Haemophilus influenzae* and *Staphylococcus aureus*[19–21]. *M. tuberculosis* DNA has been found in in epithelial cells in human

lung samples of TB patients, yet limited research has been done to examine the role this cell type plays in *M. tuberculosis* infection[22,23]. Work by our laboratory and others have shown the *M. tuberculosis* can invade and replicate in alveolar epithelial cells[24,25]. The Locht laboratory at the Pasteur Institute in Lille, France has identified the Heparin-Binding Hemagglutinin Adhesin (HBHA) as an *M. tuberculosis* surface protein that plays a direct role in the infection of alveolar epithelial cells, but not macrophages[26,27]. Deleting *hbha* from *M. tuberculosis* decreases dissemination from the lung to the spleen and liver in mice[27,28]. Early Secretory Antigen Target-6 (ESAT-6) is another secreted protein from *M. tuberculosis* that is able to bind to and lyse alveolar epithelial cells and may play a role in dissemination of *M. tuberculosis* from the lungs. *M. tuberculosis* with both *hbha* and the gene encoding ESAT-6 (*esxA*) deleted disseminates less from the lungs than strains with either single deletion alone[29]. Our laboratory has identified another *M. tuberculosis* protein that is involved in alveolar epithelial cell infection, Rv3351c[30]. An *Rv3351c*-deficient mutant strain replicates to lower numbers and is less capable of killing host cells than the parent strain, however, unlike Δ*hbha* mutant bacteria, ΔRv3351c bacilli are not deficient in internalization into alveolar epithelial cells, indicating that the host cell target is downstream of these initial processes. Elucidating the differences in intracellular trafficking between ΔRv3351c and the virulent parent strain *M. tuberculosis* Erdman will not only allow us to ascertain the function of Rv3351c but will provide a deeper insight into how alveolar epithelial cells respond to *M. tuberculosis* infection, and ultimately a more complete understanding of host/pathogen interactions. Furthermore, constructing a subunit aerosol vaccine with HBHA and Rv3351c proteins has the potential to prevent or decrease early infection of alveolar epithelial cells and reduce dissemination from the lungs. Therefore, this thesis will focus on two specific aims. The first will be to characterize the intracellular trafficking differences

between ΔRv3351c and parent strain Erdman bacteria in the A549 Type II alveolar epithelial cell line, while the second aim will examine the immune response to mice immunized with a novel aerosol subunit vaccine with Rv3351c and HBHA.

Specific Aim 1: Characterize trafficking differences between an *M. tuberculosis* strain lacking *Rv3351c* (ΔRv3351*c*) and *M. tuberculosis* parent strain Erdman. Work from our laboratory has shown that *Rv3351c* is required for virulence of A549 Type II alveolar epithelial cells[30]. Other work from our lab has shown that the autophagy pathway and lipid rafts are important in *M. tuberculosis* infection of these cells[31,32]. Because ΔRv3351c is able to internalize into A549 cells at numbers equal to the parent strain, we hypothesize that the observed less-virulent phenotype results from alternate intracellular trafficking of ΔRv3351*c* to the degradative lysosome outside of the autophagy pathway, and that this trafficking difference is initiated by disturbances to the host cell membrane and subsequent cell signaling through a decrease in lipid raft formation. To test our hypothesis, we will compare the abilities of ΔRv3351c and the Rv3351c protein applied to A549 cell monolayers to induce lipid rafts and examine if inducing or disrupting lipid raft formation changes infection outcomes. Similarly, we will observe the interaction of ΔRv3351c bacilli with the autophagy pathway and examine if disrupting the autophagy pathway changes infection outcomes. We will examine these outcomes through a variety of microbiological, biochemical, and microscopic methods.

Specific Aim 2: Examine the immune response to mice immunized with a novel aerosol subunit vaccine of Rv3351c and HBHA, using the VacSIM vaccine delivery system (vaccine self-assembling immune matrix). VacSIM solution can easily be mixed with antigens, organisms, and adjuvants for injection. Postinjection, the peptides self-assemble into hydrated nanofiber gel

matrices, forming a depot with antigens and adjuvants in the aqueous phase. This depot provides slow release of immunogens, leading to increased activation of antigen-presenting cells that then drive enhanced immunogenicity. We hypothesize that by mimicking the natural route of *M. tuberculosis* infection and targeting our vaccine to alveolar epithelial cells, we will induce robust correlates of immune protection at the mucosal surface of the lung, which parenterally delivered BCG fails to do. To test our hypothesis, we will immunize mice with the novel VacSIM-HBHA-Rv3351c vaccine alone, or as a boost to the current BCG vaccine, and compare the immune response to mice vaccinated with BCG alone or unvaccinated controls.

CHAPTER 2

REVIEW OF THE LITERATURE

2.1 Mycobacterial Disease Overview

Within the phylum Actinobacteria, the genus *Mycobacterium* contains over 180 species, most of which live freely in the environment, but a small number are obligate pathogens and a few dozen are opportunistic pathogens of various animal species[33]. Host species for the mycobacterial pathogens are many and widespread, ranging from humans and mammals to birds and fish. Examples of obligate pathogens include *Mycobacterium marinum* that infects fish and other cold-blooded mammals, *Mycobacterium avium* subspecies *paratuberculosis* that has been isolated from wild and domestic ruminants, and *Mycobacterium lepraemurium*, is the causative agent of rat leprosy[34]. One human pathogenic species is the etiological agent of Hansen's Disease (leprosy), *Mycobacterium leprae,* which also can naturally infect armadillos.

The nine mycobacterial species that cause a form of tuberculosis or tuberculous-like disease in humans and/or other animals are collectively known as the *Mycobacterium tuberculosis* complex (MTBC)[35]. These mycobacteria include the primarily human pathogens *M. tuberculosis, Mycobacterium africanum* and *Mycobacterium canettii*, the rodent pathogen, *Mycobacterium microti*, primarily bovid pathogens *Mycobacterium bovis*, *Mycobacterium caprae*, *Mycobacterium mungi*, and *Mycobacterium orygis*, and the primarily pinniped (such as seals and walruses) pathogen, *Mycobacterium pinnipedii*. Importantly, the four species responsible for most of the bovid infections are also responsible for a growing problem in a wide range of wildlife and domestic animals, including badgers, boars, deer, opossums, coyotes,

raccoons, llamas, lions, pigs, and cats[36,37]. Collectively, the species primarily associated with animal tuberculosis and the species primarily associated with human disease are increasingly observed to cross the zoonotic boundary.

Zoonotic transmission of *Mycobacterium bovis* has been shown to occur in at least 2.8% of human TB cases in African countries and 1.4% of the time in countries outside of Africa, with up to 76% of extrapulmonary TB cases caused by *M. bovis* in Tunisia[38,39]. However, the true burden of zoonotic TB is underestimated due to a lack of routine surveillance data from most countries. Zoonotic transmission of *M. bovis* from animals to humans and *M. tuberculosis* transmission from humans to animals can occur through close animal-human contact or in the case of transmission to humans, through the consumption of contaminated animal products, such as unpasteurized animal milk[39].

Lastly, many environmental saprophytic mycobacteria are emerging as opportunistic diseases of humans such as *M. avium* complex (the closely related species of *M. avium and Mycobacterium intracellulare), Mycobacterium kansasii, Mycobacterium xenopi, Mycobacterium marinum* (swimming pool granuloma), *Mycobacterium ulcerans* (Buruli ulcer), *Mycobacterium fortuitum, Mycobacterium abscessus, and Mycobacterium chelonae*[33].

2.2 Mycobacterial Physiology

Mycobacteria are non-motile, non-spore forming, rod-shaped bacteria. They are characterized by their unique very thick, waxy, lipid-rich hydrophobic cell wall that stains "acid fast" and is a defining marker for this genus. This unique cell wall confers the bacteria the ability to resist many classic antibiotics, to withstand extracellular stressors, and to survive in the hostile intracellular environment[40].

Though the mycobacterial cell envelope contains a traditional cytosolic (inner) membrane, the peptidoglycan layer is covalently linked to an arabinogalactan layer consisting of arabinose and galactose moieties, which in turn is covalently linked to mycolic acids (Figure 1)[41]. These long branched fatty acids (up to 90 carbon atoms) represent 60% of the mycobacterial cell wall and form the characteristic waxy coat of mycobacterial outer membrane, which also contains free lipids. Phosphatidylinositol mannosides also form a large portion of the cell wall. Phosphatidyl-myo-inositol mannosides, lipomannan and lipoarabinomannan (LAM) have been reported to be important for bacterial interaction with host cells[42]. Due to its overall virulence, the most well studied species in the genus is *M. tuberculosis.* This and the other closely-related virulent species contain mannose-capped LAM (ManLAM), a cell wall molecule that protects the bacterium from killing in the degradative host lysosome[43,44].

Mycolic acids make up the inner leaflet of the mycobacterial outer membrane (MOM), while the glycolipids make up much of the outer leaflet. The structure and complexity of mycolic acids can vary by species[45]. The outer leaflet is highly heterogeneous and consists of lipids, lipoglycans, and proteins[46]. Due to its complexity and species-specific constitution, it remains poorly characterized outside of *M. tuberculosis* and closely related slow-growing pathogenic mycobacteria[41]. The lipids associated with the external leaflet include phthiocerol dimycocerosate (PDIM), phenolic glycolipid (PGL), and lipooligosaccharides (LOS). These lipids are involved in the infection of macrophages, as well as in modification of the host immune response to create a more permissive environment for survival[47–49].

The final layer of the cell envelope is the capsule, mainly consisting of polysaccharides with α-glucan being the most abundant, followed by arabinomannan and mannan, and proteins[50,51].

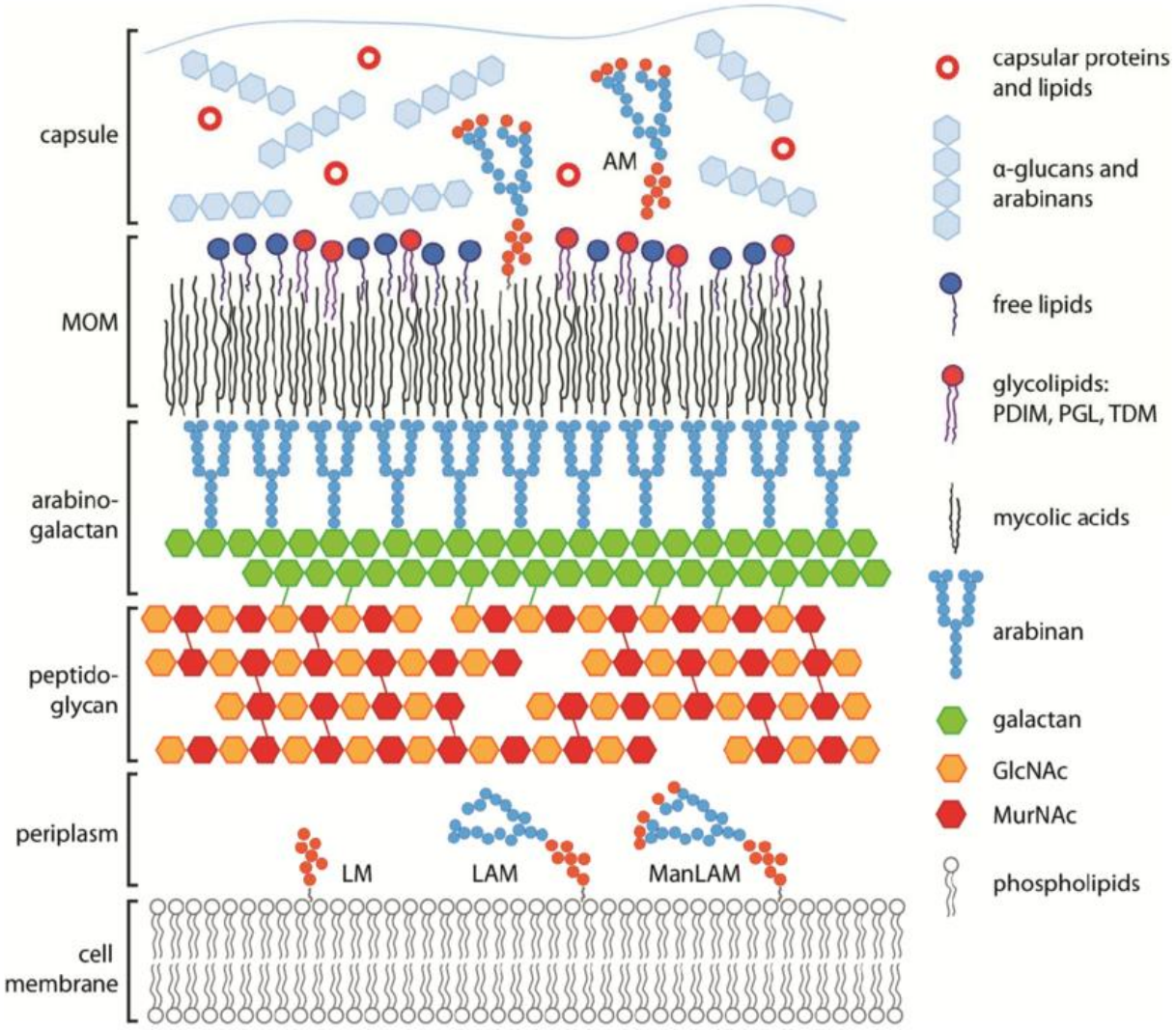

Figure 1: Illustration of a mycobacterial cell wall composition. MOM = mycobacterial outer membrane, LM = lipomannan, AM = arabinomannan, LAM = lipoarabinomannan, ManLAM = mannose-capped LAM, GlcNac = N-acetyl-glucosamine, MurNAc = N-acetyl-muramic acid.[52]

Like that of many other prokaryotes, the *M. tuberculosis* cell envelope is likely to contain proteins functioning as enzymes, receptors, transporters or signal transducers that could be vital to the microbe as it navigates varied environments within the host. In contrast to outer membrane proteins of pathogenic Gram-negative bacteria, many of which are involved in interactions with

host cells, far less is understood regarding the functions of cell envelope proteins in *M. tuberculosis* due to the difficulty in lysing mycobacterial cells for protein extraction[53–56], Some of the membrane proteins that have been studied are considered to be immunogens with the pore-forming protein OmpATb as an example of a known virulence factor essential for the adaptation of *M. tuberculosis* to acidic environments [49]. It is essential that we identify roles for additional *M. tuberculosis* membrane proteins to better understand the physiology, as well as the pathogenicity, of this microorganism.

2.3 Virulence Genes of *Mycobacterium tuberculosis*

The genome of *M. tuberculosis* is approximately 4.4 x10^6 base pairs, which consists of approximately 4,000 genes[57]. Ten percent of the coding capacity of the *M. tuberculosis* genome is dedicated to large families of proteins containing Pro-Glu (PE) or Pro-Pro-Glu (PPE) motifs. These PE and PPE proteins, found predominantly in the slow-growing pathogenic species, may be responsible for antigenic variation and immune evasion[58]. Another component of the *M. tuberculosis* genome that is known to be crucial for virulence is the Region of Difference 1 (RD1)[35]. Notably, the nine genes encoded in this region are missing from the attenuated vaccine strain *M. bovis* BCG. Introduction of RD1 into BCG increases its pathogenicity, while deletion of RD1 from *M. tuberculosis* results in attenuation similar to BCG in mice[59,60]. Several RD1 genes encode a unique mycobacterial secretion system, ESX-1, which has been shown to facilitate the release of virulence factors ESAT-6 (early secretory antigenic target-6) and CFP-10 (culture filtrate protein-10), which are also encoded in this section of genome. Mutants defective for ESX-1 secretion system are found to exhibit a range of diverse phenotypes, including defects in immune modulation, phagosomal trafficking, growth inside macrophages, and dissemination from the lungs[47,61,62].

2.4 History

It is believed that *M. tuberculosis* has been associated with humans since the first migration out of Africa 70,000 years ago. Based on the geographical distribution of other more broad-ranging pathogenic species with larger genomes including *M. marinum* and *M. ulcerans*, it has been hypothesized that the genus *Mycobacterium* originated more than 150 million years ago[1]. However, recent studies using ancient *M. tuberculosis* genomes from mummified remains track the oldest common ancestor of the *M. tuberculosis* complex to the Neolithic era, no more than 6,000 years before present[63]. Referred to as consumption, phthisis, or the white plague, TB has persisted throughout human history. Egyptian mummies, dating back to 2,400 BC, reveal skeletal deformities typical of advanced TB, known as Pott's lesions. Texts describing TB appear in ancient China and India as early as 3,300 years ago. In ancient Greece, Hippocrates described the symptoms of Phthisis, while Isocrates and Aristotle suggested its infectious nature[1]. In the 18th and 19th century in Western Europe, TB reached epidemic proportions, affecting 30-50% of adults living in London. During the industrial revolution, problematic social conditions such as extremely deprived work settings, poorly-ventilated and overcrowded housing, primitive sanitation, and malnutrition were intimately associated with the disease[1]. The first step in treating TB was the discovery of its infectious nature in 1865 by Jean-Antoine Villemin. He successfully gave a rabbit TB after inoculating it with liquid from a tuberculous lesion from a patient who had succumbed to the disease[1]. Several years later in 1882, Robert Koch identified the tubercle bacillus and demonstrated the organism as the etiological agent of the disease in his famous postulates for which he would win the Nobel prize[64]. It was also Koch who identified an extract of the mycobacterial cell wall called tuberculin and presented the idea that it could be used to prevent or diagnose the disease. Although attempts at prevention were unsuccessful, using

diluted tuberculin, doctors Clemens Freiherr von Pirquet and Charles Mantoux were able to diagnose active and latent (discussed below) forms of TB[6]. In the 1930s, Florence Seibert developed the current form of the tuberculin skin test (TST) using a standardized cell wall preparation called 'purified protein derivative' (PPD), which remains today the most widely used TB diagnostic[65].

Successful prevention of TB occurred in 1921 when the first vaccine was tested. The vaccine was developed by Albert Calmette and Camille Guérin at the Pasteur Institute of Lille using the closely-related *M. bovis* species[66]. The strain was attenuated by repeatedly subculturing the bacteria on a media of potato, glycerol, and ox bile. After 230 subcultures over 11 years, they had generated a tubercle bacillus which failed to produce progressive TB when injected into guinea pigs, rabbits, cattle, or horses. In the 1990s, comparisons between the genome of *M. bovis* BCG and its parent strain revealed the deletion of three Regions of Difference: RD1, RD2 and RD3[67–69]. As discussed earlier, RD1 was determined to be present in both *M. bovis* and *M. tuberculosis* suggesting that the genes found there could encode or important TB virulence factors.

By 1928, over 114,000 children had been orally vaccinated with the Bacille-Calmette-Guerin (BCG) vaccine[6,70]. It is estimated that BCG has been administered to over 4 billion people worldwide since the first vaccination in 1921[71]. Today, the BCG vaccine is still the most widely used vaccine, given to new-born children in most of the world, and is the oldest vaccine still in use today.[71] Unfortunately, TB remains the world's leading cause of death from an infectious agent as approximately one-quarter of the world's population infected with *M. tuberculosis*, 10 million cases per year with active infection, and the remainder having latent TB infection [72]. Despite the vaccine's variable efficacy in the treatment of pulmonary TB and its

inability to prevent reactivation of latent TB in adults, in areas with high TB burden, vaccination is effective against childhood disseminated and pulmonary TB disease and thus will continue to be used[73–75].

In addition to prevention and diagnosis, antibiotic treatment has also played a pivotal role in the fight against TB. The antibiotic streptomycin was first used to treat TB in 1945, but resistance to the drug developed quickly. Para-aminosalicylic acid (PAS), also discovered in 1945, was found to greatly reduce the occurrence of drug resistance when combined with streptomycin. In 1952, the drug isoniazid was discovered which opened the modern era of treatment; it was inexpensive, well tolerated, and safe[76]. The triple therapy of isoniazid, streptomycin, and PAS became the standard treatment for 15 years. In 1961, ethambutol replaced PAS in the three-drug regimen, and in the 1970s, including rifampin in place of streptomycin shortened the course of treatment to nine months, and later, adding pyrazinamide to the regimen led to a further reduction of treatment duration to six months. However, poor adherence to the sixth-month course of antibiotics is a major constraint to eradicating TB[77]. Multi-drug-resistant *M. tuberculosis* began to be recognized in the 1990s[78], and multi-drug-resistant and extensively drug-resistant *M. tuberculosis* remains one of the biggest barriers to TB control today. Few new drugs since the 1990s have been developed, but that is beginning to change. Since 2012, five new drugs are either in clinical trials or available for use, although *M. tuberculosis* isolates are already showing signs of resistance to these new antibiotics[79].

2.5 Disease Transmission and Manifestation

Tuberculosis is transmitted through the aerosol route when a person with active pulmonary TB disease coughs, laughs, speaks, or sings[80]. Bacteria commonly enter the host through mucosal surfaces, usually via the lung after inhalation of infectious droplets[19].

Transmission is most likely to occur over frequent, repeated, close-proximity exposure to someone with active disease. This makes households, and high-density locations such as schools, prisons, hospitals and homeless shelters, ideal settings for passing on infections[81]. Less frequently, it enters the host through the gut following the consumption of contaminated milk or traumatic inoculation into the skin[82]. Barriers to diagnosis and treatment contribute to the spread of TB[83]. Those who smoke, have diabetes, are HIV-positive or otherwise immunocompromised, or are malnourished are at a greater risk of developing TB disease[84,85]. A person's genetic background may also contribute to disease outcomes[86,87].

Only 10% of people exposed to *M. tuberculosis* will develop active TB: 5% will within 1–5 years after exposure, and the remaining 5% can develop disease at any time[88,89]. Tuberculosis disease is usually defined as an active TB disease or latent TB infection, but infection outcomes run on a continuous spectrum with differing degrees of bacterial replication and host immune response that change the way the disease is diagnosed and treated[3]. Active TB occurs in a person with insufficient immunity to eliminate the infection through innate and active immune responses or ultimately contain the *M. tuberculosis* bacilli within immune cell structures in the lungs and lymph nodes called granulomas[2]. A person with active TB disease presents with classic clinical symptoms such as fever, night sweats, weight loss, and persistent cough. Their chest radiograph will show lung lesions and their sputum sample will be positive for *M. tuberculosis* bacilli either through a specific stain (acid-fast) or through culturing the bacilli on standard media[3,4]. Severe disease can result in extrapulmonary miliary TB and meningitis[2]. Latent TB infection, which can last from weeks to decades, is asymptomatic and non-transmissible, and the *M. tuberculosis* bacilli are thought to be contained in granulomas. In this state, there is a persistent immune response against *M. tuberculosis* antigens and a positive TST

is maintained. If that immune response is compromised, such as in those with HIV, diabetes or advanced age, granulomas can collapse, releasing the mycobacteria into the weakened host with the result being the establishment of active disease[2]. In the middle of the spectrum between active and latent disease is incipient TB infection and subclinical TB disease. Those with incipient infection are infected with viable *M. tuberculosis* bacteria but have not yet progressed to active disease, while those with subclinical TB disease do not have clinical TB-related symptoms but may have abnormalities in radiologic or microbiological assays.[27] The duration and trajectory of disease state depends on the complex interaction between pathogen and host defense, and disease outcomes differ across patients. Immunocompromised patients can progress from subclinical to active disease in a matter of weeks[11]. Because subclinical disease may be an important source of transmission that goes unnoticed due to lack of symptoms, improved diagnostics for subclinical and incipient TB infection is needed to allow treatment of patients before they become symptomatic and infectious[3,11,12]. Current diagnostics like the TST and the newer interferon-gamma release assays (IGRAs) are based on the ability of the immune system to recognize mycobacterial antigens. They cannot differentiate between active and latent infection and have low accuracy for immunocompromised individuals. Recent research has focused on finding biomarkers that may allow accurate prediction of progression from infection to active TB disease[3,11,12].

2.6 Pathogenesis

Once inhaled into the alveolar space of the lungs, droplets containing *M. tuberculosis* bacilli are engulfed by macrophages and dendritic cells. The mechanism behind this phagocytic process has been well studied. After attachment, macrophages and dendritic cells internalize the bacteria by receptor-mediated phagocytosis, with numerous different receptors contributing to

this process. Pathogen recognition receptors (PRRs) on these cells recognize pathogen-associated molecular patterns (PAMP) of *M. tuberculosis* (such as glycolipids, lipoproteins and carbohydrates), and are central to the initiation and coordination of the host innate immune response[16]. These PRRs include dectin-1, the complement receptor 3, Toll-like receptors, mannose receptor, and the dendritic cell-specific intercellular adhesion molecule (ICAM)-3-grabbing nonintegrin (DC-SIGN)[16,90–92]. Other receptors include complement receptors and Fc receptors[16]. Due to the numerous and diverse ligands on the surface of the mycobacteria, it is likely that *M. tuberculosis* engages multiple receptors simultaneously and may preferentially target specific receptors to manipulate the host response and promote its own survival. For instance, the binding of ManLAM by mannose receptors limits phagosome–lysosome fusion, favoring mycobacterial persistence within macrophages[93–95], and this may be due to upregulation of certain signaling pathways within the cell. Other studies showed that antibody-opsonized bacteria, which bind the Fc-γ receptor, traffic to the lysosome[96]. However, studies intracellular trafficking of *M. tuberculosis* bacilli is not significantly altered by blocking individual receptors[97].

After uptake of *M. tuberculosis* bacilli, macrophages either eliminate the bacteria, or serve as a niche for the replication. *M. tuberculosis* survives in the macrophage by inhibiting apoptosis, resisting damage by nitric oxide and other reactive oxygen species, blocking fusion of the bacterial-containing compartment with the microbicidal lysosome, and subsequently interfering with recognition of infected macrophages by CD4+ T cells[42]. Virulence factors used by *M. tuberculosis* to aid in inhibiting apoptosis include superoxide dismutase SodA and the NADH dehydrogenase NuoG, while AhpC (alkyl hydroperoxide reductase) and KatG (catalase-

peroxidase) enzymes protect against oxidative stress. Lipoproteins LpqH, LprA, and LprG interact with Toll-Like Receptor 2 (TLR2) to inhibit antigen presentation to T cells[42,98–100].

Infected macrophages produce inflammatory cytokines and chemokines such as IL-8, MCP-1, and RANTES that signal infection and recruit additional macrophages/monocytes and neutrophils[19,101,102]. The newly recruited cells help phagocytose the mycobacteria released by lysis of the infected macrophages. In the meantime, dendritic cells with engulfed bacilli, migrate to the regional lymph node, prime T cells (both $CD4^+$ and $CD8^+$) against mycobacterial antigens, and secrete immunoregulatory cytokines, such as IL-12[92]. However, *M. tuberculosis* alters the cytokine signaling of dendritic cells to suppress T lymphocyte activity through ManLAM[103–105]. More recently, it was shown that the LAM precursors, phosphatidyl-inositol mannosides (PIMs), have the immune-inhibitory effect, while ManLAM has a proinflammatory effect. However, the contradictory results could be the result of different sample preparations[106].

T cells migrate to the site of infection and help kill mycobacteria by secreting IFN-γ and TNF-α to activate macrophages, and by the cytotoxic functions of activated CD4+ and CD8+ T cells. Both macrophages and dendritic cells can present antigens to T cells in the context of both MHC class I and II and both play an important role in recruitment of cells at the site of infection by secreting the proinflammatory cytokines IL-1 and IL-6[16,90–92,107]. The aggregates of these many cell types form the granulomas, the pathological hallmarks of TB.

M. tuberculosis also infects nonphagocytic cells in the alveolar space, including microfold cells, alveolar endothelial, and type 1 and type 2 alveolar epithelial cells, encountering distinct environments within these different cell types[16]. The impact of these environments for *M. tuberculosis* on TB dissemination or disease progression remains unclear.

2.7 Interaction with the Lung

As mentioned above, the fight against *M. tuberculosis* infection mainly occurs in the lungs. The lungs are primary organs of the respiratory system, and the respiratory system is divided into the conducting portion that brings in air from outside the body, and the respiratory portion that facilitates gas exchange and oxygenation of the blood. The conducting portion begins at the trachea and ends at the bronchioles. Bronchioles branch out from the trachea into smaller and smaller branches, until reaching the respiratory portion of the lung that includes alveolar ducts, alveolar sacs, and ends at the alveoli where gas exchange takes place[108]. This branching maximizes the area for gas exchange. Droplets containing *M. tuberculosis* bacilli that are < 5μm in diameter pass through the conduction portion into the respiratory portion, while larger droplets are trapped in the upper conducting portion in mucus secreted by goblet cells, which are subsequently transported away by ciliated cells[19]. The walls of the alveoli are lined by epithelial cells called pneumocytes and there are two types: type I and type II. Type I pneumocytes cover 95-97% of the surface of the alveoli, and their primary function is to facilitate gas exchange. Type II pneumocytes occupy the other 3-5% of the surface area of alveoli[108]. These cells secrete a surfactant, which consist of a multimolecular complex of proteins and lipids, to reduce surface tension in the lung[20,109–113]. Type II cells can differentiate into type I pneumocytes upon damage to the epithelium[108]. Pulmonary surfactant proteins A and D participate in the lung innate and adaptive immune responses against multiple pathogens[111,112]. Pulmonary surfactant protein D (SP-D), binds *M. tuberculosis* ManLAM and prevents it from binding to the macrophage's mannose receptors and enhancing phagosome–lysosome fusion[111,113]. In contrast, surfactant protein A (SP-A) enhances attachment and phagocytosis of *M. tuberculosis* bacilli by upregulating the macrophage mannose receptors and may play a role

in the cellular immune response[109,110,112]. Alveolar epithelial cells rest on top of a permeable basement membrane, with endothelial cells below. This wall allows for the exchange of oxygen and carbon dioxide in the blood, and is referred to as the air-blood barrier (Figure 2)[24,108] .

Present free within the alveolar space are alveolar macrophages that phagocytize and remove inhaled foreign particles such as dust and bacteria. They are the dominant immune cell in the lung under steady state conditions[114]. Alveolar macrophages are predominantly immunosuppressive to prevent an unnecessary inflammatory response to inhaled foreign proteins encountered within the airway[114]. This natural immunosuppressive state may contribute to the persistence of *M. tuberculosis* in the lung. However, when a lung infection does occur, the alveolar macrophages and epithelial cells are capable of recruiting immune cells from the blood across the air-blood barrier to the blood to the alveolar surface. Unfortunately, due to severe inflammation associated with this process, life-threatening tissue damage can occur[115].

For many years, it was thought that alveolar macrophages were the first cell type *M. tuberculosis* bacilli interacted with in the lung and that the persistence of the mycobacteria in these cells drove infection outcomes, including dissemination from the lung to the lymph nodes, blood, and other organs. It is thought that the dissemination of *M. tuberculosis* bacilli from the lungs before the adaptive immune response develops is what makes this organism so successful at establishing infection[24,105,116,117]. However, there are approximately 50 macrophages per alveolus compared to the 30,000 alveolar epithelial cells, giving *M. tuberculosis* bacteria far greater opportunity to interact with these cells[19]. Interaction with alveolar epithelial cells is an important part of the infection process for other bacterial pathogens. For example, *Staphylococcus aureus* invades pneumocytes in order to evade host immunity and colonize the host. Non-typeable *Haemophilus influenzae* bacteria similarly escape from the host immune

system and reside inside alveolar epithelial cells to gain access to essential nutrients[20,118]. Likewise, *Francisella tularensis* targeting of alveolar epithelial cells is essential for its virulence in the host[21]. This has led us and other groups to believe that alveolar epithelial cells play a role in *M. tuberculosis* infection. Indeed, it has been shown that *M. tuberculosis* bacilli replicate in alveolar epithelial cells, and *M. tuberculosis* DNA has also been detected in epithelial cells of subjects with latent TB infection[22–25]. Alveolar epithelial cells have also been shown to secrete IL-8, MCP-1, and TNF-α in response to mycobacterial infection, linking these cells to recruitment of cells involved in granuloma formation, and explaining the high levels of IL-8 in bronchial lavage fluid of TB patients that could not be explained as having come from alveolar macrophages due to their small numbers in the alveoli[119–121].

It has been recently shown that alveolar epithelial cells internalize *M. tuberculosis* bacilli by receptor-mediated macropinocytosis involving actin-polymerization[122]. Once internalized, *M. tuberculosis* bacilli cause permeation, necrosis, and subsequent spread to other type II pneumocytes, while *M. bovis* BCG is attenuated for this phenotype[123–125]. Lysis of the alveolar epithelium could have a substantial effect on dissemination of these bacilli from the lungs into the blood[60,61]. ESAT-6 has been implicated in the cytolysis of these cells, and has been shown to bind to laminin, a protein of epithelial cells that is concentrated on the cell surface membrane[62]. In a bilayer model of the alveolar barrier, bacteria that replicate in A549 cells are also more likely to invade endothelial cells, and monocytes harboring *M. tuberculosis* bacilli were more likely to cross the alveolar barrier when alveolar epithelial cells were infected[24,126].. Similarly, *M. marinum* bacilli are able to cross the blood-brain barrier both via infected-macrophages and by a macrophage-independent mechanism[127]. ESAT-6 mutants and ESAT-6 secretion-deficient mutants are both attenuated for transmigration in a similar *in vitro* alveolar barrier model[29]

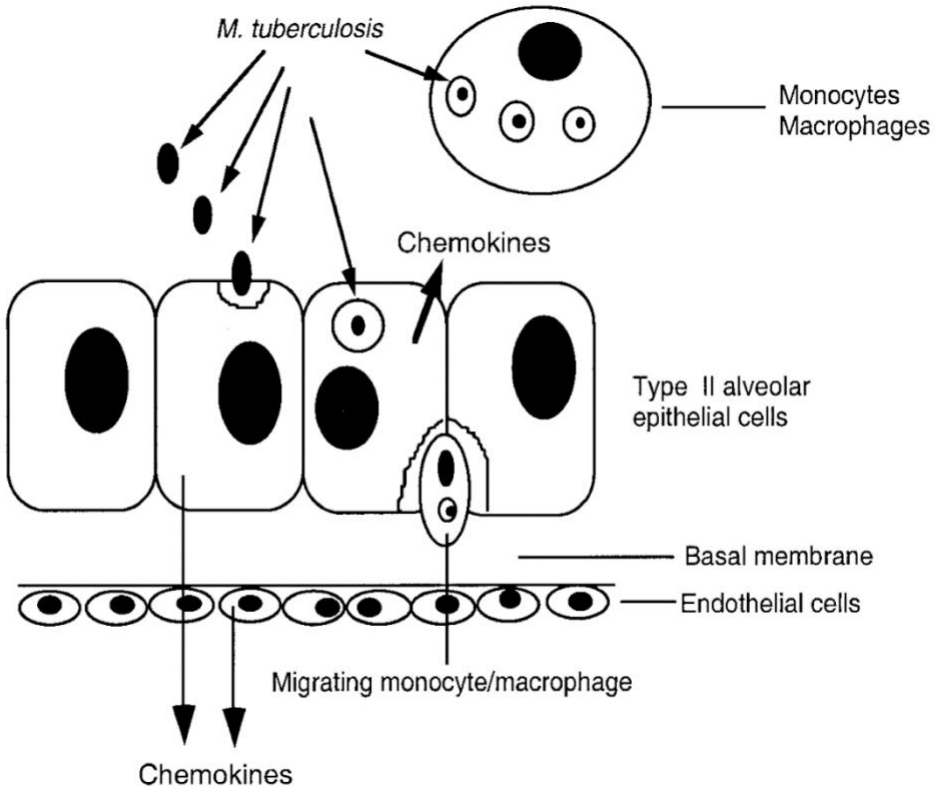

Figure 2: Schematic representation of the states of *M. tuberculosis* translocation across the alveolar wall[128]

Additionally, there are genes and associated protein products of *M. tuberculosis* that are specific for alveolar epithelial cells. One such gene product is the heparin-binding hemagglutinin adhesin (HBHA) that binds to heparin sulfate proteoglycans in the cell membrane of alveolar epithelial cells and in the underlying basement membrane[26]. *M. tuberculosis* bacilli lacking the *hbha* gene are attenuated for adherence and invasion of alveolar epithelial cells, but not of macrophages, and transcripts for *hbha* are upregulated during infection of alveolar epithelial cells but not during infection of macrophages[27]. Deleting *hbha* from *M. tuberculosis* had no effect on the ability of the bacteria to infect or grow within the lung, but impaired the ability to disseminate from the lungs to spleen in mice, showing a role for HBHA in dissemination of *M. tuberculosis* bacilli from the lungs, independent of macrophages[28]. In an *in vitro* bilayer model of

the alveolar barrier, *M. bovis* BCG *Δhbha*, which does not produce either ESAT-6 or HBHA, is even more attenuated than the single ESAT-6 deficient mutants for migration across the *in vitro* alveolar barrier[29]. Furthermore, vaccination that leads to the attenuation of the interactions of HBHA with alveolar epithelial cells has been demonstrated. Pre-incubation of wild type *M. tuberculosis* bacilli with anti-HBHA antibodies attenuates the dissemination of the intra-nasally administered bacteria from the lungs to spleen[28]. Similarly, mucosal immunization with HBHA elicits anti-HBHA antibodies, reduces the mycobacterial burden in the lungs of infected mice, and decreases dissemination of *M. tuberculosis* bacilli from the lungs to the spleen[129,130] . Targeting protein interactions with cells of the alveolar barrier has shown potential as a vaccine strategy in the case of *Streptococcus pneumoniae*[131]. Pre-incubation of A549 cells with recombinant cell wall adhesin PtsA (rPtsA) inhibited the adhesion of *S. pneumoniae* bacilli to these cells. Immunization of susceptible mice with rPtsA protected the animals against challenge with *S. pneumoniae*. The above evidence shows that targeting mycobacterial proteins that interact with alveolar epithelial cells is an attractive vaccine strategy.

2.8 Phagosome Maturation Arrest

One of the hallmarks of *M. tuberculosis* pathogenicity is its ability to survive and persist in macrophages. Once intracellular, *M. tuberculosis* can prevent fusion of its phagocytic compartment with the degradative macrophage lysosome, in a process originally called "the phagosome-lysosome fusion block, but now termed "phagosome maturation arrest"[132]. *M. tuberculosis* employs many mechanisms to prevent interaction of the mycobacterial containing phagosome with endocytic compartments in order to arrest maturation of the phagosome at a point before fusion with the lysosome occurs[16,91]. *M. tuberculosis* bacilli can reside in the phagosome to secure nutrients such as iron and manganese[133]. Small GTPases of the Rab family

regulate phagosome maturation in their GTP-bound 'active' state by modulating the recruitment of binding partners and interactions with the cytoskeleton. Early endosomal GTPase, Rab5 regulates the fusion events between the phagosome and early endosomes by recruiting early endosome antigen 1 (EEA1)[134]. Rab5 also recruits the phosphatidylinositol 3kinase (PI3K) hVPS34, which in turn generates phosphatidylinositol 3-phosphate (PI3P)[135]. PI3P also binds EEA1 at its FYVE domain, stabilizing its association with the early endosomal membrane[136]. Additionally, PI3P promotes recruitment of other proteins involved in phagosome maturation including Rab7, a marker of late endosomes[134]. Rab7 in turn, recruits other proteins to the membrane, like Rab-interacting lysosomal protein (RILP), which brings the phagosome in contact with microtubules, and lysosomes[137]. Lysosomal-associated membrane proteins (LAMPs) and luminal proteases (cathepsins and hydrolases) are incorporated into the phagocytic compartment from fusion with late endosomes. Phagolysosomes are formed when phagosomes fuse with lysosomes. Cathepsins, lipases, and proteases are also important degradative enzymes found in the lysosome[138]. Another microbicidal component of the phagosome is the nicotinamide adenine dinucleotide phosphate (NADPH) oxidase that generates reactive oxygen species[139]. Low pH is the most distinctive characteristic of phagolysosomes. During the maturation process, the membrane of the phagosome accumulates more and more active molecules of V-ATPase that translocates protons into the lumen of the phagosome using cytosolic ATP as an energy source[139]. The low pH disrupts the normal metabolism of many bacteria and is required for the activation of many hydrolytic enzymes, which degrade the ingested pathogen[140].

Early studies with *M. tuberculosis* using electron microscopy localized bacilli in phagosomes of cultured mouse peritoneal macrophages[96], and later the same group showed that

bacilli could survive and multiply both in phagolysosomes and in unfused phagosomes when the mycobacteria were pretreated with rabbit antiserum[18]. Later, Crowle *et al.* found that phagosomes containing *M. tuberculosis* bacilli or an opportunistic pathogen, *M. avium*, in human macrophages were non-acidic, suggesting a defect in phagosomal acidification[141]. In human monocytes, *M. tuberculosis* bacilli were mostly localized in phagosomes that do not fuse with late endosomes/lysosomes[142]. A subsequent study showed that while early endosomal marker Rab5 accumulated on mycobacterial phagosomes, late endosomal/lysosomal maker Rab7 was not detected[143]. A complementary study showed that early endosomal autoantigen 1 (EEA1) was excluded from *M. tuberculosis* containing phagosomes[144]. Ferrari *et al.* found that incorporation of host tryptophan aspartate coat protein (TACO or Coronin 1) onto the *M. bovis* BCG-containing phagosomal membrane prevents fusion with lysosomes[145]. Coronin 1 activates calcineurin, a Ca^{2+}-dependent phosphatase, which in turn impairs the delivery of mycobacteria to phagolysosomes[146]. ManLAM, found on the surface of virulent mycobacteria, also modulates calcium signaling by decreasing intracellular calcium levels and inactivating calmodulin kinase II activity, which prevents PI3KC3 from producing PI3P on the phagosomal membrane[147–149]. While many studies have shown that ManLAM prevents phagolysosome-fusion[150,151], others showed that insertion of ManLAM into host membrane rafts that prevents fusion with the lysosome rather than the inhibition in PI3P production[152,153]. The phosphoinositide phosphatase SapM alters phagolysosome fusion by inhibiting the generation of phosphatidylinositol 3-phosphate (PI3P)[44]. PTpA, another *M. tuberculosis* phosphatase, alters trafficking by inhibiting Vacuolar-type H^+ -ATPase (V-ATPase) on the mycobacterial phagosome and subsequent acidification of the phagosome[154,155]. V-ATPase exclusion is also associated with the STAT-5-mediated expression of cytokine-inducible SH2-containing protein, which selectively targets the

V-ATPase for ubiquitination and degradation[17]. These studies confirm reports by Sturgill-Koszycki *et al*. that the *M. tuberculosis* phagosome is not acidified[156].

Reports are contradictory on whether *M. tuberculosis* bacilli escape the phagosome in macrophages. Localization of *M. tuberculosis* bacilli to the cytosol were first reported in the early 1980s and 1990s[157–159]. Twenty years later, van der Wel *et al*. identified the 6-kDa early secreted antigenic target ESAT-6, secreted by the Type VII Secretion System (T7SS) ESX-1, as one of the main *M. tuberculosis* factors responsible for the localization of bacteria in the cytosol[160]. Another study showed that both the ESX-1 system and PDIM production were required to damage the phagosome. However, the ability of ESAT-6 to lyse membranes could be due to different procedures used by these groups for the purification of the recombinant ESAT-6[161,162]. A study by Simeone *et al*. supported the lytic activity of ESAT-6 when they showed that *M. tuberculosis* induces phagosomal rupture in the mouse model of infection[163]. While significant research has gone into identifying trafficking patterns of *M. tuberculosis* in the macrophage, little research has gone into elucidating trafficking patterns in other cell types.

2.9 Lipid Rafts and Pathogenesis

Receptor molecules such as pattern recognition receptors cluster in lipid rafts, which are isolated, tightly-packed regions on the plasma membrane that are also rich in cholesterol, glycosphingolipids, and regulatory and signaling proteins[164]. Rafts float freely in the plasma membrane but coalesce upon stimulation of receptor molecules, which brings surface receptors in close contact with co-stimulatory molecules that initiate signaling cascades. Bacteria such as *Escherichia coli, Brucellae* species, and *Pseudomonas aeruginosa* use lipid rafts to modulate their internalization, trafficking, and influence host cell-signaling pathways to establish a protective niche[165–171]. Most studies use cholesterol-disrupting agents, such as filipin, to disrupt

lipid rafts, and subsequently observe the effects on invasion and survival of bacteria, as well as the host cell response, or employ the cholera toxin receptor GM1 as a marker of glycolipid raft domains in confocal microscopy[172]. When FimH of *E. coli* binds to its receptor in lipid rafts, the bacteria are internalized by a type of lipid raft known as caveolae and survive intracellularly[165]. The binding of this receptor also triggers mast cells to secrete TNF-α, a proinflammatory cytokine that recruits other cells to the site of infection[166]. *E. coli* that enter macrophages through this route are not trafficked to the lysosome for degradation[167]. *Brucellae* species associate with lipid raft components, such as GM1, upon entry into macrophages to avoid phagosome-lysosome fusion and inhibit macrophage activation to promote their intracellular survival[168,169]. *P. aeruginosa* binding also triggers lipid raft signaling platforms to enter cells, induce apoptosis and regulate the cytokine response of infected cells to initiate the host immune response[170,171]. There is evidence that *Mycobacterium* species utilize lipid rafts to their advantage. *M. avium* and *M. bovis* bind to cholesterol, which is important for internalization of the bacteria into macrophages, neutrophils, and mast cells[146,173,174]. Cholesterol-dependent incorporation of host tryptophan aspartate coat protein (TACO) onto the *M. bovis* BCG-containing phagosomal membrane and incorporation of *M. tuberculosis* lipoarabinomannan into macrophage membrane rafts prevents fusion with the lysosome[145,152] . The 19-kDa protein of *M. tuberculosis* LpqH colocalizes with lipid rafts and initiates TLR2 signaling in macrophages[175]. Our laboratory has shown that *M. tuberculosis* induces lipid raft formation in A549 cells, and disruption of lipid rafts impacts mycobacterial survival in these cells[176]. How *M. tuberculosis* stimulates lipid rafts and the mechanism that promotes survival in A549 cells is currently being investigated. In macrophages, *Legionella pneumophila* and FimH+ *E. coli* internalized through lipid rafts recruit the autophagic machinery and avoid immediate killing[177]. Due to our

laboratory's previous observation that *M. tuberculosis* interacts with both lipid rafts and the autophagy pathway to support survival, it would be interesting to see whether these two pathways are also connected in *M. tuberculosis* infection of alveolar epithelial cells.

2.10 Autophagy and LC3 Associated Phagocytosis

One way that *M. tuberculosis* avoids fusion with the phagosome is by manipulating the autophagy pathway. Macroautophagy (hereafter termed autophagy) refers to the general cellular process of "self-eating" superfluous or potentially harmful cytosolic components (i.e. damaged mitochondria) within a double membrane autophagosome followed by proteolytic degradation in the lysosome[178]. This process allows the cell to maintain cellular homeostasis and generate amino acids for maintaining cell viability. Autophagy occurs at a basal level in most cell types, but can be induced by nutrient deprivation, oxidative stress, and infection[178]. One of the hallmarks of autophagy is the microtubule-associated protein 1 light chain 3 (MAP1LC3, best known as LC3) LC3 (specifically LC3-II), which is the major protein of the autophagosome and remains with the autophagosome until fusion with the lysosomes[179]. GFP-tagging of LC3 (GFP–LC3) has become indispensable for visualizing autophagosomes in mammalian cells[180].

The kinase mammalian target of rapamycin complex 1 (mTOR1) and AMPK kinase are downstream of many nutrient signaling pathways and serve as the gatekeepers of autophagy in mammalian cells, and under nutrient rich conditions[179], mTOR inhibits autophagy by phosphorylation of the most upstream autophagy related gene (ATG), unc-51 like autophagy-activating kinase (ULK1), and inhibition of mTOR results in activation of autophagy. While mTOR negatively regulates autophagy, (AMP)-activated protein kinase (AMPK) positively regulates autophagy by phosphorylating ULK1[178,179].

Invasion by intracellular pathogens can also trigger autophagy. The subclass of autophagy called xenophagy, refers to the specific ubiquitin tagging of intracellular pathogens[181]. Ubiquitin normally has a role in targeting misfolded proteins for degradation in proteasomes but has been linked to autophagy when aggregates of misfolded proteins become too large for proteasomes and accumulate in the cytosol where they are degraded by autophagy[182]. Ubiquitinated bacteria are delivered to autophagosomes by autophagy receptors that bind both ubiquitin and LC3 such as p62/sequestosome (SQSTM)1 and nuclear dot protein 52 (NDP52)[181]. The autophagosome then fuses with the lysosome to degrade the pathogen. Xenophagy was first reported in *M. tuberculosis* infection as a way for macrophages to overcome the phagosomal maturation block[183]. Subsequent research showed *M. tuberculosis* ESAT-6 mediates phagosomal permeabilization, allowing cytosolic components of the ubiquitin-mediated autophagy pathway to access phagosomal *M. tuberculosis*[184]. However, *M. tuberculosis* is able to prevent fusion of its autophagic compartment with the lysosome. The EIS protein of *M. tuberculosis* was shown to inhibit autophagy in macrophages by modulating the host immune response and inhibiting Rab7, an endosomal marker that is also involved in the maturation of *M. tuberculosis*-containing autophagosomes into autolysosomes[185]. ESAT-6 is also important for inhibiting autophagic flux in human dendritic cells and macrophages to promote survival of the bacteria[186,187].

Other pathogens subvert the autophagy pathway to mediate and source nutrients for their own survival. For example, *L. pneumophila*, an opportunistic human pathogen, inhibits autophagy directly by secreting RavZ, a cysteine protease which cleaves LC3 from the membrane and inhibits autophagosome formation. *S. aureus* can exploit the autophagy machinery to form its replicative niche, and like *M. tuberculosis*, *S. aureus* resides in a double membrane, LC3-positive compartment that does not fuse with the lysosome[188]. *Coxiella burnetii*

bacilli activate autophagy to gain access to the lysosome, which they convert into a parasitophorous vacuole for replication[181]. Lysins of *L. monocytogenes* rupture the endosome membrane to release the bacteria into the cytosol where autophagy is triggered. Once in the cytosol, *L. monocytogenes* expresses ActA protein to polymerize actin for motility. *L. monocytogenes* strains that are able to polymerize actin are not targeted for xenophagy[181]. Our laboratory has shown *M. tuberculosis* prevents fusion of the autophagosome with the lysosome. Blocking this pathway decreases survival of the bacteria in A549 cells[32]. In 2016, researchers discovered that the environmental non-pathogenic species, *M. smegmatis* is targeted for degradation by the autophagy marker LC3, but unlike *M. tuberculosis*, was not ubiquitinated[189]. Recently, a non-canonical autophagy pathway termed LC3 associated phagocytosis (LAP) has been identified as a mechanism host cells use to deliver phagocytosed cargo directly to lysosomes for immediate degradation[190]. In this pathway, components of autophagic machinery are used to conjugate LC3 directly onto a single membrane vesicle. However, there are many components of LAP that differ from classical autophagy, starting from the stimulus (Figure 3). While autophagy is stimulated by nutrient starvation, intracellular stress signals, or invading intracellular pathogens, LAP is thought to be triggered from outside the cell upon ligation of surface receptors. For pathogens, this includes pattern recognition receptors such as Toll-Like Receptors, and Immunoglobulin (Ig) receptors that recognize opsonized pathogens[191]. While the receptors are known, the signaling cascades that lead to recruitment of LAP effectors to the phagosome are unclear. We can examine the differences between autophagy and LAP in three main stages: phagophore formation (nucleation in autophagy, phagosome cup development in

LAP), assembly of the phosphatidyl-inositol 3-kinase complex, and LC3 lipidation and conjugation onto the phagophore membrane.

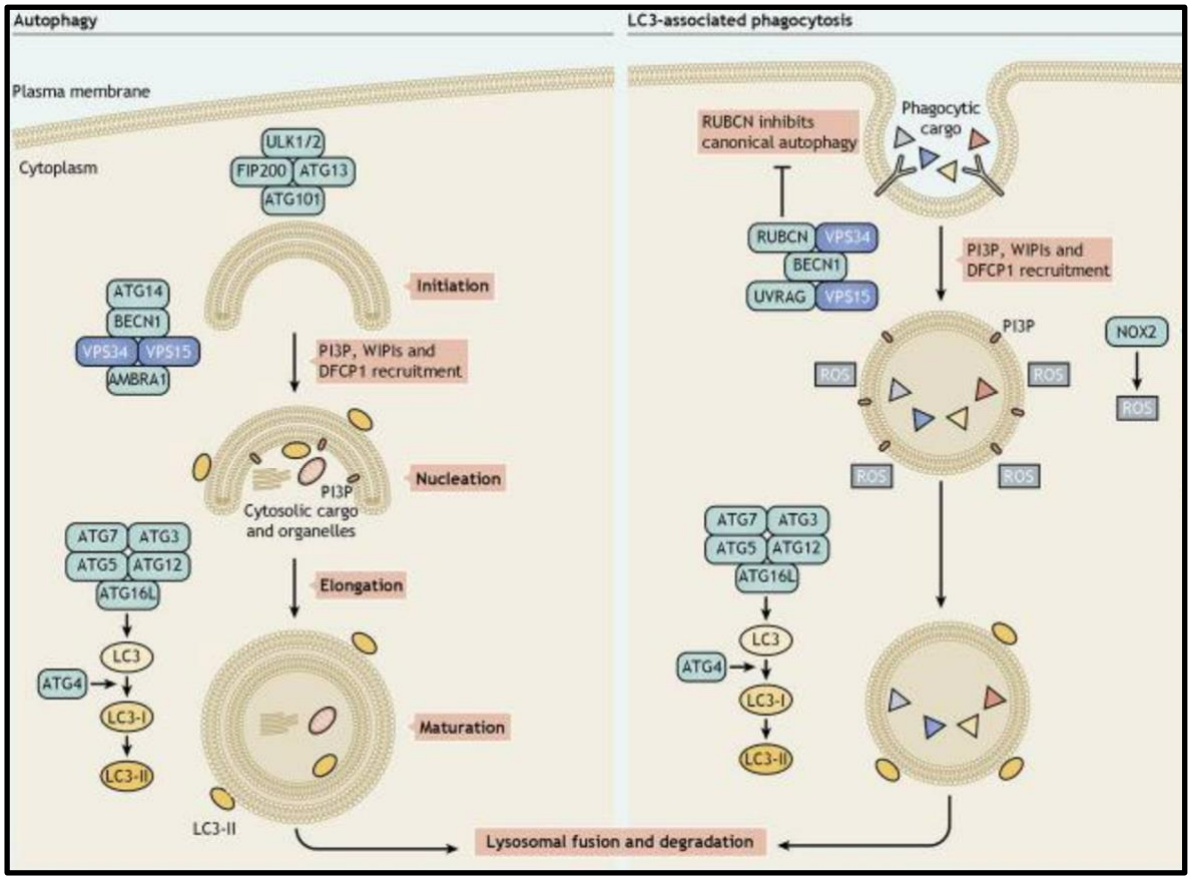

Figure 3: Illustration of the Proteins Involved in the Autophagy and LC3-Associated Phagocytosis Pathways[191][191]

When autophagy is activated, the kinase complex of ULK1, FAK family kinase-interacting protein of 200 kDa (FIP200), ATG13, and ATG101 dissociates from mTOR and redistributes to the phagophore initiation complex[191,192]. This kinase complex is dispensable for LAP, which instead follows typical phagosome formation[134]. After phagophore formation, a multimeric phosphotidylinositol 3-kinase complex (PI3KC3) is recruited. LAP and autophagy share the core PI3KC3 components of the phosphoinositide 3-kinase VPS34, Beclin-1, and VPS15, but the autophagy complex includes the subunits ATG14L and autophagy and Beclin-1 regulator 1 (AMBRA1), while the LAP complex includes UV Radiation Resistance Associated

(UVRAG) and with Run domain Beclin-1-interacting and cysteine-rich domain-containing protein (RUBICON)[191]. VPS34 is a kinase that produces phosphatidylinositol-3-phosphate (PI3P), which recruits the ubiquitin-like conjugation systems that process and ligate the protein LC3 (or LC3-I) to phosphatidylethanolamine (PE) molecules at the autophagosome/phagosome creating LC3-PE conjugates or LC3-II[178]. Interestingly, RUBICON inhibits autophagy by abrogating PI3P production by VPS34, but is required for PI3P generation during LAP[191]. Moreover, unlike WIP (WD-repeat phosphoinositide-interacting protein) I2, a WD β-propeller PROPPIN that utilizes an alternative lipid-binding domain from the common PX or FYVE domains in autophagy, there are no known proteins in LAP that link the PI3KC3 and the lipidation machinery[191,193]. An intermediate step specific to LAP that occurs after PI3KC3 recruitment but before LC3-I lipidation, is generation of reactive oxygen species (ROS) at the phagosomal membrane[192]. In macrophages, ROS is produced by the nicotinamide adenine dinucleotide phosphate (NADPH) oxidase-2 (NOX2). Interaction with RUBICON activates NOX2, and NOX2 is required for the recruitment of the LC3 conjugation machinery, but the precise role of NOX2 and ROS in LAP are unknown[192]. Additionally, LC3 conjugation to the phagosome in LAP occurs after closure of the phagosome membrane, while the lipidation of LC3 promotes phagosome closure in autophagy. In both cases, LC3-II recruitment occurs prior to autophagosome/phagosome fusion with the lysosome[192].

Interestingly, it has been suggested studies that use pharmacological means to overcome the phagosome-lysosome block in *M. tuberculosis* infection are actually inducing LAP[194]. *M. tuberculosis and M. marinum* are both targeted by LAP in macrophages. *M. marinum* resides in a LC3-decorated, single-membrane compartment that does not fuse with lysosomes[195]. Mutants of *M. tuberculosis* lacking *cpsA* are degraded by LAP while wild type bacteria are able to avoid this

process[196]. Another pathogen, *B. pseudomallei* resides in single-membrane LC3-positive compartments that do not fuse with lysosomes, and a proportion of the bacteria escape into the cytosol. However, mutants of *B. pseudomallei* lacking the type III secretion system are not able to prevent fusion with the lysosome and do not escape from the phagosome[190]. Transmission electron microscopy (TEM)-as well as correlative light and electron microscopy (CLEM) analyses at 1 hour post-infection revealed the LC3-positive *L. monocytogenes*-harboring compartment to be surrounded by a single membrane[197,198]. Transmission electron microscopy (TEM)- as well as correlative light and electron microscopy (CLEM)-analyses at 1 hour post infection revealed the compartments harboring *L. monocytogenes*, were LC3 positive surrounded by a single membrane[197,198]. *Legionella dumoffii, Shigella flexneri,* and *Yersinia pseudotuberculosis* have all been shown to be targeted by LAP in non-phagocytic cells[190]. Whether *M. tuberculosis* is targeted by LAP in cell types other than macrophages remains to be investigated.

2.11 Current Vaccine Strategies

Since its first use in 1921, *M. bovis* BCG has been the only approved human TB vaccine. Because of the limited efficacy of this vaccine and the rise in antibiotic resistant strains of *M. tuberculosis*, development of new vaccines are a cornerstone of the World Health Organization's "End TB" strategy[5]. Current vaccine strategies involve subunit, viral-vectored vaccines expressing one or more antigens of *M. tuberculosis,* live whole-cell mycobacteria, or inactivated whole-cell vaccines, but to date none of the candidates in clinical trials have been proven to be more effective than *M. bovis* BCG alone[199]. Vaccine candidates have the goal of inducing an immune response to control progression of *M. tuberculosis* infection and can be administered as a preventative, as a therapeutic for current infections, to prevent reactivation of latent TB, or as a

boost to the current *M. bovis* BCG vaccine[14]. While the correlates of protective immunity to *M. tuberculosis* infection aren't completely defined, vaccines should generate a memory response to infection, resulting from the clonal expansion and differentiation of antigen-specific lymphocytes[200]. T cells can differentiate into effector memory T (T_{EM}) cells that produce cytokines and migrate to affected tissues, as well as central memory T (T_{CM}) cells that migrate to secondary lymphoid organs where they can proliferate and differentiate into new effector cells upon re-exposure to antigen[200]. Protective immunity to *M. tuberculosis* in the lung requires T helper 1 (Th1) and 17 (Th17) type CD4 effector memory cells secreting interferon γ (IFNγ)/tumor necrosis factor α (TNF-α)/interleukin 2 (IL-2), and IL-17, respectively. CD8 T-cell response is also important for successful control of disease through effector cytokine secretion and cytolytic functions to kill *M. tuberculosis*-infected cells[201]. It is thought that the shortcoming of the current *M. bovis* BCG vaccination strategy is its inability to induce a long-lived central memory T-cell population with the ability to migrate to the lung[202]. Most recently, T-resident memory cells (T_{REM}) that home to the lung have been found to be important in controlling TB disease[203]. Mucosal and intravenous administration of *M. bovis* BCG induces a stronger T_{REM} response than the classical intradermal and intramuscular routes of vaccination[204]. The benefits of mucosal administration were reported as early as the 1970s in animal models, but this route of vaccination has been understudied throughout the years[13,205,206]. Novel vaccines should also aim to increase the number and quality of T_{CM} cells generated, and aerosol-delivered vaccines as well as novel adjuvants administered with M. *tuberculosis* antigens have shown success in this regard[82,202]. Even though there are over 4,000 genes in the *M. tuberculosis* genome, only 11 mycobacterial antigens have progressed to human clinical trials as part of subunit vaccines, with antigens from the antigen 85 (Ag85) complex being the most commonly used[57,207]. The

identification of novel antigens for inclusion in subunit vaccines is a critical step in the TB vaccine-development process. More consideration is also being given to the role of humoral immunity in TB control. *Mycobacterium tuberculosis* infection has been shown to induce the humoral immune responses against various mycobacterial antigens[208,209]. In addition, *M. bovis* BCG vaccination can induce antibody responses to several mycobacterial antigens, which elicits both innate and cell-mediated immunity against mycobacteria[209–213]. New vaccine approaches should aim to elicit both the cellular and humoral immune response against *M. tuberculosis* in vaccinated individuals.

2.12 Conclusion

While extensive research has examined *M. tuberculosis* and its interactions with various animal hosts and phagocytic cells, it is evident that there are still significant gaps in our knowledge. The goal of the research described in this dissertation was to characterize interactions and trafficking of a *M. tuberculosis* mutant within alveolar epithelial cells. Our data suggest major differences exist in the mechanisms used by wild-type *M. tuberculosis* and the ΔRv3351c bacilli to survive in alveolar epithelial cells. The localization of the Rv3351c protein to the membrane of *M. tuberculosis,* its ability to elicit antibodies in patients with active TB, and its ability to reduce *M. tuberculosis* killing of A549 cells, makes it an attractive candidate for a mucosal subunit vaccine with other proteins that target alveolar epithelial cells. This work has important implications for our understanding of this ancient pathogen, its many mechanisms for virulence, and identifying and exploiting novel targets for vaccination.

CHAPTER 3

ROLE OF RV3351C IN TRAFFICKING OF *MYCOBACTERIUM TUBERCULOSIS* BACILLI IN ALVEOLAR EPITHELIAL CELLS[1]

1 Megan Prescott, Kari Fine-Coulson, Maureen Metcalfe, Tuhina Gupta, Rebecca Pavlicek1, Barbara Reaves, Russell Karls, and Frederick Quinn.

To be submitted to *Cellular Microbiology*

Abstract

Although interactions with alveolar macrophages have been well characterized for *Mycobacterium tuberculosis*, the roles epithelial cells play during *M. tuberculosis* infection have not been well studied. Recent reports indicate that *Rv3351c* is one of at least three *M. tuberculosis* genes whose products that have been shown to function in the support of *M. tuberculosis* attachment, internalization, replication and/or survival in alveolar epithelial cells. In infected human type II pneumocyte cell lines, we previously showed that the ΔRv3351c mutant bacilli replicate less efficiently and generate less necrosis compared to the virulent parent strain Erdman. In the present study, we analyze infections of *M. tuberculosis* ΔRv3351c and parent strain Erdman in A549 type II cells. Results confirm our previous observation demonstrating lipid raft aggregation on A549 cell plasma membranes during *M. tuberculosis* Erdman infection or after addition of infected A549 cell filtered supernatants. However, we demonstrate here that Rv3351c is responsible for the observed lipid raft formation, as the addition of *Escherichia coli* recombinant Rv3351c protein to A549 cell cultures induces lipid rafts, and the ΔRv3351c mutant induces fewer lipid rafts on the surface of A549 cells compared to the wild-type strain. We also show that ΔRv3351c mutant as well as wild type bacilli attach and are internalized via an actin pseudopod engulfment mechanism. Endosomal trafficking studies demonstrate that the mutant strain traffics through LAMP-2-labeled endosomes 30% more frequently than the parent strain. These data suggest that ΔRv3351c bacilli once internalized are less able to survive and multiply intracellularly and are thus less cytotoxic compared with the parent strain. Thus, the role of Rv3351c in trafficking and survival of *M. tuberculosis* bacilli through epithelial cells may begin with modifications to the plasma membrane prior to attachment.

Introduction

Mycobacterium tuberculosis, the causative agent of tuberculosis (TB), infects an estimated one-quarter of the world's population, and 60-90% of these individuals may harbor latent infection[5,214]. To date, no vaccine reproducibly protects against the pulmonary form of the disease in post-adolescents.

The alveolar macrophage is generally believed to control the initial success or failure of *M. tuberculosis* infections. While based in large part on the lack of *in vivo* data from late-stage infection and clinical studies, alveolar pneumocytes were not considered to be important players in *M. tuberculosis* pathogenesis[96]. However, recent studies and clinical observations are changing this concept[215,216], and corresponding *in vitro* studies have demonstrated that *M. tuberculosis* bacilli can enter and replicate to high numbers in type II alveolar pneumocytes in both monolayer and in epithelial/endothelial bilayer systems. However, internalization of alveolar epithelial cells is much slower than that observed in macrophages[19,30,31,122,126,128,217]. An understanding of the receptors and mechanisms responsible for microbial attachment and internalization in alveolar epithelial cells is important but incomplete, although the heparin-binding hemagglutinin protein and the process of lipid raft development may play important roles[31,218]. Once internalized, vacuolar trafficking is crucial to the ultimate survival of the pathogen and host cell. Hsu, et al. (2003) showed that pneumocytes and macrophages infected with a strain of *M. tuberculosis* deficient in the critical virulence factor Early Secretory Antigenic Target-6 (ESAT-6) resulted in the loss of the cytolytic phenotype in both cell types[61]. Chitale *et al*. determined that products of the *M. tuberculosis mce* locus promoted uptake into human epithelial (HeLa) cells[219]. Our laboratory demonstrated that intracellular trafficking patterns for *M. tuberculosis* bacilli in alveolar epithelial cells significantly differ from those in

macrophages, and that autophagy is a crucial part of this process[32], observations that were later confirmed by other labs[220,221]. Additional *in vitro* studies have suggested that the actual movement through this tissue layer can cause phenotypic changes in the bacteria themselves, which could contribute to enhanced virulence[123]. The alveolar epithelial layer, therefore, may play an important role, particularly in early stages of *M. tuberculosis* infection.

While cell death in macrophages resulting from virulent or avirulent mycobacterial infections can proceed via apoptotic or non-apoptotic pathways, alveolar epithelial cell death following *M. tuberculosis* infection is reported to result primarily in necrosis by an undefined mechanism[124,222,223]. The ability of *M. tuberculosis* bacilli to kill type II pneumocytes is potentially an indicator of strain virulence. Our laboratory generated a *M. tuberculosis* mutant lacking the *rv3351c* gene, which like the filamentous hemagglutinin (*hbha*) mutant, kills type II pneumocytes at reduced rates compared to the virulent parent strain[30,218].

In the present study, attachment, internalization and trafficking within type II pneumocytes infected with virulent *M. tuberculosis* strain Erdman and mutant ΔRv3351c bacilli were examined. Using mutants such as ΔRv3351c should help develop a better understanding of the infection process in epithelial cells and may shed light on the role of pneumocytes in mycobacterial respiratory disease.

Results

Rv3351c induces lipid rafts on epithelial cell plasma membranes.

We previously observed that A549 alveolar epithelial cells infected with *M. tuberculosis* Erdman bacilli or culture filtrates from those infections added to fresh monolayers induce lipid raft formation on the host cell plasma membranes to levels equal or more than lipid raft super-aggregator listeriolysin O (LLO) (Fine-Coulson, 2012). In the present study, we show that

ΔRv3351c bacilli induce lipid raft formation on infected A549 cells at a significantly lower rate than wild-type Erdman bacilli in fluorescent confocal microscopic examinations of *M. tuberculosis*-infected and cholera toxin subunit B-labeled A549 monolayers; cholera toxin binds to lipid raft marker GM1. At 6 hours post-infection, 1.5 versus 0.2 lipid rafts per cell, respectively, were observed in cells infected with the wild type versus mutant strain (Figure 1.4, panels A-F). In addition, exogenous addition of recombinant Rv3351c protein alone induced lipid raft formation on A549 cells (Figure 4, panels A and E), and this was unique to Rv3351c compared to another recombinant mycobacterial protein of similar molecular weight (Supplemental Figure 1). Additionally, the Rv3351c protein bound to GM1 by the thin layer chromatography overlay analysis (Supplemental Figure 2), suggesting Rv3351c may interact directly with lipid raft components.

Induction of lipid rafts by Rv3351c is essential for M. tuberculosis *virulence*

We previously observed that the induction of lipid rafts is critical to *M. tuberculosis* Erdman survival in A549 cells[224]. Specifically, disrupting lipid rafts with lipid raft/cholesterol disrupting agent Filipin III decreased the viability of virulent *M. tuberculosis* bacilli. To determine if the observed absence of lipid rafts in cells infected with ΔRv3351c was the reason for the loss of virulence, we induced lipid rafts with the Rv3351c protein before infection with the ΔRv3351c bacilli. Briefly, A549 monolayers were incubated with 5 μg of Rv3351c protein, and after 30 minutes, the cells were washed and maintained in cell culture medium for the duration of the experiment. The addition of Rv3351crestored the virulence phenotype of ΔRv3351c bacilli over the course of infection as measured by lactate dehydrogenase (LDH) release into the cell culture medium (Figure 5, A and B). Lactate dehydrogenase is only released from cells with a damaged cell membrane such as those undergoing necrosis or late state

apoptosis. Similar to our previous study, disrupting lipid rafts with Filipin III significantly decreased the rate of host cell killing by Erdman bacteria, but had no effect on cells infected with ΔRv3351c bacilli (Figure 5C and D). No cytotoxic effects due to the addition of Rv3351c or Filipin III were observed at the concentrations and time points used (data not shown).

Mycobacterium tuberculosis *Erdman and* ΔRv3351*c bacilli attach to A549 type II pneumocytes via actin-mediated engulfment.*

To investigate the earliest time points of infection, we examined mycobacterial interactions at the surface of the host cell by transmission electron microscopy (TEM). A549 cells were infected with the mutant ΔRv3351c and the parent strain, *M. tuberculosis* Erdman. Images of specimens collected from 3 to 24 hours post infection (hpi) suggest that both strains attach and internalize through an actin-mediated mechanism (Figure 6, panels A & B).

To confirm this finding, A549 cells were allowed to attach to coverslips in 6-well dishes and were then infected with DsRed-expressing *M. tuberculosis* Erdman or GFP-expressing ΔRv3351c bacilli at a MOI of 100. Preliminary experiments suggested that *M. tuberculosis* Erdman bacilli attached to A549 cells and became internalized between 6 and 24 hpi. Thus, we chose these time points to focus on early infection. Specimens were fixed and stained with Alexa Fluor 488 or 546 phalloidin to visualize potential surface interactions via confocal microscopy. At 6 hpi, top slices from z-stack images showed *M. tuberculosis* Erdman and ΔRv3351c bacilli within coils of polymerized actin suggesting that both the mutant and parent strains interact with the alveolar epithelial host cell using a similar mechanism during initial infection (Figure 6, panels C & E).

Previous observations have been made indicating actin-associated internalization of virulent *M. tuberculosis* strain H37Rv in A549 and mast cells[128,225,226]. To determine if actin is

critical for engulfment of both *M. tuberculosis* Erdman and ΔRv3351c, the actin-depolymerizing agent cytochalasin D was utilized. Drug-treated A549 cells infected at a MOI of 100 with strain *M. tuberculosis* Erdman ΔRv3351c were examined at 6 and 24 hpi by confocal microscopy. These images revealed an absence of actin tendrils around either strain; however, no significant differences in the adherence of *M. tuberculosis* Erdman or ΔRv3351c bacilli to the surface of host cells at either time point were observed with and without cytochalasin D suggesting that attachment can proceed in the absence of actin polymerization for both strains (Figure 6, panels D, F, G, H, M, N). At 24 hpi, the rate of internalization for ΔRv3351c and *M. tuberculosis* Erdman bacilli were significantly reduced compared to infected A549 cells not treated with cytochalasin D (p-value = 0.060 or <0.001, respectively; (Figure 6, panels I-N). Taken together, these data suggest that both *M. tuberculosis* Erdman and ΔRv3351c bacilli preferentially utilize an actin-based mechanism for internalization, while attachment is not inhibited by the absence of polymerized actin for either strain.

Mycobacterium tuberculosis *Erdman and ΔRv3351c bacilli co-localize with LAMP-2 and cathepsin-L in A549 cells at 12 to 96 hours post-infection.*

The Rv3351c protein has been found to bind to lipid raft component GM1 by thin layer chromatography overlay assays. We hypothesize the binding to, and induction of lipid raft formation leads to the trafficking of the wild-type parental strain through the desired canonical autophagy pathway. To demonstrate, we showed that even though ΔRv3351c bacilli are more associated with autophagy marker LC3 at 12 hours post-infection compared to the *M. tuberculosis* parent Erdman strain, they are less associated with LC3 at later timepoints (Figures 9 and 10) and are more associated with lysosome fusion markers Lamp2 and Cathepsin L at 72 hours post-infection (Figures 7 and 8).

To investigate the difference observed between *M. tuberculosis* Erdman and ΔRv3351c intracellular bacterial numbers over time, intracellular trafficking studies comparing infections with these strains in type II pneumocytes were initiated. Because virulent *M. tuberculosis* bacilli inhibit phagosome-lysosome fusion in macrophages, confocal and immuno-electron microscopy (IEM) studies were performed using antibodies against lysosomal targets, such as lysosomal associated-membrane protein 2 (LAMP-2) and cathepsin-L, to determine if a similar process occurs in infected pneumocytes. Co-localization of GFP-expressing *M. tuberculosis* Erdman with LAMP-2 was examined by confocal microscopy from 6 to 96 hpi with co-localization detected from 24 to 96 hpi (Figures 7, panels A-D; I-K). ΔRv3351c bacilli were also detected co-localizing with LAMP-2 during the same time period (Figure 7, panels E-H; L-N).

Co-localization of lysosomal markers with *M. tuberculosis* Erdman or ΔRv3351c bacteria-containing compartments was analyzed by IEM. At both 12 and 72 hpi, significantly more LAMP-2 and cathepsin-L antibodies were associated with endosomes containing bacilli of the mutant strain compared to the parent strain (Figure 8, panels A-F). To demonstrate that delivery of ΔRv3351c bacteria to the acidic environment of the lysosome is responsible for the decreased intracellular numbers, the vacuolar type H+-ATPase inhibitor Bafilomycin A1 was added to during the course of A549 cell infection. Inhibiting lysosomal acidification with Bafilomycin A1 restored the LDH phenotype to wild-type levels (Figure 8, panel G). Studies showed no deleterious effects produced by the drug at the dose utilized (data not shown).

M. tuberculosis Erdman and ΔRv3351c *induce production of autophagy proteins in A549 cells*.

We previously showed that induction of the autophagy pathway is crucial for *M. tuberculosis* Erdman survival in A549 cells. To determine if Rv3351c was directly involved in autophagy induction, A549 cells were infected with strain Erdman or ΔRv3351c bacilli

expressing dsRed or GFP, respectively for 12 (Figures 9A and C) or 24 hours (Figures. 9B and D). Confocal microscopy examination demonstrated greater amounts of LC3 puncta at 12 hours post-infection in ΔRv3351c-infected cells than those infected with Erdman, but no difference by 24 hours post-infection was observed. (Figures 9E and F, respectively).

These results were confirmed by western blot. A549 cells were incubated for 12 or 24 hours with *M. tuberculosis* Erdman or ΔRv3351c at a MOI of 100. Extracellular bacteria were then removed, and infected cells were treated for 2 hours with Bafilomycin A1 to inhibit autophagic flux. Autophagy levels were analyzed by LC3-II immunoblotting assay with GAPDH as a loading control. The LC3-II/GAPDH ratio is higher upon *M. tuberculosis* Erdman and ΔRv3351c infection than uninfected controls (Figure 10). However, the LC3-II/GAPDH ratio is higher at 12 hours pos- infection for A549 cells infected with ΔRv3351c than Erdman or cells induced for autophagy by amino acid starvation with EBSS (Figure 10A and C). This difference disappears by 24 hours (Figure 10 B and D).

Due to the early observed differences in LC3-II production between A549 cells infected with Erdman and ΔRv3351c, we sought to determine if there were differences in the production of other autophagy proteins. ULK1 is involved in autophagosome formation upstream of LC3 recruitment[227]. Densitometric analysis showed[227]. Densitometric analysis shows differences in the ULK1/GAPDH ratios in Erdman and uninfected cells at 24 hours post infection, while no differences are seen between ΔRv3351c and uninfected cells at that timepoint (Figure 11B and D), indicating ΔRv3351c may not be trafficking through the autophagy pathway.

Cytokine profiles of A549 cells infected with ΔRv3351c *or Erdman.*

Epithelial cells at the mucosal surface are capable of secreting proinflammatory cytokines, which are important mediators in both lung defense and inflammation in response to

bacterial infection[228]. This suggests that epithelial cells can act as an early warning system for local immune and inflammatory cells. For example, tumor necrosis factor alpha (TNF-α) plays a critical role in the control of *M. tuberculosis*[228]. The bacilli can inhibit host cell TNF-α production via expression of specific mycobacterial components and evade antituberculosis immunity[229]. Additionally, alveolar epithelial cells recruit other immune cells through the production of IL-8 and MCP-1 in response to *M. tuberculosis* infection[119–121]. To determine the ability of *M. tuberculosis* Erdman and ΔRv3351c to induce A549 cells to generate cytokines in response to infection, A549 cells were infected at a MOI of 100 with either strain. At 12, 24, and 72 hours post-infection, supernatants were removed and assayed for TNF-α, IL-8, or MCP-1 production. The results demonstrated that only ΔRv3351c stimulated high levels of TNF-α after A549 infection (Figure 12A). In contrast, low levels of TNF-α were detected in response Erdman infection. A549 cells infected with Erdman or ΔRv3351c produced high levels of MCP-1 or IL-8, respectively (Figure 12B and C), confirming previous observations[119–121].

Rv3351c is detected in the outer membrane and recognized by the host immune response in human TB patients, and ΔRv3351c *bacilli are less virulent in the mouse aerosol-infection model.*

Due to its role in the generation of epithelial cell lipid rafts, it is likely that Rv3351c localizes to the cell surface and/or extracellularly secreted by *M. tuberculosis*. Previous studies have shown mycobacterial surface protein HBHA interacts with alveolar epithelial cells induces humoral immune responses in humans and elicits a protective immune response in mice[230,231]. Our results also show that the Rv3351c protein is detected in the membrane of *M. tuberculosis* Erdman bacilli (Supplemental Figure 3) allowing it to be more easily recognized by the immune system during infection. To test whether Rv3351c is antigenic, we screened human sera from patients with culture-confirmed active and latent TB by ELISA. Latent TB infection (LTBI) is defined as a state

of persistent immune response to stimulation by *M. tuberculosis* antigens without evidence of clinically-manifested active TB[232]. Patients with LTBI had negative bacteriological tests and the presumptive diagnosis is based on a positive result of a tuberculin skin test or blood (interferon-gamma release assay, IGRA) test indicating an immune response to *M. tuberculosis* infection[232]. Our assessment demonstrated that human sera from patients with active, but not latent TB, produce antibodies against the Rv3351c protein (Figure 13). Lastly, we observed that BALB/c mice intratracheally-infected with the ΔRv3351*c* bacilli have fewer replicating bacilli in lungs and fewer bacilli disseminated to the spleens and livers by 21 days post-infection compared to control infections with the complemented mutant, CM ΔRv3351c (Supplemental Figure 4). Infection with either the mutant or complemented strain generated similar immune cell infiltration by the 3-week post-infection time point (Supplemental figure 5). SCID mice aerosol infected with these strains showed similar death rates (Supplemental figure 6) indicating basic *M. tuberculosis* virulence was maintained in ΔRv3351c in this immunocompromised mouse strain.

Due to its role in the generation of epithelial cell lipid rafts, it is likely that Rv3351c is expressed on the cell surface and/or extracellularly secreted by *M. tuberculosis*. Previous studies have shown another mycobacterial surface protein, HBHA that interacts with alveolar epithelial cells is able to induce humoral immune responses in humans, and is able to elicit a protective immune response in mice[230,231]. Our results also show that the Rv3351c protein is expressed in the membrane of *M. tuberculosis* Erdman bacilli (Supplemental Figure 3) allowing it to be more easily recognized by the immune system during infection. To test whether Rv3351c is antigenic, we screened human sera from patients with culture-confirmed active and latent TB by ELISA. Latent TB infection is defined as a state of persistent immune response to stimulation by *M. tuberculosis* antigens without evidence of clinically manifested active TB[232]. Patients with

presumptive LTBI had negative bacteriological tests and either a positive tuberculin skin test, or blood (interferon-gamma release assay, IGRA) test indicating an immune response to *M. tuberculosis* infection[232]. Our assessment demonstrated that human sera from patients with active but not latent TB, produce antibodies against the Rv3351c protein (Figure 13). Lastly, we show that BALB/c mice intratracheally-infected with the ΔRv3351*c* bacilli have fewer replicating bacilli in lungs and fewer bacilli disseminated to the spleens and livers by 21 days post infection compared to control infections with the complemented strain, CM ΔRv3351c (Supplemental Figure 4). Infection with either the mutant or complemented strain generates similar immune cell infiltration by the 3-week post-infection time point (Supplemental figure 5), and SCID mice aerosol infected with these strains show similar death rates (Supplemental figure 6) indicating basic *M. tuberculosis* virulence is maintained in ΔRv3351c in this immunocompromised mouse strain

Effects of Rv3351c on the ability of M. tuberculosis to infect A549 cells.

To test a possible protective effect of the Rv3351c protein, we incubated A549 cells with 5 μg of Rv3351c for 30 minutes prior to infection. After 30 minutes, cells were washed and infections proceeded as previously described. Pre-incubating A549 cells with Rv3351c recombinant protein increased the survival of A549 cells infected with the Erdman or the CMΔRv3351c strain (Figure 5B). Preincubating with another recombinant mycobacterial protein, Rv0097 which is of similar molecular weight and is also proposed to be surface expressed[233], did not generate the same protective effect (Supplemental Figure 7). CFU analysis revealed that fewer bacteria of the Erdman or CMΔRv3351c strain were internalized into A549 cells at internalization time point 0 as defined in the methods. (Figure 14). These results indicate that Rv3351c may be a protective antigen.

Discussion

To better characterize the role of type II pneumocytes in TB, particularly during early infection, detailed studies of the interaction between the bacilli and alveolar pneumocyte at the cellular level are needed. In the experiments described herein, a process of bacterial attachment, internalization and trafficking through type II pneumocytes has been established, including measurements of bacterial and host cell viability. A deletion mutant of *M. tuberculosis* Erdman lacking *Rv3351c* was previously found to target alveolar epithelial cells, as well as macrophages[30]. In the present study, the attachment, internalization and trafficking within alveolar epithelial cells by ΔRv3351c bacilli were compared to those of its parental strain.

We previously demonstrated microscopically that viable *M. tuberculosis* Erdman bacilli induce lipid raft formation on infected A549 cells to similar or greater levels than lipid raft super aggregator LLO[31]. Additionally, we showed that culture filtrates from infected A549 cells also induce lipid rafts when added to fresh monolayers indicating the responsible factor is mycobacterial and likely secreted during or prior to infection[31]. In this current study, we demonstrate that infection with ΔRv3351c cells did not generate lipid rafts as efficiently as the parental strain, and the recombinant Rv3351c protein can alone induce similar levels of lipid raft formation rates on A549 cell plasma membranes compared to the LLO-positive control (Figure 4). Interestingly, the difference in lipid raft formation between A549 cells infected with the wild-type and ΔRv3351c bacilli did not appear at the gross level to affect the method or rate of bacterial attachment and internalization but did alter the intracellular trafficking pattern between the two strains. Thus, the overall studies described herein provide for a more thorough understanding of the role of Rv3351c in the process of *M. tuberculosis* attachment, internalization and trafficking within type II pneumocytes. However, these data also contribute to the body of knowledge

indicating a larger role for alveolar pneumocytes as they may not simply provide a barrier to infection, but may also contribute to the pathology associated with TB[234–236] . What was surprising is the apparent role Rv3351c protein plays in modifying the host cell membrane to induce lipid raft formation that may be responsible for the optimal trafficking pattern not observed with the mutant strain; potentially causing the ΔRv3351c mutant to attach to and enter the pneumocyte and traffic through a sub-optimal pathway.

The process of attachment and internalization is readily observed with both *M. tuberculosis* Erdman and ΔRv3351c bacilli between 6 and 24 hpi. Other studies have shown mycobacterial internalization in these cells occurring as early as 2 hpi[128,237]. Thus, our results are comparable, although different *M. tuberculosis* strains and different methods of quantification make direct comparisons difficult. There has been some degree of discussion regarding the actual mechanism of internalization in type II pneumocytes. Some studies suggest a membrane ruffling process may occur[225]. In this study, microscopic examination did not reveal evidence of ruffling, but did support previous observations of actin-pseudopod engulfment[225]. Furthermore, addition of the actin-depolymerizing agent, cytochalasin D, resulted in a significant reduction of internalized bacteria for the mutant and wild-type strains at 24 hpi (Figure 6). This suggests that *M. tuberculosis* Erdman and ΔRv3351*c* bacilli internalize using the same actin-mediated mechanism.

We previously demonstrated microscopically that viable *M. tuberculosis* Erdman bacilli induce lipid raft formation on infected A549 cells to similar or greater levels than lipid raft super aggregator LLO[31]. Additionally, we showed that culture filtrates from infected A549 cells also induce lipid rafts when added to fresh monolayers indicating the responsible factor is mycobacterial and likely secreted during or prior to infection[31]. In this current study, we demonstrate that infection with ΔRv3351c cells did not as efficiently generate lipid rafts

compared to the parent strain, and the *E. coli* recombinant Rv3351c protein can alone induce similar levels of lipid raft formation rates on A549 cell plasma membranes compared to the LLO positive control (Figure 4). Interestingly, the difference in lipid raft formation between A549 cells infected with the wild type and ΔRv3351c bacilli did not appear at the gross level to affect the method or rate of bacterial attachment and internalization, but did alter the intracellular trafficking pattern between the two strains. Thus, the overall studies described here provide for a more thorough understanding of the role Rv3351c in the process of *M. tuberculosis* attachment, internalization and trafficking within type II pneumocytes. However, these data also contribute to the body of knowledge indicating a larger role for alveolar pneumocytes; they may not simply provide a barrier to infection, but may also contribute to the pathology associated with TB[234–236] . What was surprising is the apparent role this protein plays in modifying the host cell membrane to induce lipid raft formation that may be responsible for the optimal trafficking pattern not observed with the mutant strain; potentially causing the mutant bacteria to attach to and enter the pneumocyte and traffic through a sub-optimal pathway.

The process of attachment and internalization is readily observed with both *M. tuberculosis* Erdman and ΔRv3351c bacilli between 6 and 24 hpi. Other studies have shown mycobacterial internalization in these cells occurring as early as 2 hpi[128,237]. Thus, our results are comparable, although different *M. tuberculosis* strains and different methods of quantification make direct comparisons difficult. There has been some degree of discussion regarding the actual mechanism of internalization in type II pneumocytes. Some studies suggest a membrane ruffling process may occur[225]. In this study, microscopic examination did not reveal evidence of ruffling but did support previous observations of actin-pseudopod engulfment[225]. Furthermore, addition of the actin-depolymerizing agent, cytochalasin D, resulted in a significant reduction of

internalized bacteria for the mutant and wild-type strains at 24 hpi (Figure 6). This suggests that *M. tuberculosis* Erdman and ΔRv3351*c* bacilli internalize using the same actin-mediated mechanism.

Although internalization was reduced by the addition of cytochalasin D, adherence of mycobacteria to treated host cells was not significantly different from the infected, untreated host cells. Other microscopic experiments conducted in our laboratory using a PI3K inhibitor, which also interferes with actin polymerization, reveal an alternate mechanism of attachment to A549 cells (unpublished data). These data suggest that *M. tuberculosis* bacilli can attach to alveolar epithelial cells through multiple mechanisms, with actin-pseudopod engulfment being the preferred and perhaps more efficient means of intimate cellular association/internalization. The timeline for the process of attachment and internalization in human macrophages has been reported to occur within one hour[157]. The longer time period required for bacterial internalization in the pneumocyte compared to the macrophage is not unexpected given that epithelial cells are not phagocytic by nature and thus an alternative, potentially slower, means of internalization likely exists. The precise nature of the attachment and internalization mechanism is currently being investigated.

Although similar rates of attachment and internalization by Erdman and ΔRv3351c bacilli were initially observed, analysis of the trafficking pathway demonstrated that the mutant bacilli are more often associated with endosomes possessing lysosomal markers LAMP-2 and cathepsin-L compared to the parent strain at 12 and 72 hpi (Figure 8). Similarly, inhibiting lysosome fusion restores the mutant phenotype to wild type levels. Thus, the mutant bacilli may be exposed to higher levels of degradative lysosomal enzymes that are inhibitory or ultimately lethal, helping to explain the decrease in intracellular mutant bacterial numbers observed over

time. The *Rv3351c* gene product might facilitate efficient trafficking by providing exposure to the appropriate host cell ligand associated with lipid rafts. Early association of mutant bacteria with LC3, and their ultimate delivery to the lysosome could suggest a mechanism similar to LC3-associated phagocytosis (LAP), in which LC3 and other autophagy proteins target single membrane bacterial containing compartments to the lysosome for degradation[238]. *M.*[238]. *Mycobacterium tuberculosis* and the related fish pathogen *M. marinum* are both targeted by LAP in macrophages, and mutants of *M. tuberculosis* bacilli lacking *cpsA* are degraded by LAP, while wild type is able to subvert this process[195,196]. *Legionella dumoffii, Shigella flexneri*, and *Yersinia pseudotuberculosis* are all targeted by LAP in non-phagocytic cells[190]. ULK1 is a protein specific to the autophagy pathway[191], and is not essential in the LAP pathway. The inability of ΔRv3351c to induce ULK1 above uninfected cell levels supports the hypothesis that ΔRv3351c is trafficked through this pathway (Figure 11D). While we have previously shown that *M. tuberculosis* Erdman bacteria are contained in double-membrane compartments, further investigation into the structure of ΔRv3351c-containing compartments needs to be completed, as well as examining bacterial association with other markers specific to either LAP or canonical autophagy.

Studies with other bacteria have shown that lipid raft induction may be a means to manipulate the host immune response[168]. In our study, we observed that cells infected with *M. tuberculosis* Erdman did not produce the cytokine TNF-α to the same levels as those infected with ΔRv3351c (Figure 12), suggesting induction of lipid rafts might provide an additional mechanism by which *M. tuberculosis* modulates the host immune response.

HBHA was the first pneumocyte-targeting *M. tuberculosis* protein to be identified and shown to be involved in mycobacterial attachment and intracellular trafficking. However, due to its surface localization and likely constitutive expression, this protein also was shown to induce

immune responses in the human host and subsequently to be an effective mucosal vaccine target[231]. HBHA-deficient mutant strains of *M. tuberculosis* also replicate to lower numbers in the lungs of aerosol-infected mice compared with a wild-type strain and disseminate from the lungs less efficiently[218]. Similarly, in this study, we showed that in addition to its role in pneumocyte internalization and trafficking, bacterial surface-localized Rv3351c induces a humoral response in human TB patients (Figure 13), protects A549 cells from *M. tuberculosis* Erdman infection, and the ΔRv3351c mutant strain replicates to lower numbers in the lungs of mice and disseminates less effectively. These data infer that HBHA and Rv3351c perform similar extracellular functions and thus are similarly exposed to the host immune response during infection. With HBHA, our studies of Rv3351c support a hypothesis that *M. tuberculosis* has a mechanism to target the alveolar epithelium, enhancing the importance of these cells in the disease process. Elucidation of this process continues to be explored *in vitro* and *in vivo*.

Experimental procedures

Bacterial strains

M. tuberculosis strain Erdman was obtained from the Tuberculosis/Mycobacteriology Branch of the Centers for Disease Control and Prevention. The *M. tuberculosis* strains were grown in Middlebrook 7H9 broth supplemented with 0.5% glycerol, 0.05% Tween 80, 0.5% bovine serum albumin (fraction V, Boehringer-Mannheim), and 0.085% NaCl. Strain ΔRv3351c was developed from strain Erdman using the method of Bardarov *et al.* (2002) and is described in Pavlicek *et al.*, 2015. The ΔRv3351c -complementing strain (CMΔRv3351c) was constructed by amplifying the *Rv3351c* gene plus 366 bp of upstream and 14 bp of downstream DNA with primers 5'-GTG AAG CTT ATA CTG GTG AAG GTT TGCGC-3' and 5'-GGA ATT CTT CGA CTG CTG GCG GAG-3' and inserting the amplicon into the integrative plasmid

pMV306[239]. This plasmid was then electroporated into strain ΔRv3351c and transformants were selected for by inclusion of kanamycin (25 μg/ml) in the medium.[239]. This plasmid was then electroporated into strain ΔRv3351c and selected for with kanamycin (25 μg/ml). For confocal microscopy, *M. tuberculosis* strains Erdman and ΔRv3351c were transformed with replicating plasmid pFJS8gfpmut2 expressing green fluorescent protein[240] or replicating plasmid pGCRed2 expressing DsRed2, and maintained by inclusion of 50 μg/ml kanamycin or 50 μg/ml hygromycin, respectively. Plasmid pGCRed2 was a generous gift from Dr. Mary Hondalus, Department of Infectious Diseases, University of Georgia. Bacterial plating studies utilized Middlebrook 7H11 agar supplemented with 0.5% glycerol, 0.05% Tween 80 and 1 x ADS[241].

Epithelial cell infection

A549 human type II alveolar epithelial cells were obtained from ATCC (CCL-185) and maintained in DMEM supplemented with 5% FBS at 37°C, in 5% CO_2 and 95% air. Twenty-four hours prior to infection, A549 cells were seeded into 6-well Costar® dishes at 1.0 x 10^6 cells per well. On the day of infection, epithelial cell monolayers were first prepared for a cold-synchronized infection by incubating at 4°C for 1 hour. Cells were then infected at a MOI of 100 (100 bacteria per host cell) with *M. tuberculosis* strains. To disperse the inoculant, bacteria were passed through an insulin syringe directly into the appropriate wells. After an hour incubation at 4°C post infection, cells were incubated at 37°C, 5% CO_2. This was considered time point 0. Infections were maintained for up to 96 hours with samples examined at the indicated times. For actin-depolymerization experiments, cytochalasin D [1 μM final] was added to cells 2 hours prior to cold-synchronization and infection at a MOI of 100 and maintained in culture medium throughout the experiment.

Intracellular bacterial viability studies

Epithelial cell monolayers infected at a MOI of 100 with *M. tuberculosis* strains Erdman, ΔRv3351c, or CM ΔRv3351c, were incubated for 6 hours before being washed 3 times with PBS and incubated for 2 hours in DMEM with 5% FBS and 200 μg/ml amikacin (added to inhibit the growth of remaining extracellular bacteria). The medium was then replaced with fresh DMEM. This was defined as time point 0. At 24 and 72 hpi, monolayers were washed and cells lysed with 0.1% Triton X-100. Viable bacilli were enumerated by serial dilution of each lysate in 1 x PBS/ 0.05% Tween 80 and plating on 7H11 agar. All infection assays were performed in triplicate.

Lactate dehydrogenase (LDH) assay

For lactate dehydrogenase (LDH) release studies, A549 cells were seeded into 6-well Costar® dishes at 1.0 x 10^6 cells per well 24 hours prior to infection. On the day of infection, monolayers were washed 3 times with Hanks Balanced Salt Solution (HBSS) and fresh medium was added. Cells were infected in parallel with *M. tuberculosis* strains Erdman, ΔRv3351c and CM ΔRv3351c at a MOI of 100. All infections were performed in triplicate. For studies testing Rv3351c recombinant protein and Filipin III, 5 μg of Rv3351c and Filipin III were added to appropriate wells 30 minutes before infection using the methods of Fine-Coulson et al. (2012)[31]. After 30 minutes, cells were washed and Filipin III-treated cells were maintained in 2.5 μg /mL of the chemical[31]. After 30 minutes, cells were washed and Filipin III cells were maintained in 2.5 μg /mL for the duration of the experiment. Filipin III was obtained from Sigma (Sigma-Aldrich, St. Louis, MO) and reconstituted with DMSO. For Bafilomycin A1 treatment, Bafilomycin A1 (Sigma-Aldrich, St. Louis, MO) was added to 100 nm to appropriate wells for the entirety of the experiment. Host cells treated with Filipin and Bafilomycin A1 were evaluated for cytotoxic effects by LDH release assay. Supernatants were sampled over a time

course and filtered through PVDF membranes (0.22 μm). Immediately following filtration, supernatants were assayed for LDH activity using the Cytotoxicity Detection Kit (Roche, Indianapolis, IN)[30,124]. Percent LDH release was calculated using the following formula: [(Release from Strain - Background)/(Max release – Background)] x 100.

Confocal and immunofluorescent microscopy

For confocal microscopy, A549 cells were grown as monolayers to confluency, harvested with trypsin-treatment for 3 minutes at 37°C, and 5 x 10^5 cells were seeded onto sterile cover slips placed within 6-well Costar® dishes. The cells were allowed to adhere for 12 hours at 37°C in 5% CO_2 and then infected as described. Specimens were fixed at indicated time points with either 2% or 3.7% paraformaldehyde for 1 hour. The specimens were washed 3 times with 1 x PBS and the cells permeabilized for 10 minutes with 0.1% Triton X-100. The samples were then blocked for 30 minutes with PBS containing 3% BSA. For attachment studies, cells were blocked and then labeled with Alexa Fluor®488 or 546 phalloidin (Invitrogen, Carlsbad, CA) for 35 minutes at room temperature. For lysosomal studies, LAMP-2 monoclonal antibody (Abcam Inc., Cambridge, MA) was added to each coverslip at a dilution of 1:200 and incubated at room temperature for 1 hour. After washing with PBS, mouse-anti-human antibody conjugated with Texas Red was then added at a dilution of 1:500 and incubated for 1 hour at room temperature. Cytoskeletal staining was achieved by 35-minute incubation with Alexa Fluor®647 phalloidin (Invitrogen). Images were obtained with a Zeiss LSM 510 or Leica SP5 confocal microscope.

For LC3 studies, LC3b rabbit polyclonal antibody (Abcam Inc., Cambridge, MA) was added to each coverslip at a dilution of 1:200 and incubated at room temperature for 1 hour. After washing with PBS, goat-anti-rabbit antibody conjugated with Alexa Fluor®633

(Invitrogen, Carlsbad, CA) was then added at a dilution of 1:500 and incubated for 30 minutes at room temperature.

For GM1 studies, 2 μg listeriolysin O (LLO) (Abcam Inc., Cambridge, MA), Rv3351c, or Rv0097 recombinant protein were added to appropriate wells for 30 minutes at room temperature before staining. Cholera toxin subunit B conjugated to Alexa Fluor 488 (Invitrogen, Carlsbad, CA) was added at a dilution of 1:250 to all coverslips 30 minutes prior to fixation with 4% paraformaldehyde. All staining steps were carried out at 4°C. A total of 10 fields were imaged per coverslip for each experiment, incorporating approximately 50–100 host cells per field. Images were captured at 63x magnification. Two coverslips were obtained for all conditions at the designated timepoint for all three experimental replicates. Aggregates of cholera toxin and LC3 puncta were quantified and analyzed for size and area using ImageJ. Numbers of aggregates were normalized to the number of host cells imaged per field to acquire an average number of aggregates per host cell/per field for each condition

Total cell protein extraction

At 12 and 24 hours post-infection, cell lysates were harvested with Pierce™ IP Lysis Buffer (Pierce Biotechnology, Rockford, IL), according to the manufacturer's instructions. For amino acid starvation conditions, cell monolayers were washed 3 times with Earle's Balanced Salts Solution (EBSS), and 2 mL of fresh EBSS was added for 4 hours. To inhibit autophagic flux, 100 nm Bafilomycin A1 was added 2 hours before each time point. Supernatants were filtered through 22 μmμM PVDF membranes before being removed from the biosafety level 3 lab. Total protein concentration was determined by BCA protein quantification. (ThermoFisher Scientific, CA). Protein samples were mixed with sodium dodecyl sulfate buffer (1× final concentration) and heated at 90°C for 10 minutes. Proteins were separated by electrophoresis on

a 12% sodium dodecyl sulfate polyacrylamide gel. Total protein was transferred to a PVDF membrane (Bio-Rad, Hercules, CA), which was then preincubated with blocking solution (5% nonfat dry milk in Tris-buffered saline containing 0.01% Tween 20; pH, 7.4) for 1 hour, followed by overnight incubation with anti-LC3B or anti-ULK1 rabbit monoclonal antibodies (1:1000), or anti-GAPDH mouse monoclonal antibody (1:1000), (Cell Signaling Technology, Inc, Danvers, Massachusetts) at 4°C. After primary incubation, the membrane was washed 3 times with Tris-buffered saline containing 0.01% Tween 20 and incubated for 1 hour with secondary rabbit (Cell Signaling Technology, Inc, Danvers, Massachusetts) or goat anti-mouse HRP-conjugated antibody (Abcam Inc., Cambridge, MA). All incubations and wash steps were performed at room temperature except when otherwise stated. Cross-reactivity was visualized by using enhanced chemiluminescence (SuperSignalWestPico; Pierce Biotechnology, Rockford, IL).

Transmission electron microscopy (TEM)

For transmission electron microscopy (TEM), cells were harvested and seeded into T25 flasks at a density of 5.0 x 10_6 cells/ml. The cell cultures were synchronized by incubation at 4°C for 2 hours: 1 hour preceding infection and 1 hpi. Infections were conducted as previously described. Specimens were fixed with 2.5% glutaraldehyde for 1 hour and then placed in phosphate buffer prior to treatment with 1% osmium tetroxide for 45 minutes and a phosphate buffer wash. An ethanol series was used to dehydrate the specimens that were then infiltrated using propylene oxide. Thorough infiltration was completed with three ratios of propylene oxide: resin (Epon-araldite). Resin recipes were based on previous protocols by Mollenhauer[242]. Specimens were incubated 1 hour in resin followed by an exchange and overnight incubation at room temperature. After an additional resin exchange, samples were embedded and polymerized

overnight at 60°C. Ultrathin sections were mounted onto copper grids and stained with 4% uranyl acetate and lead citrate. Imaging was performed using a Tecnai BioTwin (FEI Company, Hillsboro, OR) electron microscope operating at 80 or 120 kV. Digital images were captured using a 2K x 2K camera (AMT, Danvers, MA). Images were edited using Microsoft® Picture Manager and Adobe® Photoshop 7.0.

Immuno-electron microscopy (IEM)

For immuno-electron microscopy (IEM), cells were harvested and seeded into T25 flasks at a density of 5.0 x 10_6 cells/ml. The cell cultures were synchronized by incubation at 4°C for 2 hours; 1 hour preceding infection and 1 hpi with *M. tuberculosis* strains at a MOI = 100. At the indicated time points, cells were fixed with a 1.5% paraformaldehyde/0.025% glutaraldehyde solution for 1 hour, and then placed in phosphate buffer. The fixed specimens were then dehydrated using a graded ethanol series. Cells were incubated in increasing ratios of ethanol: LR White embedding media as outlined by Goldsmith *et al.*[243]. Samples were then allowed to incubate 1 hour in 100% LR White followed by a fresh exchange and overnight incubation at 4°C. The following day, specimens were incubated in fresh LR White for 1 hour, placed in gelatin capsules, centrifuged (1,500 x g, 5 minutes) and the blocks allowed to polymerize for 20-24 hours at 58°C. Ultrathin sections were mounted onto nickel grids and blocked with normal goat serum diluted 1:100. Each grid was incubated with a 1:500 dilution of cathepsin-L (Abcam Inc., Cambridge, MA) or LAMP-2 (Invitrogen, Carlsbad, CA) antibody for 75 minutes. Gold-conjugated secondary labels: 12-nm goat-anti-rabbit or 20-nm goat-anti-mouse IgG (Jackson ImmunoResearch), were used at a 1:20 dilution with 1 hour incubation. Samples were imaged using a Tecnai BioTwin (FEI Company, Hillsboro, OR) electron microscope operating at 80 or

120 kV. Digital images were captured using a 2K x 2K camera (AMT, Danvers, MA). Images were edited using Microsoft® Picture Manager and Adobe® Photoshop 7.0.

Intracellular quantification

Total bacteria from TEM experiments were counted within at least 20 grid fields containing 10-15 infected pneumocytes per field. The number of bacteria inside the cells was divided by the total number of bacteria within the defined grid fields to determine the percent internalization. Infections were performed in duplicate and experiments repeated three times. For confocal attachment/internalization studies, z-stack images were obtained for each field of view and external/internal bacteria quantified by slice. Infections were performed in duplicate and experiments repeated three times. For each coverslip, 10 fields of view were captured and quantified (~250 host cells counted per coverslip).

M. tuberculosis membrane fraction analysis

Cultures of *M. tuberculosis* Erdman or ΔRv3351c were grown to an OD_{600} of 0.8. Cultures were centrifuged at 2,000 x g for 10 minutes to pellet bacteria, and pellet and supernatant fractions stored at -80ºC until further processing. Pellets were thawed and washed with equal volumes of ice-cold PBS. Washed pellets were resuspended in PBS containing cOmplete EDTA- Free protease inhibitor (Roche, Indianapolis, IN), 2 mM EDTA, and 0.5 mM PMSF, and lysed by bead beating. Lysed samples were transferred to clean microcentrifuge tubes and centrifuged at 8,000 x g for 10 minutes at 4ºC. Supernatants were filtered through 22 μm PVDF membranes and pellets heat-killed before being removed from the biosafety level 3 lab. Total protein concentration was determined by BCA protein quantification. Protein samples were mixed with sodium dodecyl sulfate buffer (1× final concentration) and heated at 90°C for 10 minutes. Proteins were separated by electrophoresis on a 12% sodium dodecyl sulfate

polyacrylamide gel. Total protein was transferred to a nitrocellulose membrane (Bio-Rad, Hercules, CA), which was then preincubated with blocking solution (5% nonfat dry milk in Tris-buffered saline containing 0.01% Tween 20; pH, 7.4) for 1 hour, followed by overnight incubation with anti-Rv3351c mouse monoclonal antibody (1:100) (provided by the Centers for Disease Control by the methods of Goldstein et al.[244]), or recombinant anti-RNA polymerase beta antibody (Abcam Inc., Cambridge, MA) at 4°C. After primary incubation, the membrane was washed 3 times with Tris-buffered saline containing 0.01% Tween 20 and incubated for 1 hour with secondary mouse HRP-conjugated antibody (Abcam Inc., Cambridge, MA). All incubations and wash steps were performed at room temperature unless otherwise stated. Cross-reactivity was visualized by using enhanced chemiluminescence (SuperSignalWestPico; Pierce Biotechnology, Rockford, IL)

TNF-a, MCP-1, IL-8 ELISA

Supernatants of infected cells were assayed for cytokine levels by ELISA using the BD OptEIA™ kits for TNF-α, MCP-1, or IL-8 (BD Pharmingen, Franklin Lakes, NJ) according to manufacturers' protocols.

Subcloning, expression and purification of recombinant Rv3351c

Plasmid pET19b-Rv3351c (Supplemental Figure 8) or pET19b-Rv97 was generated by incorporating the *Rv3351c* or *Rv0097* genes into a pET-19b backbone. A 830-bp *Rv3351c* gene fragment was amplified by PCR using *M. tuberculosis* H37Rv genomic DNA (Supplemental Figure 9) with primers 5' - GGAATTC**CATATG**CTGGCGAGCTGCCCGG - 3'(**NdeI**, for) and 5' – GA**AGATCT**TCACCGTGGAGTACGACGAACCGGC - 3' (**BglII**, rev). A 869-bp *Rv0097* gene fragment was amplified by PCR using *M. tuberculosis* H37Rv genomic DNA with primers 5'-GGAATTC**CAT**ATGACGCTTAAG GTCAAAGGCGAGGG-3' (**NdeI**, for) and 5'-

GA**AGATCT**CATGCCGCGTATCCCGG-3' (**BglII**, rev) . Plasmid pET19b and the PCR products were prepared for ligation by digestion with *Nde*I and *Bgl*II, and subsequent dephosphorylation of the cut ends. The digested PCR products and the digested pET19b plasmids were ligated and used to transform *E. coli* Rosetta™ (DE3) competent cells. Plasmid DNA from transformants was digested with *Nde*I, to determine gene insertion. Plasmids yielding bands of 6501 or 6595 bp (784 bp greater than the size of the empty plasmid for *Rv3351*c or 878 bp above the size of the empty plasmid for *Rv0097*) were expected to have the *Rv3351c* or *Rv0097* on the plasmid. Plasmid constructs were confirmed by DNA sequencing using the T7 promotor and T7 terminator primers found to have *Rv3351c* or *Rv0097* inserted without mutations. *E. coli* Rosetta™ (DE3) transformed with pET19b-Rv3351c or pET19b-Rv97 was plated on LB solid medium containing carbenicillin (50 µgµg/ml) and chloramphenicol (34 µgµg/mL), and grown overnight at 37°C. An overnight culture (10 ml) of the resulting strain was used to inoculate 2 L of LB and grown at 37°C. When the OD_{600} reached 0.6, isopropyl- β -D-thiogalactopyranoside (IPTG) was added to a final concentration of 200 µM, and the cells were incubated for another 4 hours. Cells were then harvested by centrifugation at 6,000 X g for 15 minutes at 4°C (Beckman Coulter Centrifuge, Avanti J-25I), the supernatant was discarded, and the cell pellets were frozen at -80°C. To disrupt the cells containing pET19b-Rv3351c, cell pellets were suspended (5 mL/gram of biomass) at room temperature in B-PER Complete Bacterial Protein Extraction Reagent (Pierce Biotechnology, Rockford IL,) with 0.5 mM PMSF, and resuspended by pipetting until homogenous. Pellets were incubated for 1 hour with gentle rocking at room temperature. Lysates were centrifuged at 16,000 x g for 20 minutes at 4°C to separate soluble from the insoluble proteins. The pellets containing insoluble recombinant Rv3351c protein (inclusion bodies) were washed three times with 50 mM Tris–HCl, 10 mM

EDTA, 100 mM NaCl, and 0.5% Triton X-100 (pH 8.0). The pellet was resuspended in buffer (1 ml/50 ml starting culture) containing 8 M urea, 10 mM Tris–HCl, (pH 7.4), and solubilized for 4 hours with stirring at room temperature. The solubilized inclusion bodies were centrifuged at 15,200 x g for 40 minutes at 4°C, and the supernatants collected.

To disrupt cells containing pET19b-Rv97, cells were suspended in BugBuster® Protein Extraction Reagent (Sigma-Aldrich, St. Louis, MO After lysis, samples were centrifuged at 21,000 x g for 15 minutes and supernatants were collected for protein purification. Bacterial pellets were re-suspended in Buffer C_{245} without urea (1 M Tris HCl pH 7.9, 2 M KCl, 0.5 M EDTA, 50% glycerol, 30 mM $ZnSO_4$, 0.035% BME), with 0.5 mM PMSF. After lysis, samples were centrifuged at 21,000 x g for 15 minutes and supernatants were collected for protein purification.

Nickel–NTA chromatography was used to purify the recombinant 6His-tagged Rv3351c and Rv0097 proteins. The supernatants of solubilized inclusion bodies from 8 M urea described above was applied, to Ni2+-charged HiTrap columns pre-equilibrated with 8 M urea in 20 mM sodium phosphate buffer, pH 7.4. After sample loading, the column was washed with 8 M urea, pH 7.4. Recombinant proteins were eluted using a linear gradient of imidazole (10–500 mM) in 8 M urea, pH 7.4. All flow rates were 0.5 ml/min. Recombinant proteins were analyzed by 10% Tris–sodium dodecyl sulfate–polyacrylamide gel electrophoresis (Tris–SDS–PAGE), followed by Coomassie Brilliant Blue R250 staining. Refolding was achieved by sequential dialysis with 1L volumes of freshly-made 5 mM Tris (pH 7.4) containing 6, 4, 2, 1, 0.5, and 0.01 M urea, respectively, with 5 mM Tris (pH 7.4). With each concentration, the protein was dialyzed with 12 hour incubation at 4°C in each buffer.

Human clinical serum ELISA

Two or 4 ng of Rv3351c protein was immobilized on a microtiter plate (Nunc,ThermoFisher Scientific, CA) overnight at 4°C. The next day, the plate was washed 3x with phosphate-buffered saline (pH 7.4) containing 0.05% Tween 20 (PBS-Tween20) and blocked for 30 minutes with 5% bovine serum albumin diluted in PBS-Tween20. The plate was washed 3 times with PBS-Tween20 before incubation for 1 hour at room temperature with human sera diluted 1:20, 1:50. 1:100, 1:200 in PBS from patients determined to have culture-confirmed active or latent TB infection or from uninfected controls[232]. After washing, 30-minute incubation with goat anti-human HRP-conjugated secondary antibody (Invitrogen, Carlsbad, CA) was performed prior to incubation with 1-Step™ Ultra TMB-ELISA Substrate Solution (ThermoFisher Scientific, CA) for color development, which was measured spectrophotometrically at 405 nm.

Mouse aerosol infections

BALB/c and SCID mice were obtained from Charles River Laboratory. BALB/c mice were challenged with $1X10^5$ CFU *M. tuberculosis* Erdman or the CMΔRv3351c complemented strain in 0.025 ml PBS via the intratracheal route[203]. Four mice per group were sacrificed 24 hours post-challenge to confirm actual exposure dose in the lungs. All mice were monitored daily over the course of the 3-week study for malaise or other adverse reactions. After euthanasia, portions of tissues including lungs, livers, and spleens were harvested, fixed in 10% neutral-buffered formalin, and processed for histopathology. The histologic slides were scored by a pathologist blinded to the identity of the individual experimental samples[246]. In addition, portions of the collected tissues were placed in PBS with 0.05% Tween 80 and homogenized. The homogenates were serially-diluted and plated onto 7H10gtADC agar plates and incubated at 37° C for three weeks prior to colony count assessments.

SCID mice were challenged with 50–100 CFU of *M. tuberculosis* Erdman, the ΔRv3351c mutant strain or the CMΔRv3351c complemented strain using a Madison aerosol chamber[246]. Unvaccinated mice were sacrificed 24 hours post-challenge to confirm actual exposure dose to be 50 to 100 CFU in the lungs. All mice were monitored daily over the course of the 140-day study for weight loss, malaise or other adverse reactions. Mice were euthanized based on a quantitative assessment of disease endpoints. Euthanasia procedures were consistent with the recommendations of the Panel on Euthanasia of the AVMA.

Thin Layer Chromatography Overlay

Thin layer chromatography overlay technique was conducted as described in Meisen et al., 2011. Briefly, 5 μL of A549 lipid extracts or neutral glycosphingolipid, ganglioside, and lactosylceramide lipid standards were absorbed onto a silica gel-coated glass plate and allowed to migrate using a mobile phase solvent composed of chloroform, methanol and water ((120/70/17, v/v/v). The plate was allowed to air dry and then blocked for 30 minutes with PBS plus 0.5% BSA on ice. After blocking, 50 μg of recombinant Rv3351c protein and anti-6xHIS antibody conjugated to horse radish peroxidase (1:500; Abcam Inc., Cambridge, MA) were combined in PBS plus 0.05% BSA on ice. The combined protein/antibody was added to the plate for an hour. The plate was then washed 3 times for 5 minutes in 0.01% BSA/PBS and was incubated with DAB for detection of HRP. For the reference plate, lipid standards and A549 extracts were imaged with Orcinol.

Statistical analysis

Statistical significance was determined by ANOVA and Tukey's HSD post-hoc comparison using GraphPad Prism 8.0 (GraphPad Software, San Diego, CA, USA). Animal organ mycobacterial burden comparisons were made using Student's t test and the Mann-

Whitney U test within the program GraphPad Prism 5.0 (GraphPad Software, San Diego, CA, USA). Animal survival curves were analyzed using the Kaplan Meier estimator in GraphPad Prism 5.0.

Acknowledgements

This work was supported in part by research grants from the University of Georgia Faculty of Infectious Diseases/Southeastern Center for Emerging Biologic Threats (F.Q.), and the American Lung Association (R.K.).

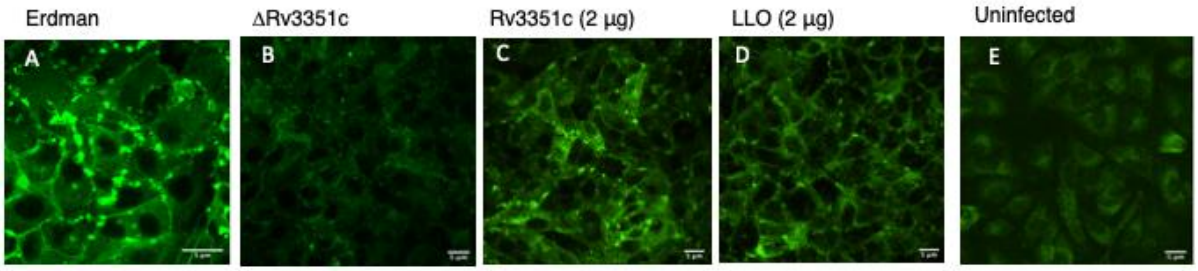

F

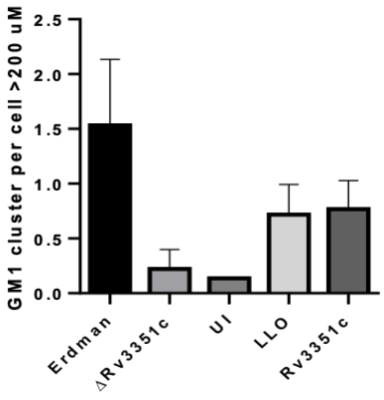

Figure 4. Confocal microscopy demonstrates differences in lipid raft numbers between *M. tuberculosis* Erdman and ΔRv3351*c* bacilli in A549 cells at 6 hours post infection. A549 human type II alveolar epithelial cells were infected at a MOI of 100 and specimens were prepared for confocal microscopy as described. At 6 hpi, confocal z-stack images show fewer GM1 staining (green) in ΔRv3351c infected cells (B) than in Erdman infected cells (A), while adding Rv3351c protein alone (C) induces lipid rafts comparable to LLO positive control levels (D). Uninfected cells showed limited GM1 staining (E). Lipid rafts were defined as GM1 clusters greater than 200 nM in size. (F) Data shown are means of 3 experiments performed in triplicate. (****p-values: <0.001, ***p-values: 0.001). Error bars represent one standard deviation.

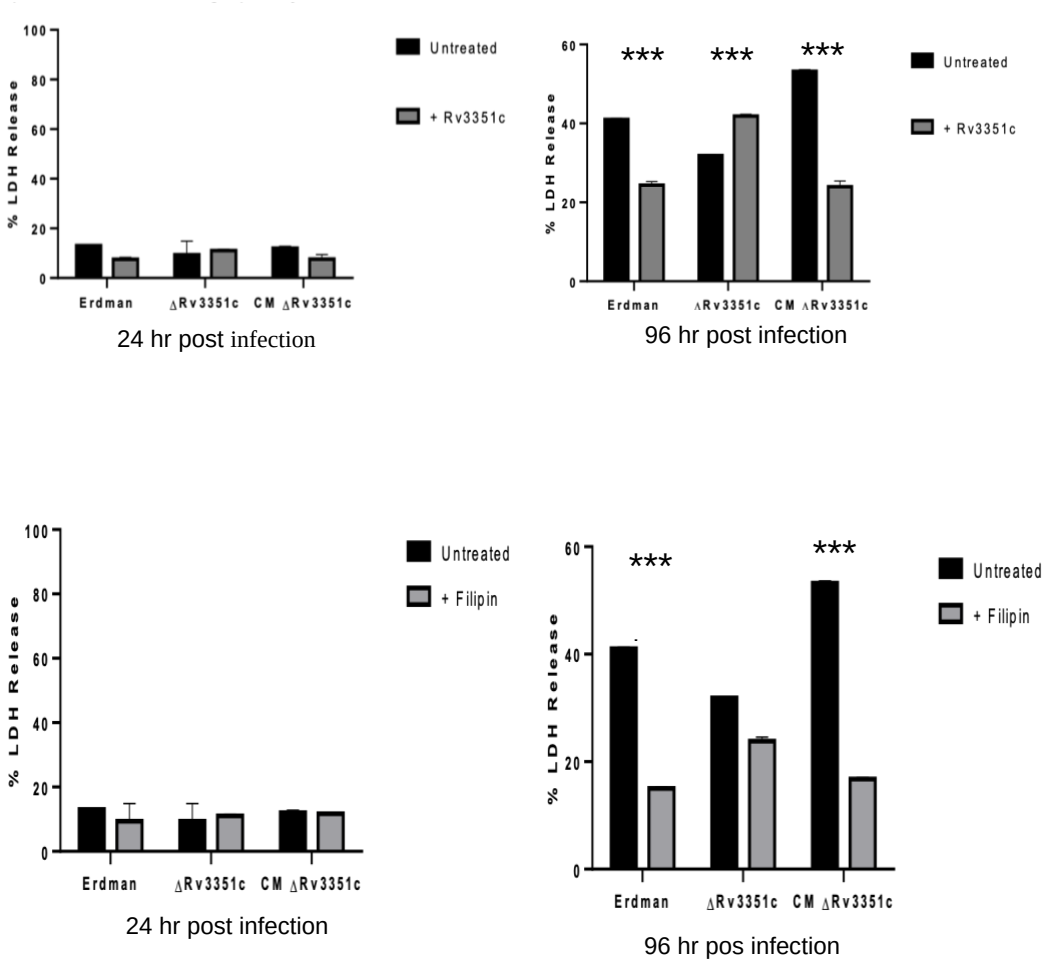

Figure 5. Pretreating cells with 5 μg of Rv3351c protein prior to infection bring mutant LDH levels equal to Erdman at 96 hours post-infection (B), while treatment with the cholesterol-binding agent Filipin III brings Erdman LDH levels down to mutant levels at the same time point (D). No differences were observed in any conditions at 24 hours post infection (A and C). Data shown are the means of 3 experiments performed in triplicate (****p-values: <0.001). Error bars represent one standard deviation.

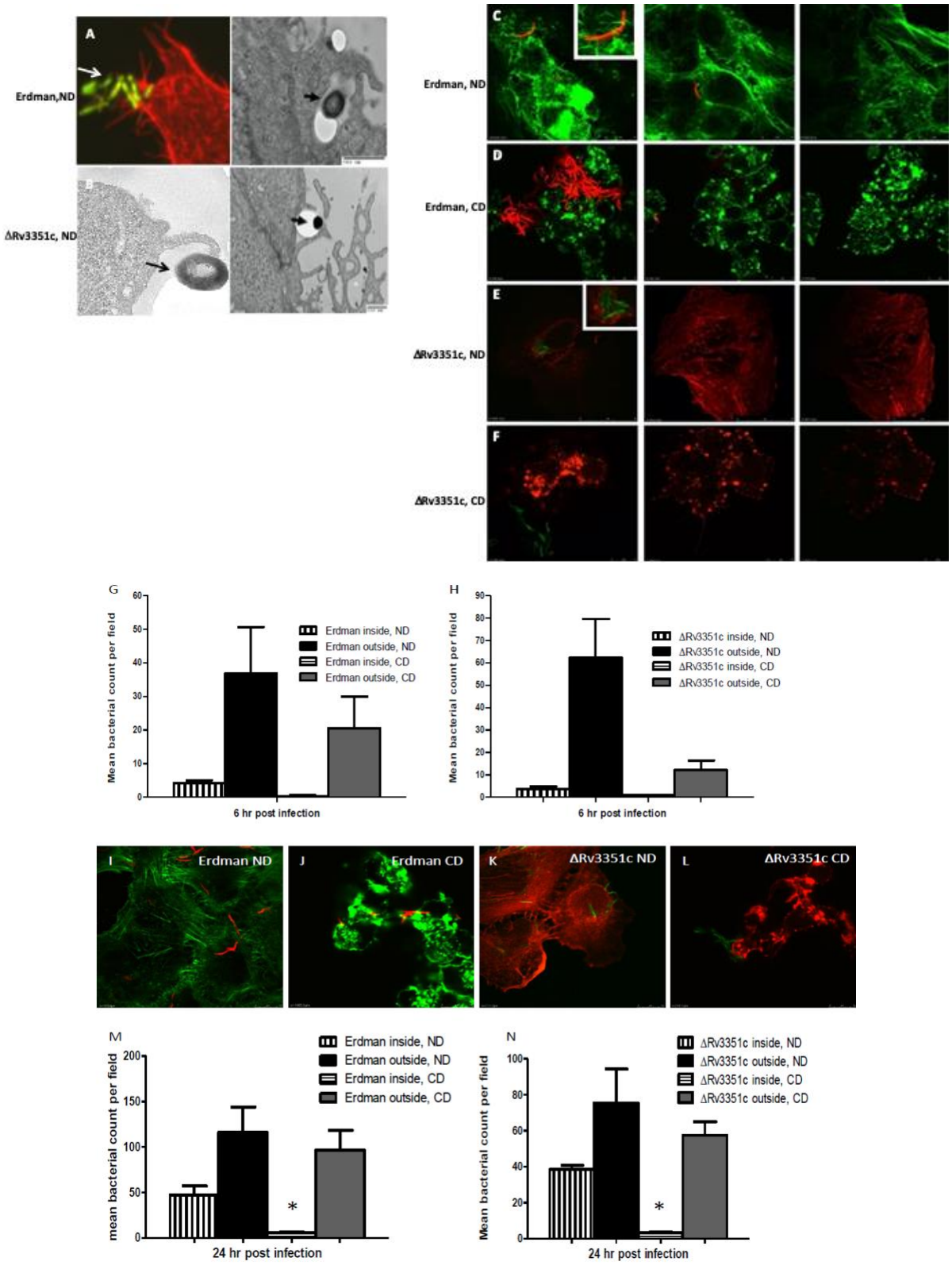
A
Erdman,ND
ΔRv3351c, ND
C
Erdman, ND
D
Erdman, CD
E
ΔRv3351c, ND
F
ΔRv3351c, CD
G
Mean bacterial count per field
Erdman inside, ND
Erdman outside, ND
Erdman inside, CD
Erdman outside, CD
6 hr post infection
H
Mean bacterial count per field
ΔRv3351c inside, ND
ΔRv3351c outside, ND
ΔRv3351c inside, CD
ΔRv3351c outside, CD
6 hr post infection
I
Erdman ND
J
Erdman CD
K
ΔRv3351c ND
L
ΔRv3351c CD
M
mean bacterial count per field
Erdman inside, ND
Erdman outside, ND
Erdman inside, CD
Erdman outside, CD
24 hr post infection
N
Mean bacterial count per field
ΔRv3351c inside, ND
ΔRv3351c outside, ND
ΔRv3351c inside, CD
ΔRv3351c outside, CD
24 hr post infection

Figure 6. *Mycobacterium tuberculosis* Erdman bacilli attach to A549 cells via actin-mediatedengulfment at 3, 6, 18 and 24 hours post infection. A549 human type II alveolar epithelial cells were infected at a MOI of 100 and specimens were prepared for confocal microscopy or TEM as described. At 6 hpi, (A) confocal z-stack images reveal phalloidin-stained red actin pseudopods wrapping around *M. tuberculosis* Erdman (green), and TEM images also showing *M. tuberculosis* Erdman bacilli interacting with host cell surface membrane projections, and (B) TEM are showing ΔRv3351c bacilli interacting with host cell surface membrane projections (arrows indicate bacilli; scale bar = 500 nm). For a comparative view with cytochalasin D-treated cells, confocal z-stack images reveal phalloidin-stained green (C) or red (E) actin pseudopods wrapping around *M. tuberculosis* Erdman (red) and ΔRv3351c (green) bacilli at the surface of the host cell (C, E). Images of A549 cells treated with cytochalasin D show similar attachment numbers for both bacterial strains in the absence of actin polymerization (D, F). Quantification from confocal studies shows no significant difference in numbers of bacteria adhering to or internalized by host cells at 6 hpi (G, H). At 24 hpi, mid sections from z-stack images of cytochalasin D treated cells show an absence of internalized *M. tuberculosis* Erdman (red) and ΔRv3351c (green) bacilli while untreated A549 cells have numerous internalized bacteria from both strains (I-L). Quantification of the images in panels I-L revealed significant differences in numbers of internalized bacteria from cytochalasin D treated A549 cells compared to untreated cells infected with either strain (G, H *p-values: <0.001 and M, N *p-values: 0.060). Error bars represent one standard deviation. (A) Image was captured at 100X magnification; all other confocal images were captured at 63x magnification with a 3x zoom. (ND, no drug added; CD, cytochalasin D added).

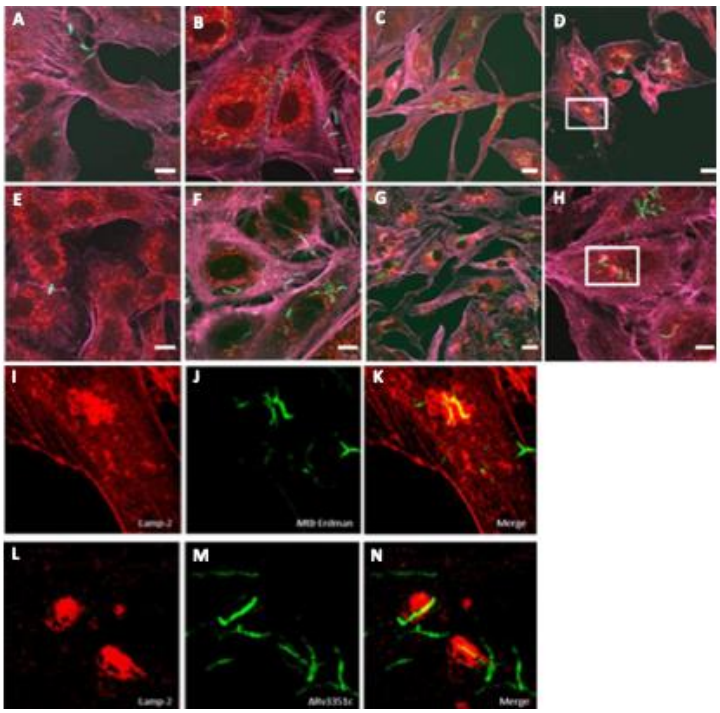

Figure 7. Confocal microscopy demonstrates intracellular differences between *M. tuberculosis* Erdman and ΔRv3351c bacilli in A549 cells at 24, 72 and 96 hours post infection. Infected A549 cells were prepared for confocal microscopy as described. Plasmid pFJS8gfp-mut2-transformed (green) strains *M. tuberculosis* Erdman (A through D) and ΔRv3351c (E through H) were examined following staining with LAMP-2 (red) for co-localization (yellow). Boxed regions in panels D and H identify the regions displayed in overlay series I-K (Erdman) and L-N (ΔRv3351c). (Scale bars, 10μm for panels A, B, D, E, F, H; 20 μm for panels C and G).

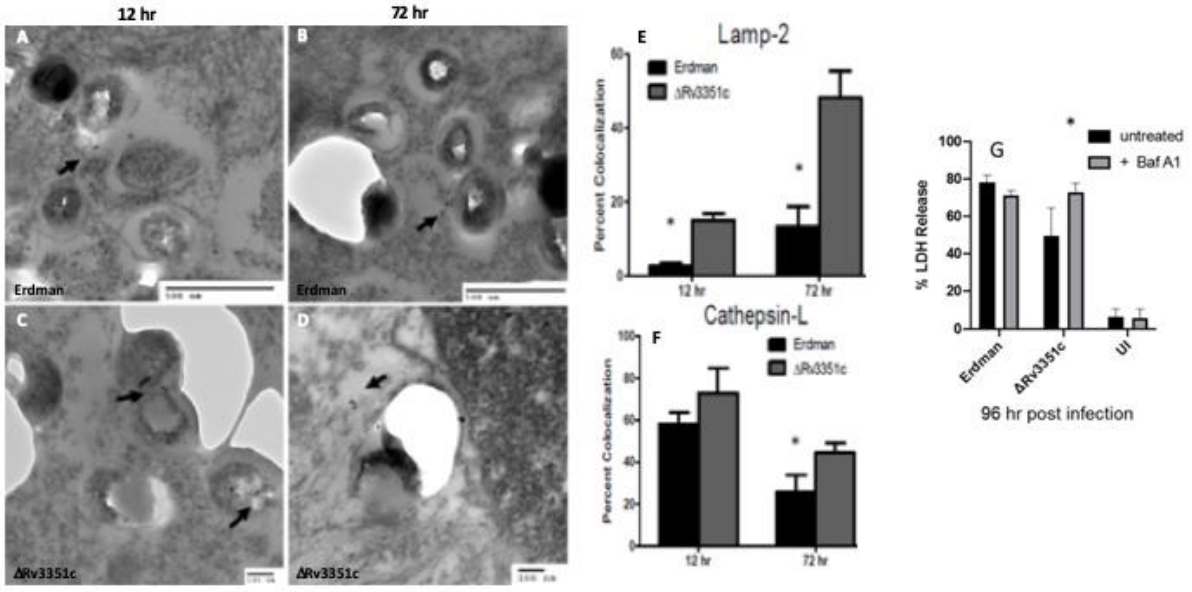

Figure 8. Immuno-electron microscopic quantification of LAMP-2 and cathepsin-L co-localization with *M. tuberculosis* Erdman or ΔRv3351c in A549 cells indicates the mutant is less efficient at preventing lysosomal delivery. Following infection with either *M. tuberculosis* strain Erdman or ΔRv3351c, specimens were prepared for IEM as described with cathepsin-L labeled with 12-nm gold particles (A-D). Bacilli are denoted by (*) and gold particles are identified with an arrow in each panel. Experiments were repeated with gold-labeling of LAMP-2 (data not shown). Co-localization of bacilli with either LAMP-2 or cathepsin-L was quantified (E, F, respectively). Significantly more LAMP-2 co-labeling with ΔRv3351c versus Erdman was observed at both 12 and 72 hpi (p-value 0.003 and <0.001, respectively). Co-localization of cathepsin-L with ΔRv3351c was also significantly greater at 72 hpi than with strain Erdman (p-value 0.012; scale bars = 500 nm for panels A and B or 100 nm for panels C and D). Inhibiting lysosomal acidification with bafilomycin A1 restored the ΔRv3351c LDH phenotype to wild type levels (G) (p-value <0.05). Error bars represent one standard deviation.

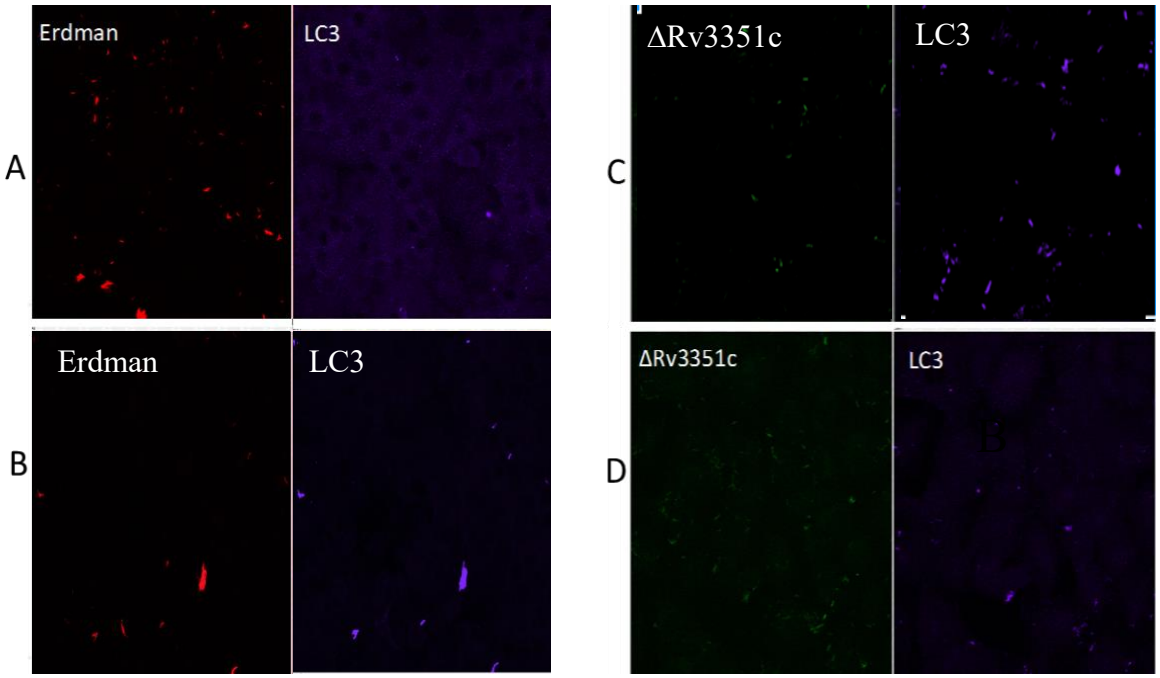
A
Erdman
LC3
B
Erdman
LC3
C
ΔRv3351c
LC3
D
ΔRv3351c
LC3

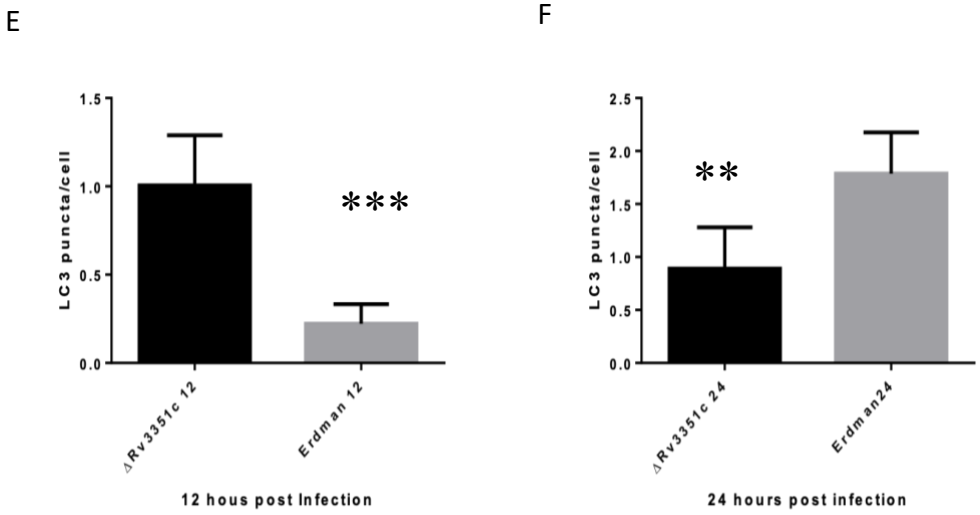
E
LC3 puncta/cell
1.5
1.0
0.5
0.0
***
ΔRv3351c 12
Erdman 12
12 hous post Infection
F
LC3 puncta/cell
2.5
2.0
1.5
1.0
0.5
0.0
**
ΔRv3351c 24
Erdman24
24 hours post infection

Figure 9. Confocal microscopy images demonstrate *M. tuberculosis* Erdman and ΔRv3351*c* bacilli induce autophagy marker LC3 in A549 cells. A549 cells were infected with strain Erdman or ΔRv3351c expressing dsRed or GFP, respectively for 12 (A and C) or 24 hours (B and D). LC3 immuno-labeling appears purple. DsRed-expressing *M. tuberculosis* bacilli appear red. GFP-expressing ΔRv3351c bacilli appear green. Punctate LC3 staining is observed in cells infected with strain Erdman (A and B) and ΔRv3351c (C and D). Puncta of LC3 were quantified at 12 hours and 24 hours post-infection (E and F, respectively). Images are representative of three experiments with similar results Data shown are the means of 3 experiments performed in triplicate ***p-values: ($p<0.005$), **p-values: ($p<0.05$). Error bars represent one standard deviation.

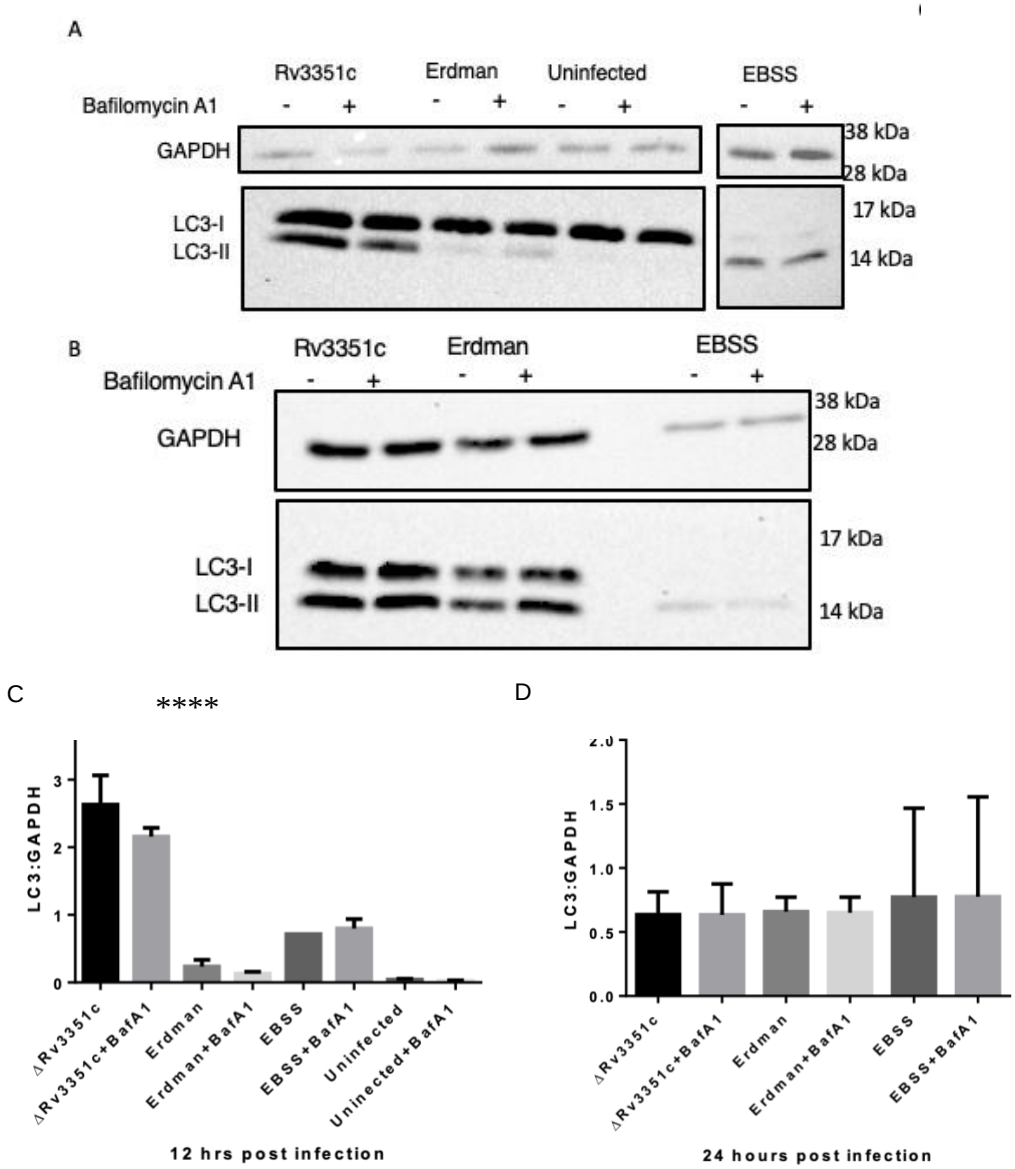

Figure 10. Western-blot analysis demonstrates LC3-II conversion. Cell lysates were obtained from infected A549 cells, uninfected cells, or cells under starvation (EBSS) conditions at 12 (A) and 24 hours (B) in the presence or absence of autophagy inhibitor Bafilomycin A1 (100 nM) as described under materials and methods. LC3 to GAPDH loading control ratios were quantified (C and D). Blots are representative of two experiments with similar results. Data shown are the means of two experiments ****p-values: ($p<0.0001$). Error bars represent one standard deviation.

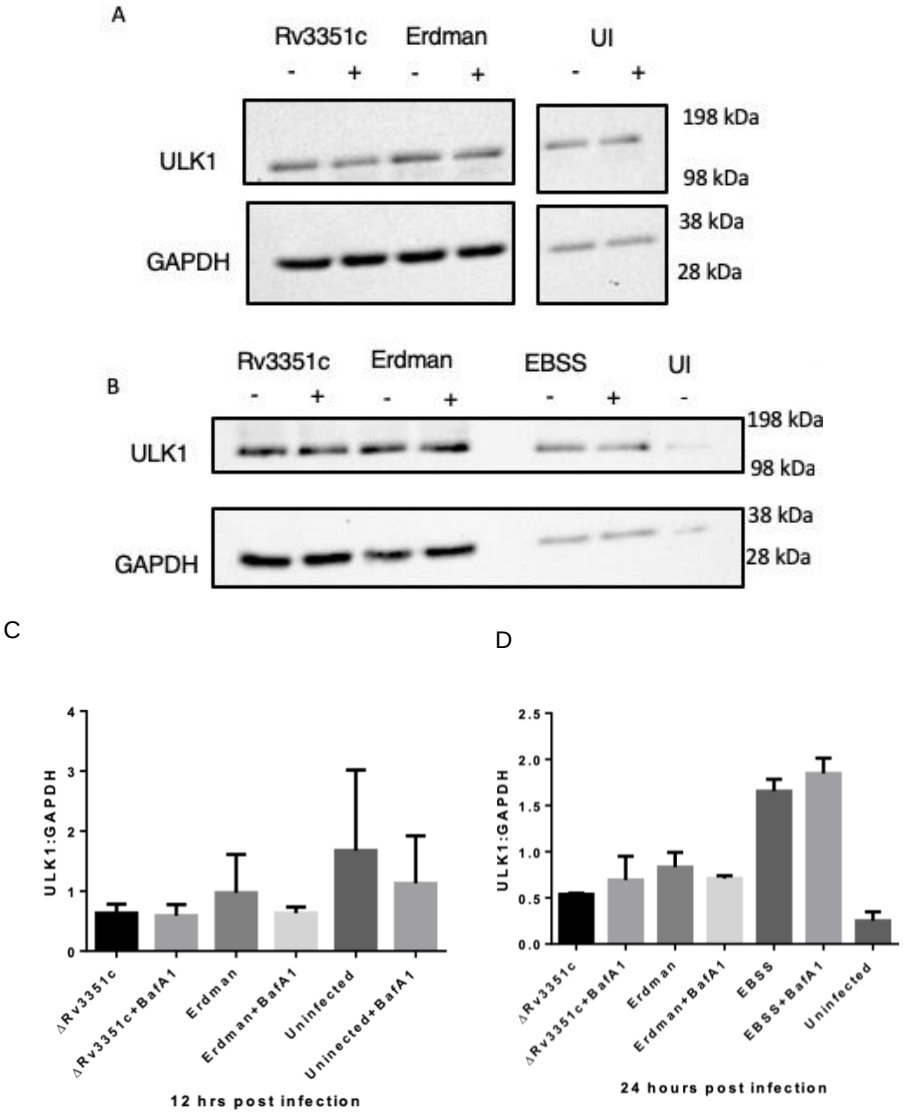

Figure 11. Western-blot analysis demonstrates induction of ULK1. Cell lysates were obtained from infected A549 cells, uninfected cells, or cells under starvation (EBSS) conditions at 12 (A) and 24 hours (B) in the presence or absence of autophagy inhibitor Bafilomycin A1 (100 nM) as described under materials and methods. ULK1 to GAPDH loading control ratios were quantified (C and D). Erdman infected cells were significantly different from uninfected cells (*p value < 0.05). Blots are representative of two experiments with similar results. Data shown are the means of two experiments. Error bars represent one standard deviation.

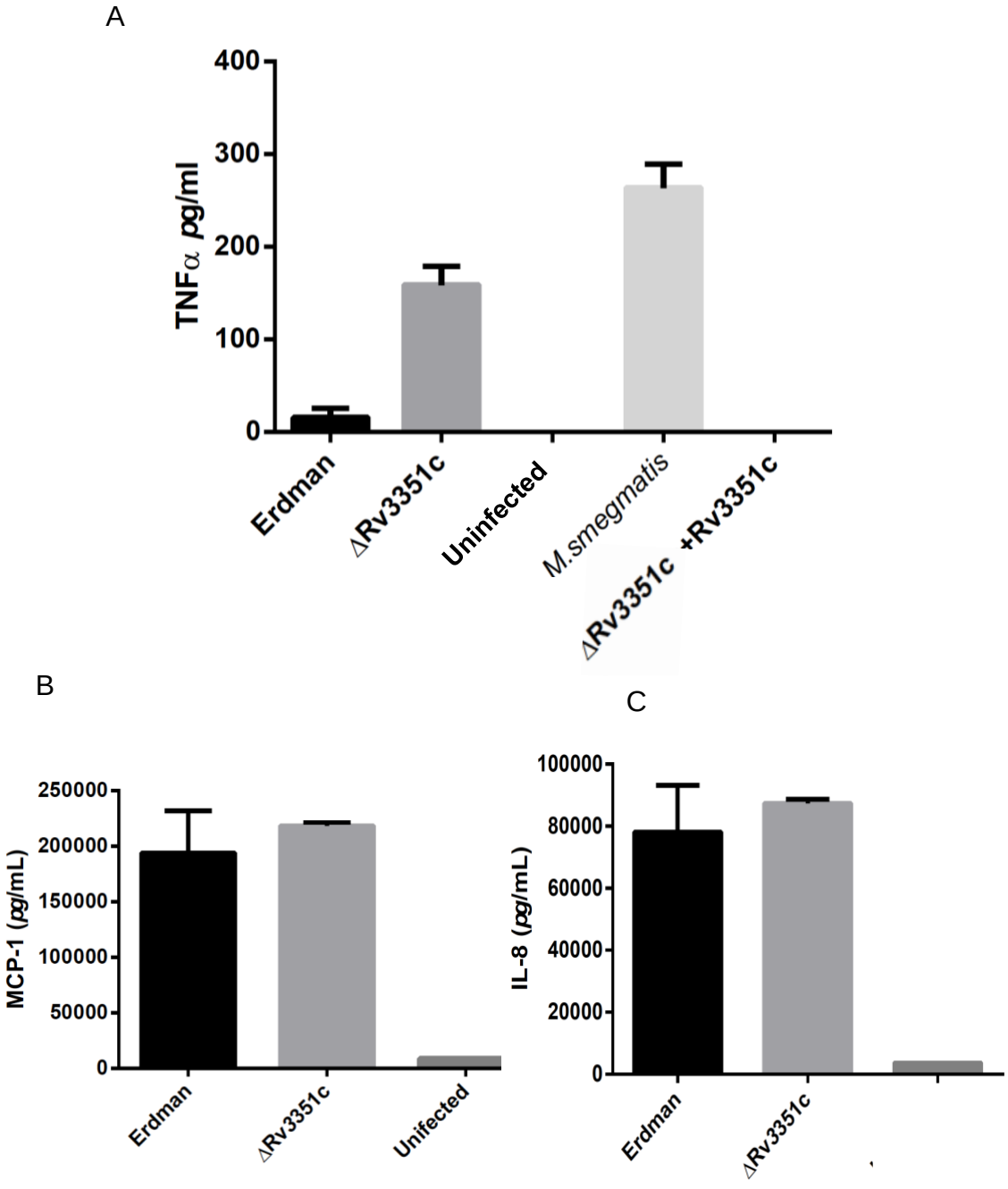

Figure 12. ELISA of infected cell culture supernatants demonstrate A549 cells produce TNF-α (A), IL-MCP-1 (B), and IL-8 (C) in response to ΔRv3351c infection ****p-values ($p<0.0001$). Data shown are the means of three experiments. Error bars represent one standard deviation.

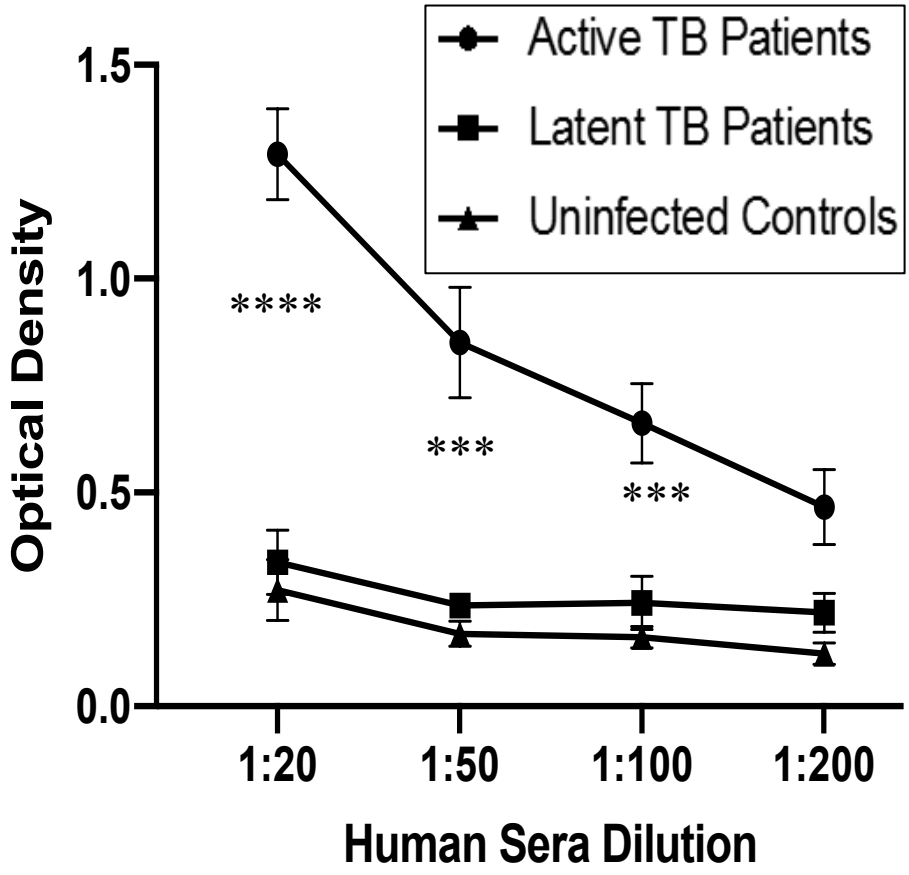

Figure 13. Screening of human sera from patients with culture-confirmed active versus latent TB and negative control volunteers by ELISA show that these patients produce antibodies against the Rv3351c protein. Images are representative of three experiments with similar results. ****p-values ($p<0.0001$), ***p-values: 0.001. Error bars represent one standard deviation.

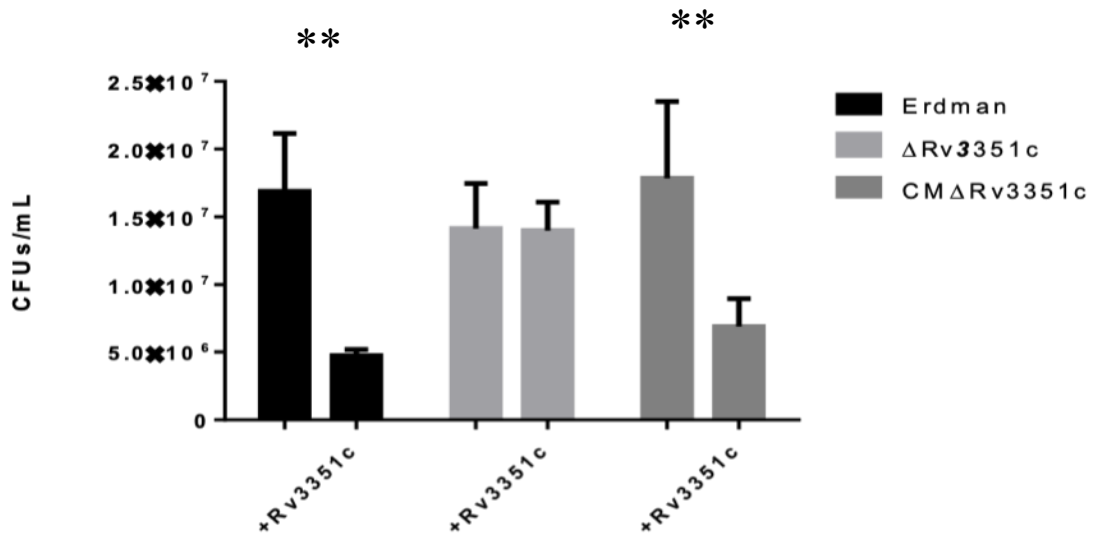

Figure 14. Intracellular viability of *M. tuberculosis* strains demonstrates that preincubating with recombinant Rv3351c protein reduces bacterial entry into A549 cells.
Cells were infected with the indicated *M. tuberculosis* strains as described in Materials and methods. At 6 hours post-internalization (T==0), cells were lysed and bacterial colony-forming units (CFU) per milliliter were enumerated. Data shown are the means of 3 experiments performed in triplicate. **p-values: ($p<0.05$). Error bars represent one standard deviation.

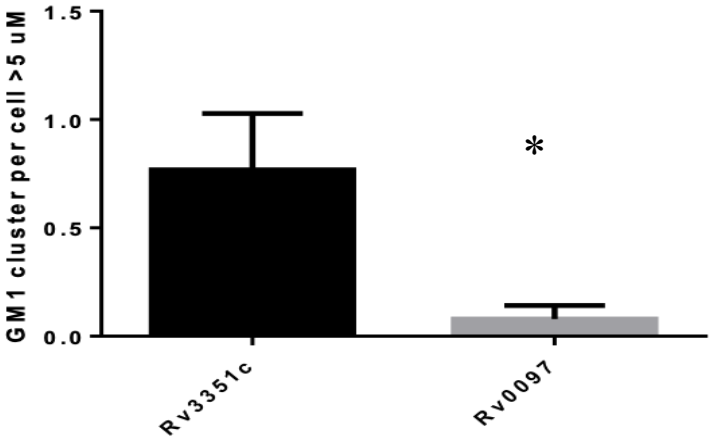

Supplemental Figure 1. Counts of GM1 clusters demonstrates differences in lipid raft numbers between A549 cells incubated for 30 minutes with *M. tuberculosis* Rv3351c or Rv0097 proteins. **p-values: ($p<0.05$) Error bars represent one standard deviation.

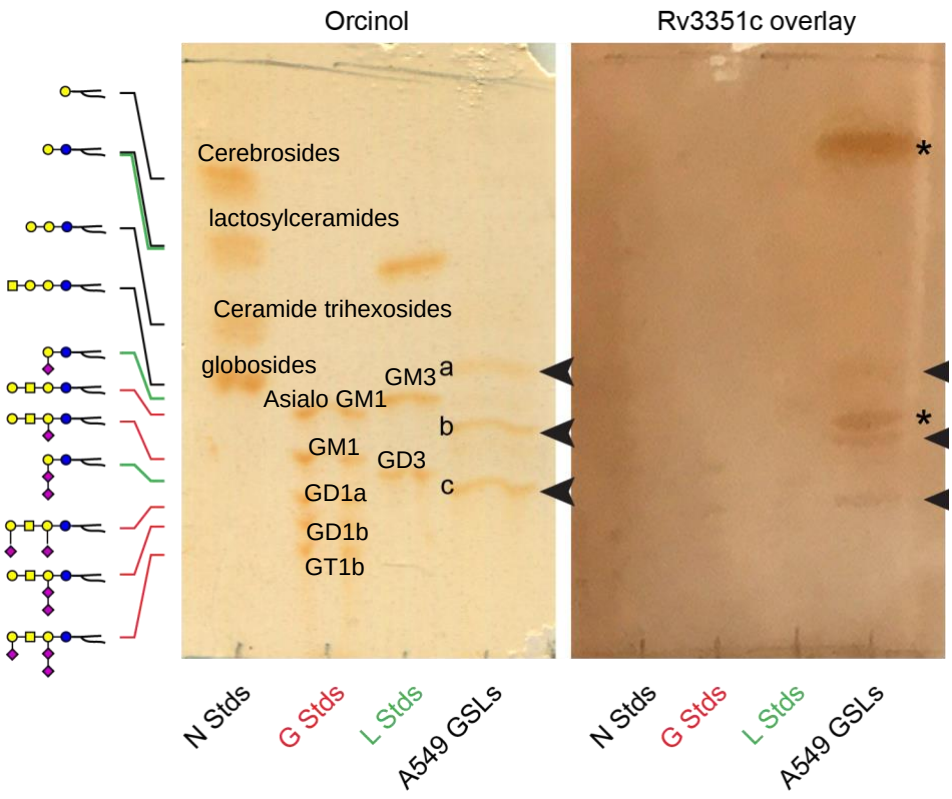

Supplemental Figure 2. ***Rv3351c binds hydrophobic compounds and glycolipids extracted from A549 cells.*** Lipid extracts were spotted and resolved on thin-layer silica plates along with three sets of well-characterized sets of glycosphingolipid standards. One plate was sprayed with Orcinol (***left panel***) to detect glycosylated lipids. An identical plate was prepared, developed, coated with plastic for probing with recombinant Rv3351c (***right panel***). Standards included in each of the indicated sets and their migration positions are shown on the left. The N Standard set included glucosyl-ceramide, lactosyl-ceramide, globotriaosyl-ceramide, and globotetraosylceramide (from fastest to slowest migrating). The G Standard set included asialo-gangliotetraosylceramide as well as GM1, GD1a, GD1b, and GT1b gangliosides. The L Standard set included lactosyl-ceramide (also in the N-Standard set) as well as GM3, and GD3 ganglioside. Orcinol staining indicates that the major glycolipids in the A549 extract have chromatographic mobility consistent with the assignment as asialo-gangliotriosylceramide GA1 (***a***), GM1 (***b***), and GD1a (***c***). Rv3351c binds to a major orcinol-negative, hydrophobic component in the lipid extract of A549 cells, most likely cholesterol, and another minor orcinol-negative component (both indicated by asterisk). Rv3351c also binds to orcinol-positive glycolipids extracted from A549 cells (indicated by arrowheads). The major glycolipids bound by Rv3351c do not migrate with any of the standard set lipids and the standard set lipids bind Rv3351c poorly, despite being presented at equal or higher density to A549 components on the silica plates.

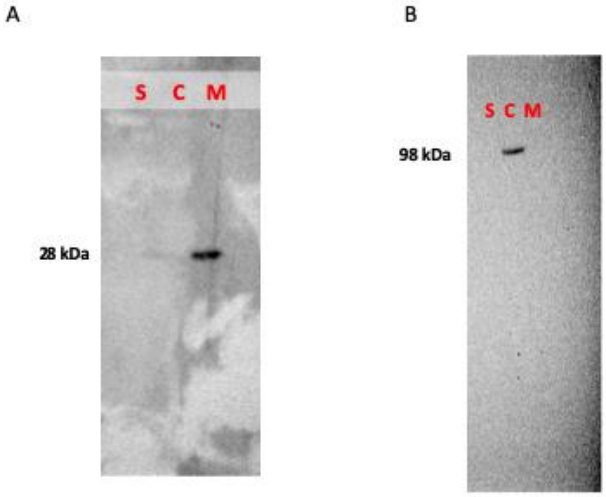

Supplemental Figure 3. A) Monoclonal antibodies made against *E. coli* recombinant Rv3351c recognize a protein the expected size for the *M. tuberculosis* protein in the membrane fraction and to a lesser extent in the cytoplasmic fraction of *M. tuberculosis* strain Erdman cell lysates by western blot. B) Anti-RNA polymerase β subunit antibody served as a control for the cytoplasmic fraction. S = supernatant; C = cytoplasmic; M = membrane fraction.

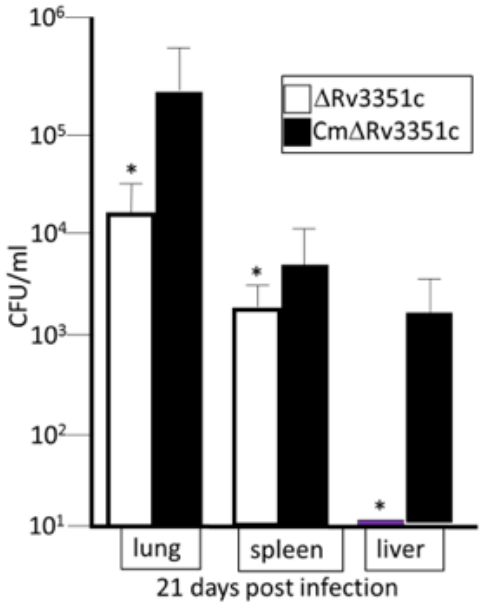

Supplemental Figure 4. BALB/c mice intranasally-infected with the ΔRv3351c bacilli have fewer replicating bacilli in lungs and fewer disseminated to the spleen and liver 21 days post-infection compared to control infections with the complemented mutant, CM ΔRv3351c. The intratracheal dose of these strains given was $1X10_5$ CFU in 0.025 ml PBS. Tissues were collected after euthanasia and processed for viable counts as described. *p value< 0.05. Error bars represent one standard deviation.

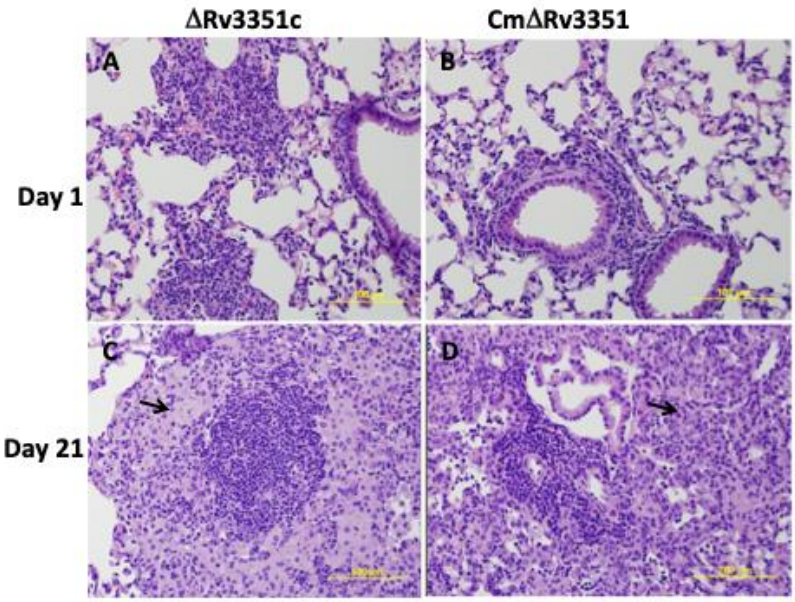

Supplemental Figure 5. Lung sections from BALB/c mice intranasally-infected with ΔRv3351c or bacilli from the complemented strain, CM ΔRv3351c show similar infiltration in BALB/c mouse lungs 21 days post-infection. Arrows highlight the areas of lymphocyte infiltration on day 21 post-infection compared with day 1. The intratracheal dose of these strains given was $1X10^5$ CFU in 0.025ml PBS. Tissues were collected after euthanasia and processed for histopathology as described.

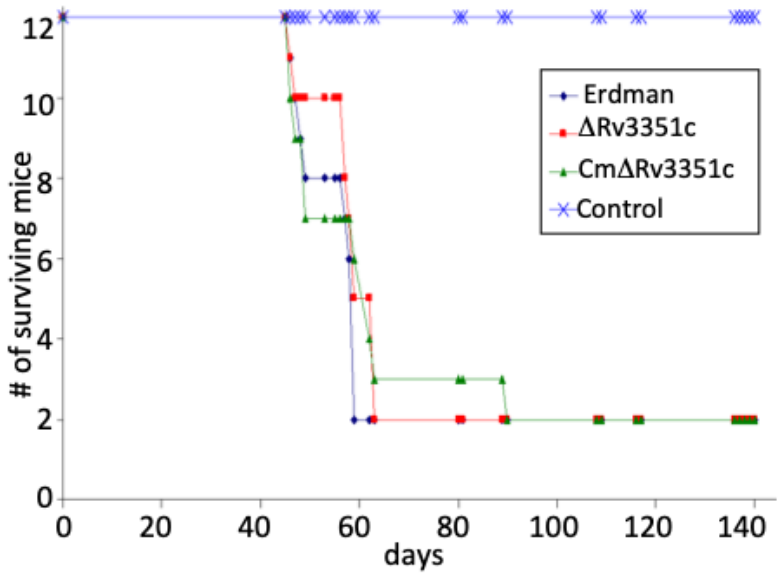

Supplemental Figure 6. SCID mouse survival study following aerosol infection with *M. tuberculosis* strains Erdman, ΔRv3351c, or CM ΔRv3351c. SCID mice were infected with a l0-50 CFU dose of the indicated *M. tuberculosis* strains using a Madison aerosol chamber. Mice were monitored daily by defined criteria over the course of the 140-day study for weight loss, malaise or other adverse reactions prior to euthanasia.

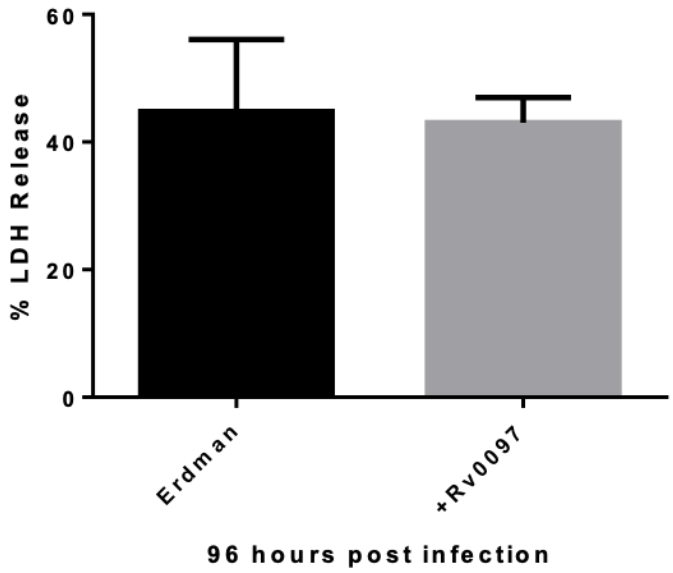

Supplemental Figure 7. Lactate dehydrogenase assay of infected A549 cell culture supernatants demonstrate that adding recombinant protein (5 μg) 30 minutes prior to infection does not reduce the cytotoxicity of Erdman or CMΔRv3351c at 96 hours post-infection (p value=0.8555) Error bars represent one standard deviation.

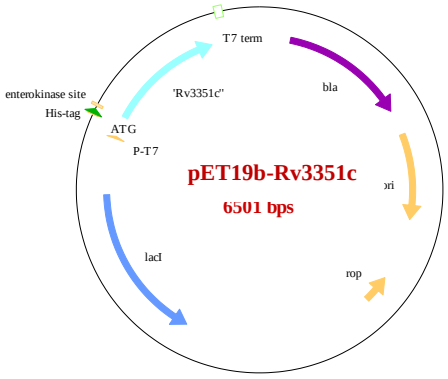

Figure 16. Plasmid map for pET19b-Rv3351c showing each individual plasmid components, including the β-lactamase ampicillin resistance gene, origin of replication of *E. coli*, and the N-terminal his-tag. The teal arrow indicates the inserted *Rv3351c* gene.

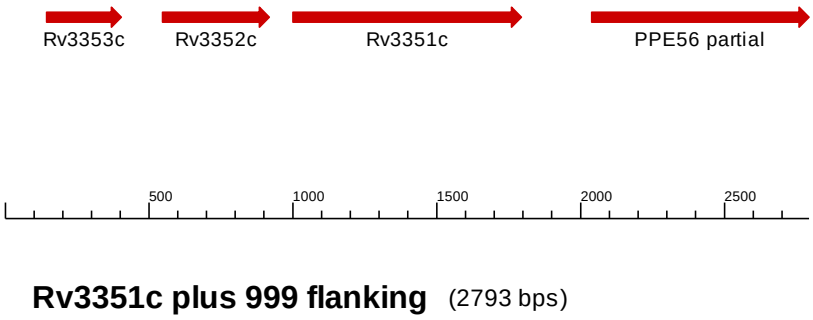

Figure 15: Gene map of *Rv3351c* and flanking region including the upstream genes *Rv3352c and Rv3353c* and downstream *ppe56.* Figure was generated using Clone Manager Software (Sci Ed, Colorado).

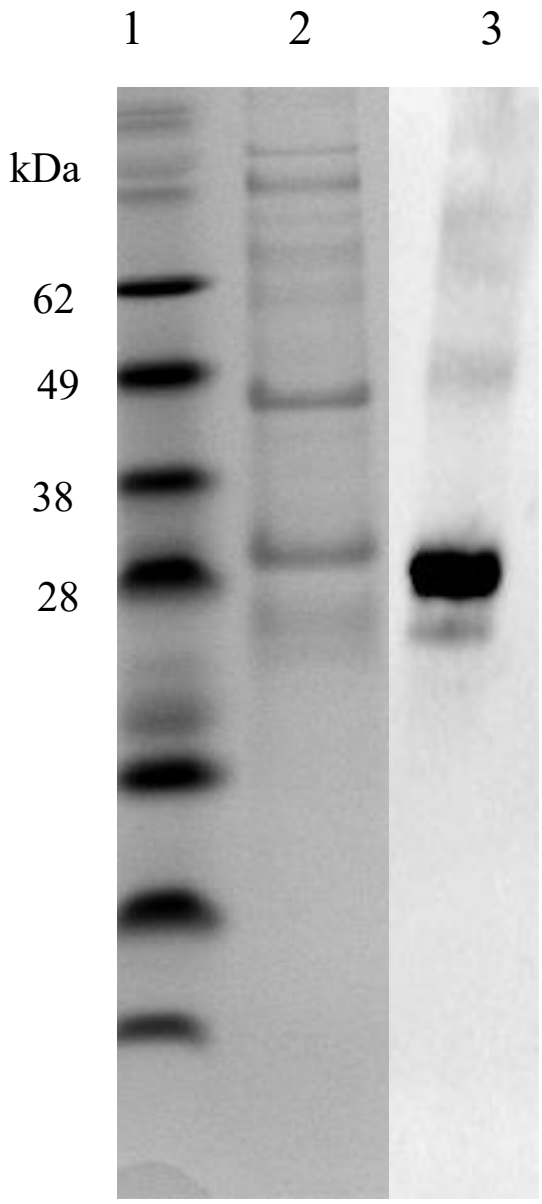

Figure 17. Generation of recombinant Rv3351c protein and analysis by SDS-PAGE and immunoblotting. Following bacterial lysis, the homogenate was divided into soluble and insoluble (inclusion bodies) fractions. Rv3351c was purified from inclusion bodies by nickel affinity chromatography and dialyzed against decreasing concentrations of urea with 5mM Tris until a 0.01M urea concentration was reached. Lane 1: Protein Markers. Lane 2: Coomassie Staining of Rv331c (5 µg). Lane 3: immunoblot of Rv3351c (5 µg) detected with anti-6x his-tag HRP antibody. Data are representative of three experiments with similar results.

CHAPTER 4

SIGNIFICANCE AND FUTURE DIRECTIONS

Our studies of Rv3351c support a hypothesis that *M. tuberculosis* has a mechanism to target the alveolar epithelium, enhancing the importance of these cells in the disease process and providing a candidate for mucosal vaccination.

Since its first use in 1921, the BCG vaccine has been the only approved human vaccine for the lung disease tuberculosis (TB). However, BCG shows variable efficacy against adult pulmonary TB, the most dangerous form of the disease. BCG is also not suitable for those with HIV co-infection, a population in which TB is a major cause of death[247]. Because of the limitations of the BCG vaccine and an increase in multidrug resistant and extremely drug resistant TB, development of new vaccines is a cornerstone of the World Health Organization's "End TB" strategy[5]. Current alternatives to BCG involve viral vectored vaccines expressing one or more antigens from *M. tuberculosis*, purified *M. tuberculosis* antigens (subunit), live whole cell mycobacteria, or inactivated whole cell *M. tuberculosis* candidates, but to date no vaccine candidates in clinical trials have been proven to be more effective than BCG alone[199]. All vaccine candidates to date are designed to prevent or lessen the development of systemic disease, they are not constructed or administered to prevent for example, initial respiratory tract infection and subsequent dissemination from the lung. In addition, a new TB vaccine will ideally work as an effective booster to BCG vaccination, due to the its continued efficacy against severe childhood forms of the diseases such as TB meningitis, and its potential ability to reduce deaths from other infectious diseases through nonspecific mechanisms[248,249].

An alternative to either live, whole cell or vector-based vaccines is immunization with a subunit vaccine; antigens determined to be critical to the disease process that are extracted from the pathogen or produced via recombination. Subunit approaches provide significant flexibility since they can specifically target the various stages of the infection process; in the case of *M. tuberculosis*, infection of the lung alveoli. In addition, this type of vaccine is safe for use in immunocompromised populations[199]. However, subunit vaccines are not very immunogenic, requiring combination with an adjuvant and a physiologically appropriate delivery system in order to make them maximally effective. So far, only a few antigens have been tested as potential booster vaccines to BCG; one of them is the heparin binding hemagglutinin adhesin (HBHA), a protein involved in binding of *M. tuberculosis* bacilli to Type II alveolar epithelial cells with resulting extrapulmonary dissemination[26,28,250]. Vaccination with HBHA has been shown to provide some protection against mycobacterial replication in the lung and subsequent dissemination after aerosol challenge with *M. tuberculosis* bacilli in mouse models[251,252]. HBHA is also recognized by T cells from latently infected individuals in contrast to patients with active TB[253]. However, in one study, the protective effect of HBHA in mice strongly depends on the use of the adjuvant dimethyldioctadecyl-ammonium bromide/monophosphoryl lipid A (DDA/MPL) that induces the TH1 response important in *M. tuberculosis* immunity[254]. This adjuvant is not suitable for human use, and thus to overcome the shortcomings observed in this study, we generated and tested a novel vaccine delivery system i) incorporating two mycobacterial proteins that interact with alveolar epithelial cells, HBHA and Rv3351c, and ii) included an adjuvant, VacSIM shown to be exceptionally good at inducing T-cell and humoral immune responses .

Unlike HBHA which is recognized by T cells only from latently infected individuals, antibodies against Rv3351c are found in serum from patients with active TB. Deleting *rv3351c* from *M. tuberculosis* leads to decreased virulence in an A549 type II epithelial cell line. By immunizing mice intranasally with HBHA and Rv3351c, two antigens that play a role in alveolar epithelial cell infection, we hope to induce a strong mucosal immune response when delivered intranasally with VacSIM (vaccine self-assembling immune matrix). VacSIM solution can easily be mixed with antigens, vaccine backbone, and adjuvants for injection. Post injection, the peptides self-assemble into hydrated nanofiber gel matrices, forming a depot with antigens and adjuvants in the aqueous phase. VacSIM provides slow release of immunogens, leading to increased activation of antigen-presenting cells like macrophages and dendritic cells that then drive enhanced immunogenicity. VacSIM has demonstrated enhanced vaccine-protective CD4 and CD8 T cell responses with hepatitis B, HIV, *Burkholderia*, schistosomiasis, and malaria antigens, as well as with whole inactivated influenza vaccines, and influenza nucleoproteins[255].

Mucosal and intravenous administration of BCG induces stronger T cell and greater humoral responses than the classical intradermal and intramuscular routes of vaccination, and mucosal delivery of HBHA coated nanoparticles was shown to boost the BCG-induced anti-TB immunity[130,204]. We hypothesize that since this our HBHA-Rv3351c-VacSIM subunit vaccine will mimic the natural respiratory mucosal route of *M. tuberculosis* infection, that it will induce a greater immune response than intradermal BCG alone. The respiratory mucosal route of immunization is superior to the parenteral route in protecting against pulmonary TB, because of its ability to induce anti-TB T-cell immunity in the lung airways in addition to inducing T-cell responses in the lung interstitium. In contrast, parenteral immunization fails to elicit T-cell responses in the airway lumen although it induces T-cells to populate the lung interstitium that

may or may not be protective. T lymphocytes are critical players in antimycobacterial immune responses. Immunological control of *M. tuberculosis* infection is based on a type 1 T-cell response involving IFN-γ-producing or polyfunctional (IL-2-, IFN-γ-, and TNF-α-producing) CD4+and CD8+ T lymphocytes[256]. Several studies have established a link between polyfunctional CD4+ T cells and protection against *M. tuberculosis*[257]. However, other studies in mouse and human infants show no correlation between these T cell responses and protection, and other immunological signatures of protection should also be considered. For instance, the production of IFN-γ is important, but not sufficient for protection against TB[258–260]

IL-17 is also involved in vaccine-induced immunity to TB[15,203,254,261–263], and plays a crucial role in the formation of granulomas during *M. tuberculosis* infection, but is not essential to control mycobacterial growth[264]. Although cellular mediated immunity is a major component in the control of mycobacterial infections, *M. tuberculosis* infection also induces humoral immune responses against various mycobacterial antigens[208,209]. In addition, BCG vaccination can induce antibody responses to several mycobacterial antigens, which elicits both innate and cell-mediated immunity against mycobacteria[209–213]. Recent studies suggest that humoral immunity might be an effective target a new TB vaccine, and we will be looking at the ability of our vaccine to illicit humoral immunity in mice, in addition to the components of cell mediated immunity mentioned above. However, because precise immune correlates of protection are still unknown in *M. tuberculosis* infection, this study will be followed by a protection study in infected mice aerosol vaccinated the same aerosol vaccine regimens in order to match correlates of protection to the optimal vaccine combination. To examine the immune response of mice vaccinated with VacSIM, Rv3351c and HBHA, the following experimental methods have been performed and studies are currently in progress.

Purification of HBHA from M. bovis BCG

Mycobacterium bovis BCG was grown in static cultures at 37◦C using 175cm2 Roux flasks (Falcon; Becton-Dickinson, Franklin Lakes, NJ) containing ~150ml of Sauton's medium. At stationary phase, the cultures were centrifuged (10,000 x g for 20 minutes), and 500 ml of supernatant was passed through a heparin-Sepharose CL-6B (Pharmacia LKB, Piscataway, NJ) column (1 x 5 cm) equilibrated with DPBS. The column was then washed with 100 ml DPBS, and the bound material was eluted by a 0-500 mM NaC1 gradient in 100 ml DPBS. The flow rate during all steps was maintained at 1.5 ml per minute, and absorbance at 280 nm was continuously monitored. Purification was followed by reverse-phase high-pressure liquid chromatography (HPLC; Beckman Gold System), using a Nucleosil C18 column (TSK gel Super ODS; Interchim) equilibrated in 0.05% trifluoroacetic acid. The protein was eluted by a linear 0–80% acetonitrile gradient prepared in 0.05% trifluoroacetic acid. HBHA was eluted at ~60% acetonitrile. The HPLC chromatogram revealed a single peak corresponding to the HBHA molecule. Analysis by SDS-PAGE showed a single band after Coomassie-blue or silver staining. The band corresponded to the apparent molecular weight of HBHA, indicating that the final preparation was not contaminated with additional proteins as far as can be detected by HPLC and gel electrophoresis. Analysis by gas chromatography indicated that the final fraction did not contain detectable levels of lipoarabinomannan (LAM) or other glycolipids. The limulus test, which is used for possible lipopolysaccharide (LPS), contamination revealed that the LPS concentration was <10 pg/mL.

Immunization protocol

All experiments were performed with 6-week-old female C57Bl/6 mice (Charles River Laboratory, L'Arbresle, France). *Mycobacterium bovis* BCG Pasteur strain (isolate 1173P2,

WHO, Stockholm, Sweden) was grown in liquid Sauton's or on solid Middlebrook 7H11 media (Difco, Detroit, MD). Stock solutions were titrated and stored at −80°C until use.

VacSIM-M. tuberculosis protein formulation

HBHA (5 μg) and Rv3351c (5 μg) were mixed with 6 μL of VacSIM (2.5 μg) in a final volume of 40 μl. All proteins were prepared in PBS. VacSIM was a generous gift from Dr. Donald Harn at the University of Georgia.

Mice (10/group) were immunized with PBS and BCG, or the VacSIM formulation (Table 1). Mice were first primed subcutaneously with $5 \times 10_5$ colony forming units (CFU) BCG at the base of the tail, and 4 months later boosted two times intranasally under light anesthesia. Three weeks after the final immunization, mice will be culled for immunogenicity studies. Spleens and lungs will be harvested for cell preparations.

Lymphocyte preparations and cytokine production

Pulmonary cells from naive or infected mice will be prepared by classical procedures. Lungs will be perfused with PBS, excised and finely minced, followed by enzymatic digestion for 20 minutes at 37°C in RPMI 1640 containing 1 mg/ml collagenase type VIII (Sigma-Aldrich, St. Louis, MO) and 1 μg/ml DNase type I (Sigma-Aldrich, St. Louis, MO). After wash, lung homogenates will be resuspended in a 35% Percoll gradient and carefully layered onto 70% Percoll and centrifuged at 400 xg, at 22°C for 30 minutes. After centrifugation, two layers of cells will be formed. The layer in the interface between the two Percoll concentrations will be carefully aspirated and washed in PBS 2% FCS. (Sigma-Aldrich St. Louis, MO).

Spleens will be aseptically removed and forced through a 70 μM (BD Pharmingen, Franklin Lakes, NJ) sterile nylon sieve into single cell suspensions, before being centrifuged at $800 \times g$ for 15 minutes. Erythrocytes in the spleen-derived lymphocyte preparation (i.e.

splenocytes) will be lysed by incubation in isotonic ACK lysis buffer (ThermoFisher Scientific, CA) for 2-3 minutes at room temperature. After washing, cells will be then resuspended in RPMI containing 10% heat-inactivated fetal calf serum and counted before being further processed, as indicated below.

Spleen and lung cells will be added at $7.5 \times 10_5$ cells per well in 96-well plates (BD Falcon, Franklin Lakes, NJ) and stimulated with medium, 10 μg/ml HBHA, Rv3351c or PPD or 1 μg/ml of concanavalin A (St. Louis, MO). Cell supernatants will be harvested 24 hours later, and cytokine levels will be determined by ELISA using the BD OptEIA™ Mouse Th1/T22 Cytokine kit (BD Pharmingen, Franklin Lakes, NJ) accordingly to manufacturer' protocols.

For detection of cytokine levels in sera of immunized mice, the 'Mouse Th1/Th2 ELISA Ready-SET-Go!' kit from eBioscience (Hatfield, UK) will be used, according to the manufacturer's instructions. Cytokine concentrations will be determined based on internal standards (IL-2, IL-4, IFN-γ and IL-10) provided in the kit.

T cell proliferation assay

Since protective immunity against *M. tuberculosis* requires potent T-cell responses and IFN-γ production, we will test the capacity of splenocytes from the immunized mice to respond to *in vitro* stimulation with our *M. tuberculosis* antigens. Cell proliferation will be determined by the carboxyfluorescein diacetate succinimidyl ester (CFSE) dilution assay using the CellTrace™ CFSE Cell Proliferation Kit (Invitrogen, Invitrogen, Carlsbad, CA) and will be performed according to the manufacturer's protocol. Splenocytes at $2 \times 10_6$ will be stained with final concentration of 0.3 μM CFSE prior to culture. Then, $1.5 \times 10_5$ cells will be cultured in a 96-wells plate in duplicate in the presence of PHA (positive control; Sigma-Aldrich St. Louis, MO), HBHA, Rv3351c, or unstimulated (negative control) at 37°C in a 5% CO_2 humidified incubator.

The final concentration of each antigen will be 5 μg/ml. After 4 days, the cells will be harvested and stained with anti-CD3-APC, anti-CD4-PeCy5 and anti-CD8-PE (BD Biosciences, Franklin Lakes, NJ). Cells will be acquired by a FACSCalibur flow cytometer and data will be analyzed by FlowJo (TreeStar, USA). Proliferating cells will be defined as those with reduced (low or dim) CFSE expression and % specific proliferation defined as the fraction of cells with low CFSE after subtraction of unstimulated control cell values.

Intracellular cytokine staining

To determine whether our vaccine can induce polyfunctional T cells, splenocytes will be resuscitated overnight and then stimulated with either HBHA (5 μg/mL), Rv3351c (5 μg/mL), PMA (1 μg/mL), ionomycin (1 μg/mL) or medium only for 18-24 hours at 37◦C with 5% CO_2, 95% air. For the last 4 hours of stimulation, GolgiPlug (BD Biosciences, Franklin Lakes, NJ) will be added. Cells will then be washed and resuspended in 10% FCS- containing antibodies to surface antigens CD3, CD4, and CD8. Cells will be incubated for 20 minutes, washed and the pellets resuspended in Cytofix (BD Biosciences, Franklin Lakes, NJ), followed by an additional 15 minutes incubation at RT. Cells will be washed twice more and incubated at 4◦C for 15 minutes. Cells will be then pelleted and resuspended in Permwash (BD Biosciences, Franklin Lakes, NJ), and antibodies will be added and incubated for 30 minutes at RT. Intracellular antibodies will be directed against IFN-γ, IL-2, and TNF-α. Cells will be washed twice more in Permwash, resuspended in Permwash and run on the BD FACSCanto II (BD Biosciences, Franklin Lakes NJ). Compensation will be carried out using OneComp eBeads (eBioscience, UK), and data will be collected using BD FACSDiva. Data files will be analyzed using FlowJo V10 (TreeStar, Inc., USA). Lymphocytes will be identified using forward scatter height (FSC-H) and side scatter area (SSC-A), from which single cells will be identified using FSC-H and FSC-

A parameters. This population will then be used to gate CD3+ CD8+ or CD3+ CD4+ cells, followed by individual cytokine responses for IFN-γ, IL-2 or TNF-α. Boolean gates will then be created to interrogate for IFN-γ, IL-2 and TNF-α in CD4+ and CD8+ populations.

Antibody determination

Ninety-eight well plates (Nunc, ThermoFisher Scientific, CA) will be coated overnight at 4°C with 200 ng/well of HBHA or Rv3351c solution in PBS. The plates will be washed 3 times with PBS (Corning, NY) and blocked for 1 hour with 5% BSA in PBS. Control and immunized sera will be added to the wells and incubated for 2 hours at room temperature. After washing, goat anti-mouse IgG isotype-horseradish peroxidase conjugates (Southern Biotech, AL, USA), will be added, and the plates will be incubated for 1 hour. After washing, the presence of antibodies will be revealed with the TMB substrate (Pierce Biotechnology, Rockford IL, USA). Color development at OD405 nm will be measured.

Table 1. VACSIM Formulation Prime-Boost Immunization Schedule of Mice.

Vaccination Condition	**Prime**	**Boost** 3 weeks (February 24)	**Boost** 6 weeks (March 16)	**Cull** 9 weeks (April 6)
PBS				+
BCG	+			+
BCG + VacSIM + Rv3351c + HBHA	+	+	+	+
VacSIM + Rv3351c + HBHA		+	+	+

CHAPTER 5

CONCLUSIONS

Mycobacterium tuberculosis, the causative agent of the lung disease tuberculosis (TB), has been a human pathogen for millennia. The BCG vaccine has been in use for almost 100 years, making it the oldest and currently the most widely distributed vaccine, yet TB still remains the world's leading infectious killer[5,6]. One of the main hurdles in the fight to control TB is the limitation of the BCG vaccine in protecting against pulmonary disease in adults. Even though the BCG vaccine is unable to protect adults, it is able to protect children from the pulmonary, meningitis and miliary forms of the disease, and is correlated with nonspecific protection from other infectious diseases. The ability of BCG to protect children make it unlikely to be phased out of use[8–10,248,249]. Other hurdles to TB control are the six to nine month long, harsh course of antibiotic treatment, and lack of specific diagnostics that can differentiate between different stages of disease that range from the active, transmittable disease state to the inactive, non-transmittable latent state. Lack of adherence to antibiotic regimens has led to the rise of multidrug resistant and extremely-drug resistant forms of *M. tuberculosis*, while the lack of specific diagnostics prevent patients from receiving treatment and allow the continued spread of the bacteria to others, or the eventual reactivation of latent TB[3,5,11,12]. A compounding effect to this issue is the presence of HIV, as latent TB carriers co-infected with this virus have an increased chance of developing active TB disease due to a declining immune system; however, these individuals with HIV cannot receive BCG due to safety concerns with immunocompromised individuals receiving a live vaccine[199]. Thus, a new vaccine is needed that

can boost the BCG vaccine to provide protection from pulmonary TB in adults and is safe for patients with HIV.

Our inability to decrease the burden of *M. tuberculosis* infection in the human population also reinforces the need for a better understanding of the host/pathogen relationship. Until recently, the efforts to understand this relationship have focused on interactions of *M. tuberculosis* with host alveolar macrophages[18,93,143–146,150–153,160,94,95,109,110,112,113,141,142]. While these cells play an important role in controlling TB, the increase in incidence of this disease worldwide suggests that we are missing important aspects of the host/pathogen relationship which could aid in our ability towards the eventual control of TB. Previous work by our laboratory and others have shown that epithelial pneumocytes, the most numerous cell type in the lung alveolus, play a role during *M. tuberculosis* infection[22,23,29–31,128,217,265]. The Locht laboratory at the Pasteur Institute in Lille, France, has even identified the Heparin Binding Hemagglutinin Adhesin (HBHA) of *M. tuberculosis* as a gene product that interacts with alveolar epithelial cells, but not macrophages[26,28,250]. Deleting *hbha* from *M. tuberculosis* decreases dissemination from the lung to the spleen and liver in mice, indicating an important role for both HBHA and alveolar epithelial cells in *M. tuberculosis* disseminated infection[27,28] .

Our laboratory has identified another protein that is involved in alveolar epithelial cell infection, Rv3351c[30]. Mutant strains deleted for the gene encoding Rv3351c (ΔRv3351c) replicate to lower numbers and are less capable of killing host cells than wild-type *M. tuberculosis* bacilli, however, unlike *hbha* mutants (Δ*hbha*), the ΔRv3351c bacilli are not deficient in internalization into alveolar epithelial cells, indicating that the host cell target is downstream of these initial processes. In chapter 3 of this dissertation, intracellular trafficking differences between ΔRv3351 and parent strain Erdman in the A549 alveolar epithelial cell line

are examined. Work from our laboratory has previously shown that *M. tuberculosis* Erdman bacilli survive and replicate in A549 cells by inhibiting fusion of the endosomal compartment with the degradative host lysosome. The *M. tuberculosis* Erdman-containing compartment was found to have a double-membrane decorated with LC3, indicating that the bacteria are able to subvert the host autophagic machinery for their own survival. Autophagy has been shown to play an important role in the trafficking of other intracellular pathogens; *Coxiella burnetii* and *Staphylococcus aureus* have been shown to utilize and manipulate this pathway to promote survival in host cells[181,188]. Inhibition of the autophagy pathway decreases *M. tuberculosis* bacterial survival while maintaining host cell viability. *Mycobacterium tuberculosis* survival in these cells was also found to be dependent on the bacteria's ability to induce cholesterol-dense regions on the host cell plasma membrane known as lipid rafts. To determine the differences between trafficking of ΔRv3351c and parent strain Erdman bacilli, our research targeted these pathways.

As hypothesized, ΔRv3351c bacilli are not able to induce lipid rafts to the same extent as parent strain Erdman but adding purified Rv3351c protein to A549 cell cultures was sufficient to induce lipid raft formation. However, the inability of ΔRv3351c bacilli to initiate lipid rafts does not affect internalization into A549 cells, as Erdman and ΔRv3351c bacilli both internalize into A549 type II pneumocytes via actin-mediated engulfment; disrupting actin with cytochalasin D limited internalization of both strains. We found that the previously reported differences in intracellular numbers and subsequent host-cell killing between ΔRv3351c and parent strain Erdman were due to differences in intracellular trafficking via endosomes containing ΔRv3351c bacteria to the lysosome: Endosomes containing ΔRv3351c bacilli were significantly more associated with lysosomal markers LAMP-2 and Cathepsin-L at 72 hours post infection than

endosomes containing Erdman bacilli. In further support of this finding, inhibiting lysosomal acidification with the vacuolar type H+-ATPase inhibitor bafilomycin A1 restored ΔRv3351c intracellular viability and virulence to wild type levels when measuring the release of lactate dehydrogenase from dying infected A549 host cells. Trafficking of ΔRv3351c bacilli to the lysosome may involve the process of LC3 Associated Phagocytosis (LAP), a mechanism host cells use to deliver phagocytosed cargo directly to lysosomes for immediate degradation[190]. In this pathway, components of autophagic machinery are used to conjugate LC3 directly onto a single membrane vesicle. We found that ΔRv3351c bacteria are more associated with LC3 at early time points than Erdman and do not induce ULK1 above uninfected cell levels. While further experiments are needed to examine other markers of LAP, like ROS produced by the NADPH oxidase NOX2 or the presence of a single membrane, mycobacteria have been increasingly shown to traffic through a non-canonical autophagy pathway. In 2016, researchers discovered that non-pathogenic *M. smegmatis* bacilli are targeted for degradation by the autophagy marker LC3, but unlike *M. tuberculosis*, are not ubiquitinated or associated with autophagy protein ULK1, indicating *M. smegmatis* is targeted by an alternative autophagy pathway[189]. *Mycobacterium tuberculosis and M. marinum* (a fish pathogen) are both targeted by LAP in macrophages: *M. marinum* resides in a LC3 decorated, single-membrane compartment that does not fuse with lysosomes, and mutants of *M. tuberculosis* lacking *cpsA,* a gene coding for a protein involved in cell-wall metabolism, are degraded by LAP while wild-type bacteria are able to avoid this process[195,196]. This is similar to other bacterial pathogens such as *Burkholderia pseudomallei* that reside in single-membrane LC3-positive compartments that do not fuse with lysosomes, and a proportion of the bacteria escape into the cytosol. However, mutants of *B. pseudomallei* lacking the type III secretion system are not able to prevent fusion with the

lysosome and do not escape from the phagosome[190]. Other bacteria, such as *Legionella dumoffii, Shigella flexneri, and Yersinia pseudotuberculosis* have all been shown to be targeted by LAP in non-professional phagocytic cells, and trafficking through this pathway can change the inflammatory state of the cell[190]. It is possible that the induction of lipid rafts leads to signaling cascades that trigger the different trafficking outcomes and levels of inflammatory cytokines. This connection has been seen in infections with *Legionella pneumophila,* and the uropathogen FimH+ *Escherichia coli*, bacterial pathogens that are internalized through lipid rafts recruited by the autophagic machinery and avoid immediate killing[177]. *Brucellae* species associate with lipid raft components such as GM1 upon entry into macrophages to avoid phagosome-lysosome fusion and inhibit macrophage activation to promote their intracellular survival[168,266]. *Pseudomonas aeruginosa* binding also triggers lipid raft signaling platforms in order to enter cells, induce apoptosis and regulate the cytokine response of infected cells to initiate the host immune response[170,171] . Similarly, in our study, we saw that Rv3351c-dependent induction of lipid rafts leads to *M. tuberculosis* survival in the autophagy pathway and downregulation of TNF-α cytokine production by host cells. The induction of lipid rafts may be due to direct binding by Rv3351c. Thin layer chromatography overlays using glycolipid extracts from A549 cells show that Rv3351c binds to lipid raft component GM1. These results indicate that Rv3351c is important for trafficking *of M. tuberculosis* bacilli in A549 cells to avoid degradation by the host cells and, ultimately, limiting the host immune response to facilitate survival.

Chapter 3 also showed that Rv3351c is expressed in the membrane of *M. tuberculosis* bacteria, allowing them to be recognized by the host immune response in humans. Screening of human sera from TB patients by ELISA shows that patients with active TB, but not latent, produce antibodies against the Rv3351c protein. Pre-incubating A549 cells with the Rv3351c

protein led to a reduction in the LDH release of Erdman infected A549 cells, indicating a potential protective effect of Rv3351c. Furthermore, BALB/c mice intratracheally-infected with the ΔRv3351c bacilli have fewer replicating bacilli in lungs and fewer disseminated to the spleens and livers by 21 days post infection compared to control infections with the complemented strain. This work culminates in our efforts to use our understanding of a novel *M. tuberculosis* protein in order to develop a vaccine with enhanced protective efficacy. Based on these results, we hypothesized that Rv3351c could be a potential candidate for an aerosol subunit vaccine with HBHA. Subunit approaches to *M. tuberculosis* vaccines are more flexible than other approaches since they allow targeting of all stages of infection and are safe for use in immunocompromised populations[199]. HBHA is recognized by T cells only from latently infected individuals[253], and Rv3351c is only recognized in serum from patients classified as having an active TB infection, allowing us to target multiple stages of infection. Because subunit vaccines are not very immunogenic on their own, we delivered HBHA and Rv3351c with the novel vaccine delivery system VacSIM, which provides slow release of immunogens, leading to increased activation of antigen-presenting cells that then drive enhanced immunogenicity[255]. We chose the mucosal route of administration, since mucosal vaccination mimics the natural infection route of *M. tuberculosis* and has shown to induce a greater T cell response than intradermally delivered TB vaccines[204]. We hope that intranasal boosting of BCG with VacSIM will result in superior humoral and cellular immune responses compared with those induced by immunization with BCG alone. However, because precise immune correlates of protection are still unknown for *M. tuberculosis* infection, this study will be followed by a protection study in infected mice aerosol vaccinated with the described two protein-VacSIM regimen in order to match correlates of protection to the optimal vaccine combination. In conclusion, our studies of

Rv3351c support a hypothesis that *M. tuberculosis* has a mechanism to target the alveolar epithelium, enhancing the importance of these cells in the disease process and providing a candidate for mucosal vaccination.

REFERENCES

1. Barberis, I., Bragazzi, N. L., Galluzzo, L. & Martini, M. The history of tuberculosis: From the first historical records to the isolation of Koch's bacillus. *Journal of Preventive Medicine and Hygiene* vol. 58 E9–E12 (2017).
2. Hunter, R. L. The pathogenesis of tuberculosis: The early infiltrate of post-primary (adult pulmonary) tuberculosis: A distinct disease entity. *Frontiers in Immunology* vol. 9 (2018).
3. Petruccioli, E. *et al.* Correlates of tuberculosis risk: Predictive biomarkers for progression to active tuberculosis. *European Respiratory Journal* vol. 48 1751–1763 (2016).
4. Heemskerk, D., Caws, M., Marais, B. & Farrar, J. Clinical Manifestations. (2015).
5. *GLOBAL TUBERCULOSIS REPORT 2018*. (2018).
6. Daniel, T. M. The history of tuberculosis. *Respir. Med.* **100**, 1862–1870 (2006).
7. Trunz, B. B., Fine, P. & Dye, C. Effect of BCG vaccination on childhood tuberculous meningitis and miliary tuberculosis worldwide: a meta-analysis and assessment of cost-effectiveness. *Lancet* **367**, 1173–1180 (2006).
8. Abubakar, I. *et al.* Systematic review and meta-analysis of the current evidence on the duration of protection by bacillus Calmette-Guérin vaccination against tuberculosis. *Health Technology Assessment* vol. 17 1–4 (2013).
9. Mangtani, P. *et al.* Protection by BCG Vaccine Against Tuberculosis: A Systematic Review of Randomized Controlled Trials. *Clin. Infect. Dis.* **58**, 470–480 (2014).
10. Mangtani, P. *et al.* Observational study to estimate the changes in the effectiveness of bacillus calmette-guérin (BCG) vaccination with time since vaccination for preventing

tuberculosis in the UK. *Health Technol. Assess. (Rockv).* **21**, 5–53 (2017).

11. Drain, P. K. *et al.* Incipient and subclinical tuberculosis: A clinical review of early stages and progression of infection. *Clinical Microbiology Reviews* vol. 31 (2018).
12. Bekken, G. K. *et al.* Identification of subclinical tuberculosis in household contacts using exposure scores and contact investigations. *BMC Infect. Dis.* **20**, 96 (2020).
13. Barclay, W. R., Anacker, R. L., Brehmer, W., Leif, W. & Ribi, E. Aerosol-Induced Tuberculosis in Subhuman Primates and the Course of the Disease After Intravenous BCG Vaccination. *Infect. Immun.* **2**, 574–582 (1970).
14. Kaufmann, S. H. E., Weiner, J. & von Reyn, C. F. Novel approaches to tuberculosis vaccine development. *International Journal of Infectious Diseases* vol. 56 263–267 (2017).
15. Lai, R., Afkhami, S., Haddadi, S., Jeyanathan, M. & Xing, Z. Mucosal immunity and novel tuberculosis vaccine strategies: Route of immunisationdetermined T-cell homing to restricted lung mucosal compartments. *Eur. Respir. Rev.* **24**, 356–360 (2015).
16. Bussi, C. & Gutierrez, M. G. Mycobacterium tuberculosis infection of host cells in space and time. *FEMS Microbiology Reviews* vol. 43 341–361 (2019).
17. Queval, C. J., Brosch, R. & Simeone, R. The macrophage: A disputed fortress in the battle against Mycobacterium tuberculosis. *Frontiers in Microbiology* vol. 8 2284 (2017).
18. Armstrong, J. A. & D'Arcy Hart, P. Phagosome lysosome interactions in cultured macrophages infected with virulent tubercle bacilli. Reversal of the usual nonfusion pattern and observations on bacterial survival. *J. Exp. Med.* **142**, 1–16 (1975).
19. Ryndak, M. B. & Laal, S. Mycobacterium tuberculosis Primary Infection and Dissemination: A Critical Role for Alveolar Epithelial Cells. *Frontiers in Cellular and*

Infection Microbiology vol. 9 (2019).

20. García-Fojeda, B. *et al.* Lung surfactant lipids provide immune protection against haemophilus influenzae respiratory infection. *Front. Immunol.* **10**, (2019).
21. NA, E. & DM, A. Host Defense and the Airway Epithelium: Frontline Responses That Protect Against Bacterial Invasion and Pneumonia. *J. Pathog.* **2011**, (2011).
22. Hernández-Pando, R. *et al.* Persistence of DNA from Mycobacterium tuberculosis in superficially normal lung tissue during latent infection. *Lancet* **356**, 2133–2138 (2000).
23. Barrios-Payán, J. *et al.* Extrapulmonary Locations of Mycobacterium tuberculosis DNA During Latent Infection. (2012) doi:10.1093/infdis/jis381.
24. Bermudez, L. E. & Goodman, J. Mycobacterium tuberculosis invades and replicates within type II alveolar cells. *Infect. Immun.* **64**, 1400–6 (1996).
25. Mehta, P. K. *et al.* Comparison of in vitro models for the study of Mycobacterium tuberculosis invasion and intracellular replication. *Infect. Immun.* **64**, 2673–9 (1996).
26. Menozzi, F. D. *et al.* Identification of a heparin-binding hemagglutinin present in mycobacteria. *J. Exp. Med.* **184**, 993–1001 (1996).
27. Delogu, G. *et al.* The hbhA gene of Mycobacterium tuberculosis is specifically upregulated in the lungs but not in the spleens of aerogenically infected mice. *Infect. Immun.* **74**, 3006–3011 (2006).
28. Pethe, K. *et al.* The heparin-binding haemagglutinin of M. tuberculosis is required for extrapulmonary dissemination. *Nature* **412**, 190–194 (2001).
29. Ryndak, M. B., Chandra, D. & Laal, S. Understanding dissemination of Mycobacterium tuberculosis from the lungs during primary infection. *J. Med. Microbiol.* **65**, 362–369 (2016).

30. Pavlicek, R. L. *et al.* Rv3351c, a Mycobacterium tuberculosis gene that affects bacterial growth and alveolar epithelial cell viability. *Can. J. Microbiol.* **61**, 938–947 (2015).

31. Fine-Coulson, K., Reaves, B. J., Karls, R. K. & Quinn, F. D. The Role of Lipid Raft Aggregation in the Infection of Type II Pneumocytes by Mycobacterium tuberculosis. *PLoS One* **7**, (2012).

32. Fine, K. L. *et al.* Involvement of the autophagy pathway in trafficking of *Mycobacterium tuberculosis* bacilli through cultured human type II epithelial cells. *Cell. Microbiol.* **14**, 1402–1414 (2012).

33. Chalmers, R., Gray, N. F., Williams, D. W., Percival, S. L. & Yates, M. V. *Microbiology of Waterborne Diseases : Microbiological Aspects and Risks*. vol. Second edi (Academic Press, 2014).

34. Tierney, D. & Nardell, E. A. Nontuberculous Mycobacterial Infections - Infectious Diseases - MSD Manual Professional Edition. *MSD Manual* https://www.msdmanuals.com/professional/infectious-diseases/mycobacteria/nontuberculous-mycobacterial-infections (2018).

35. Mostowy, S., Cleto, C., Sherman, D. R. & Behr, M. A. The Mycobacterium tuberculosis complex transcriptome of attenuation. *Tuberculosis* **84**, 197–204 (2004).

36. Salguero, F. J. 9 The Pathology and Pathogenesis of Mycobacterium bovis Infection. *Bov. Tuberc.* 122 (2018).

37. Viljoen, I. M., van Helden, P. D. & Millar, R. P. Mycobacterium bovis infection in the lion (Panthera leo): Current knowledge, conundrums and research challenges. *Vet. Microbiol.* **177**, 252–260 (2015).

38. Djemal, S. E. *et al.* Genetic diversity assessment of Tunisian Mycobacterium bovis

population isolated from cattle. *BMC Vet. Res.* **13**, 1–8 (2017).

39. Yahyaoui-Azami, H. *et al.* Molecular characterization of bovine tuberculosis strains in two slaughterhouses in Morocco. *BMC Vet. Res.* **13**, (2017).

40. Tsukamura, M. Identification of mycobacteria. *Tubercle* **48**, 311–338 (1967).

41. Vincent, A. T. *et al.* The mycobacterial cell envelope: A relict from the past or the result of recent evolution? *Frontiers in Microbiology* vol. 9 (2018).

42. Vergne, I., Gilleron, M. & Nigou, J. Manipulation of the endocytic pathway and phagocyte functions by Mycobacterium tuberculosis lipoarabinomannan. *Front. Cell. Infect. Microbiol.* **4**, (2014).

43. Torrelles, J. B. *et al.* Identification of Mycobacterium tuberculosis clinical isolates with altered phagocytosis by human macrophages due to a truncated lipoarabinomannan. *J. Biol. Chem.* **283**, 31417–31428 (2008).

44. Vergne, I. *et al.* Mechanism of phagolysosome biogenesis block by viable Mycobacterium tuberculosis. *Proc. Natl. Acad. Sci. U. S. A.* **102**, 4033–4038 (2005).

45. Singh, P., Rameshwaram, N. R., Ghosh, S. & Mukhopadhyay, S. Cell envelope lipids in the pathophysiology of Mycobacterium tuberculosis. *Future Microbiol.* **13**, 689–710 (2018).

46. Chiaradia, L. *et al.* Dissecting the mycobacterial cell envelope and defining the composition of the native mycomembrane. *Sci. Rep.* **7**, 1–12 (2017).

47. Cambier, C. J., Falkow, S. & Ramakrishnan, L. Host evasion and exploitation schemes of Mycobacterium tuberculosis. *Cell* vol. 159 1497–1509 (2014).

48. Reed, M. B. *et al.* A glycolipid of hypervirulent tuberculosis strains that inhibits the innate immune response. *Nature* vol. 431 84–87 (2004).

49. Forrellad, M. A. *et al.* Virulence factors of the mycobacterium tuberculosis complex. *Virulence* vol. 4 3–66 (2013).

50. van Winden, V. J. C., Houben, E. N. G. & Braunstein, M. Protein Export into and across the Atypical Diderm Cell Envelope of Mycobacteria. *Microbiol. Spectr.* **7**, (2019).

51. Kalscheuer, R. *et al.* The Mycobacterium tuberculosis capsule: A cell structure with key implications in pathogenesis. *Biochemical Journal* vol. 476 1995–2016 (2019).

52. Raffetseder, J. *Interplay of human macrophages and Mycobacterium tuberculosis phenotypes*. *Linköping University Electronic Press* (2016). doi:10.3384/diss.diva-132321.

53. Song, H., Sandie, R., Wang, Y., Andrade-Navarro, M. A. & Niederweis, M. Identification of outer membrane proteins of Mycobacterium tuberculosis. *Tuberculosis* **88**, 526–544 (2008).

54. Raynaud, C. *et al.* The functions of OmpATb, a pore-forming protein of Mycobacterium tuberculosis. *Mol. Microbiol.* **46**, 191–201 (2002).

55. Niederweis, M., Danilchanka, O., Huff, J., Hoffmann, C. & Engelhardt, H. Mycobacterial outer membranes: in search of proteins. *Trends in Microbiology* vol. 18 109–116 (2010).

56. Li, H. *et al.* Analysis of the Antigenic Properties of Membrane Proteins of Mycobacterium tuberculosis. *Sci. Rep.* **9**, (2019).

57. Cole, S. T. *et al.* Deciphering the biology of mycobacterium tuberculosis from the complete genome sequence. *Nature* vol. 393 537–544 (1998).

58. Strong, M. *et al.* Toward the structural genomics of complexes: Crystal structure of a PE/PPE protein complex from Mycobacterium tuberculosis. *Proc. Natl. Acad. Sci. U. S. A.* **103**, 8060–8065 (2006).

59. Pym, A. S., Brodin, P., Brosch, R., Huerre, M. & Cole, S. T. Loss of RD1 contributed to

the attenuation of the live tuberculosis vaccines Mycobacterium bovis BCG and Mycobacterium microti. *Mol. Microbiol.* **46**, 709–717 (2002).

60. Lewis, K. N. *et al.* Deletion of RD1 from Mycobacterium tuberculosis Mimics Bacille Calmette-Guérin Attenuation . *J. Infect. Dis.* **187**, 117–123 (2003).

61. Hsu, T. *et al.* The primary mechanism of attenuation of bacillus Calmette-Guérin is a loss of secreted lytic function required for invasion of lung interstitial tissue. *Proc. Natl. Acad. Sci. U. S. A.* **100**, 12420–12425 (2003).

62. Kinhikar, A. G. *et al.* Potential role for ESAT6 in dissemination of M. tuberculosis via human lung epithelial cells. *Mol. Microbiol.* **75**, 92–106 (2010).

63. Sabin, S. *et al.* A seventeenth-century Mycobacterium tuberculosis genome supports a Neolithic emergence of the Mycobacterium tuberculosis complex. *bioRxiv* 588277 (2019) doi:10.1101/588277.

64. Sakula, A. Robert Koch: Centenary of the discovery of the tubercle bacillus, 1882. *Bull. Int. Union Tuberc.* **57**, 111–116 (1982).

65. Huebner, R. E., Schein, M. F. & Bass, J. B. *The Tuberculin Skin Test*. *Clinical Infectious Diseases* vol. 17 (1993).

66. L'infection bacillaire et la tuberculose chez l'homme et chez les animaux ... - Albert Calmette - Google Books. https://books.google.com/books?hl=en&lr=&id=PBk1AQAAMAAJ&oi=fnd&pg=PR2&dq=Calmette+et+al.,+1922&ots=DkzrCSq0Cq&sig=BCHXl4pNkSYOAdbFG15jTIkgmZ8#v=onepage&q&f=false.

67. Mahairas, G. G., Sabo, P. J., Hickey, M. J., Singh, D. C. & Stover, C. K. Molecular analysis of genetic differences between Mycobacterium bovis BCG and virulent M. bovis.

J. Bacteriol. **178**, 1274–1282 (1996).

68. Behr, M. A. *et al.* Comparative genomics of BCG vaccines by whole-genome DNA microarray. *Science (80-.).* **284**, 1520–1523 (1999).

69. Gordon, S. V. *et al.* Identification of variable regions in the genomes of tubercle bacilli using bacterial artificial chromosome arrays. *Mol. Microbiol.* **32**, 643–655 (1999).

70. Calmette, A. *La vaccination preÌventive contre la tuberculose par le 'BCG,'*. (Masson et cie, 1927).

71. Ottenhoff, T. H. M. & Kaufmann, S. H. E. Vaccines against tuberculosis: Where are we and where do we need to go? *PLoS Pathogens* vol. 8 (2012).

72. WHO | Global tuberculosis report 2019. *WHO* (2020).

73. Pereira, S. M., Dantas, O. M. S., Ximenes, R. & Barreto, M. L. BCG vaccine against tuberculosis: Its protective effect and vaccination policies. *Rev. Saude Publica* **41**, 59–66 (2007).

74. Roy, A. *et al.* Effect of BCG vaccination against Mycobacterium tuberculosis infection in children: Systematic review and meta-analysis. *BMJ* **349**, (2014).

75. RODRIGUES, L. C., DIWAN, V. K. & WHEELER, J. G. Protective Effect of BCG against Tuberculous Meningitis and Miliary Tuberculosis: A Meta-Analysis. *Int. J. Epidemiol.* **22**, 1154–1158 (1993).

76. Murray, J. F., Schraufnagel, D. E. & Hopewell, P. C. Treatment of tuberculosis: A historical perspective. *Annals of the American Thoracic Society* vol. 12 1749–1759 (2015).

77. Volmink, J. & Garner, P. Directly observed therapy for treating tuberculosis. *Cochrane Database of Systematic Reviews* (2007) doi:10.1002/14651858.CD003343.pub3.

78. Yew, W. W., Wong, C. F., Lee, J., Wong, P. C. & Chan, C. H. Do β-lactam-β-lactamase inhibitor combinations have a place in the treatment of multidrug-resistant pulmonary tuberculosis? *Tubercle and Lung Disease* vol. 76 90–92 (1995).

79. Mdluli, K., Kaneko, T. & Upton, A. The tuberculosis drug discovery and development pipeline and emerging drug targets. *Cold Spring Harb. Perspect. Biol.* **7**, 1–25 (2015).

80. Loudon, R. G. & Roberts, R. M. Singing and the dissemination of tuberculosis. *Am. Rev. Respir. Dis.* **98**, 297–300 (1968).

81. Lienhardt, C. *From Exposure to Disease: The Role of Environmental Factors in Susceptibility to and Development of Tuberculosis*. vol. 23 (2001).

82. Khademi, F., Derakhshan, M., Yousefi-Avarvand, A., Tafaghodi, M. & Soleimanpour, S. Expert Review of Vaccines Multi-stage subunit vaccines against Mycobacterium tuberculosis: an alternative to the BCG vaccine or a BCG-prime boost? Multi-stage subunit vaccines against Mycobacterium tuberculosis: an alternative to the BCG vaccine or a BCG-. *Expert Rev. Vaccines* **17**, 31–44 (2017).

83. Mathema, B. *et al.* Drivers of Tuberculosis Transmission. *J. Infect. Dis.* **216**, S644–S653 (2017).

84. Oxlade, O. & Murray, M. Tuberculosis and Poverty: Why Are the Poor at Greater Risk in India? *PLoS One* **7**, (2012).

85. Gupta, S., Shenoy, V. P., Mukhopadhyay, C., Bairy, I. & Muralidharan, S. Role of risk factors and socio-economic status in pulmonary tuberculosis: a search for the root cause in patients in a tertiary care hospital, South India. *Trop. Med. Int. Heal.* **16**, 74–78 (2011).

86. Martínez-Barricarte, R. *et al.* Human IFN- immunity to mycobacteria is governed by both IL-12 and IL-23. *Sci. Immunol.* **3**, (2018).

87. Abel, L., El-Baghdadi, J., Bousfiha, A. A., Casanova, J. L. & Schurr, E. Human genetics of tuberculosis: A long and winding road. *Philosophical Transactions of the Royal Society B: Biological Sciences* vol. 369 (2014).

88. Lee, S. H. Tuberculosis infection and latent tuberculosis. *Tuberculosis and Respiratory Diseases* vol. 79 201–206 (2016).

89. Dye, C. WHO | Breaking a law: tuberculosis disobeys Styblo's rule. *WHO* **86**, 1–80 (2008).

90. Ahmad, S. Pathogenesis, immunology, and diagnosis of latent mycobacterium tuberculosis infection. *Clinical and Developmental Immunology* vol. 2011 (2011).

91. Zhai, W., Wu, F., Zhang, Y., Fu, Y. & Liu, Z. The immune escape mechanisms of Mycobacterium Tuberculosis. *International Journal of Molecular Sciences* vol. 20 (2019).

92. Mihret, A. The role of dendritic cells in Mycobacterium tuberculosis infection. *Virulence* vol. 3 (2012).

93. Schlesinger, L. S., Kaufman, T. M., Iyer, S., Hull, S. R. & Marchiando, L. K. Differences in mannose receptor-mediated uptake of lipoarabinomannan from virulent and attenuated strains of Mycobacterium tuberculosis by human macrophages. *J. Immunol.* **157**, 4568–75 (1996).

94. Rajaram, M. V. S. *et al.* M. tuberculosis-Initiated Human Mannose Receptor Signaling Regulates Macrophage Recognition and Vesicle Trafficking by FcRγ-Chain, Grb2, and SHP-1. *Cell Rep.* **21**, 126–140 (2017).

95. Schäfer, G., Guler, R., Murray, G., Brombacher, F. & Brown, G. D. The role of scavenger receptor B1 in infection with mycobacterium tuberculosis in a murine model. *PLoS One* **4**, 1–13 (2009).

96. Armstrong, J. A. & Hart, D. Response of cultured macrophages to Mycobacterium Tuberculosis, with observations on fusion of lysosomes with phagosomes. *J. Exp. Med.* **134**, 713–740 (1971).

97. Ernst, J. D. Macrophage Receptors for Mycobacterium tuberculosis. *Infection and Immunity* vol. 66 1277–1281 (1998).

98. Gehring, A. J., Dobos, K. M., Belisle, J. T., Harding, C. V. & Boom, W. H. Mycobacterium tuberculosis LprG (Rv1411c): A Novel TLR-2 Ligand That Inhibits Human Macrophage Class II MHC Antigen Processing . *J. Immunol.* **173**, 2660–2668 (2004).

99. Gehring, A. J. *et al.* The Mycobacterium tuberculosis 19-kilodalton lipoprotein inhibits gamma interferon-regulated HLA-DR and FcγR1 on human macrophages through toll-like receptor 2. *Infect. Immun.* **71**, 4487–4497 (2003).

100. Pecora, N. D., Gehring, A. J., Canaday, D. H., Boom, W. H. & Harding, C. V. Mycobacterium tuberculosis LprA Is a Lipoprotein Agonist of TLR2 That Regulates Innate Immunity and APC Function . *J. Immunol.* **177**, 422–429 (2006).

101. Deshmane, S. L., Kremlev, S., Amini, S. & Sawaya, B. E. Monocyte chemoattractant protein-1 (MCP-1): An overview. *Journal of Interferon and Cytokine Research* vol. 29 313–325 (2009).

102. Domingo-Gonzalez, R., Prince, O., Cooper, A. & Khader, S. A. Cytokines and Chemokines in Mycobacterium tuberculosis Infection. *Microbiol. Spectr.* **4**, (2016).

103. Geijtenbeek, T. B. H. *et al.* Mycobacteria target DC-SIGN to suppress dendritic cell function. *J. Exp. Med.* **197**, 7–17 (2003).

104. Wolf, A. J. *et al.* Mycobacterium tuberculosis Infects Dendritic Cells with High Frequency and Impairs Their Function In Vivo . *J. Immunol.* **179**, 2509–2519 (2007).

105. Wolf, A. J. *et al.* Initiation of the adaptive immune response to Mycobacterium tuberculosis depends on antigen production in the local lymph node, not the lungs. *J. Exp. Med.* **205**, 105–115 (2008).

106. Mazurek, J. *et al.* Divergent effects of mycobacterial cell wall glycolipids on maturation and function of human monocyte-derived dendritic cells. *PLoS One* **7**, (2012).

107. Giacomini, E. *et al.* Infection of Human Macrophages and Dendritic Cells with Mycobacterium tuberculosis Induces a Differential Cytokine Gene Expression That Modulates T Cell Response . *J. Immunol.* **166**, 7033–7041 (2001).

108. Brown, K. & Lynch, D. T. *Histology, Lung*. *StatPearls* (2018).

109. Gold, J. A. *et al.* Surfactant Protein A Modulates the Inflammatory Response in Macrophages during Tuberculosis. *Infect. Immun.* **72**, 645–650 (2004).

110. Pasula, R., Wright, J. R., Kachel, D. L. & Martin, W. J. Surfactant protein A suppresses reactive nitrogen intermediates by alveolar macrophages in response to Mycobacterium tuberculosis. *J. Clin. Invest.* **103**, 483–490 (1999).

111. Ferguson, J. S. *et al.* Surfactant protein D increases fusion of Mycobacterium tuberculosis-containing phagosomes with lysosomes in human macrophages. *Infect. Immun.* **74**, 7005–7009 (2006).

112. Beharka, A. A. *et al.* Pulmonary Surfactant Protein A Up-Regulates Activity of the Mannose Receptor, a Pattern Recognition Receptor Expressed on Human Macrophages. *J. Immunol.* **169**, 3565–3573 (2002).

113. Ferguson, J. S., Voelker, D. R., Ufnar, J. A., Dawson, A. J. & Schlesinger, L. S.

Surfactant Protein D Inhibition of Human Macrophage Uptake of Mycobacterium tuberculosis Is Independent of Bacterial Agglutination . *J. Immunol.* **168**, 1309–1314 (2002).

114. Allard, B., Panariti, A. & Martin, J. G. Alveolar Macrophages in the Resolution of Inflammation, Tissue Repair, and Tolerance to Infection. *Frontiers in immunology* vol. 9 1777 (2018).

115. Sasindran, S. J. & Torrelles, J. B. Mycobacterium tuberculosis infection and inflammation: What is beneficial for the host and for the bacterium? *Front. Microbiol.* **2**, (2011).

116. Chackerian, A. A., Alt, J. M., Perera, T. V., Dascher, C. C. & Behar, S. M. Dissemination of Mycobacterium tuberculosis is influenced by host factors and precedes the initiation of T-cell immunity. *Infect. Immun.* **70**, 4501–4509 (2002).

117. Cohen, S. B. *et al.* Alveolar Macrophages Provide an Early Mycobacterium tuberculosis Niche and Initiate Dissemination. *Cell Host Microbe* **24**, 439-446.e4 (2018).

118. Josse, J., Laurent, F. & Diot, A. Staphylococcal adhesion and host cell invasion: Fibronectin-binding and other mechanisms. *Frontiers in Microbiology* vol. 8 (2017).

119. Chuquimia, O. D. *et al.* The role of alveolar epithelial cells in initiating and shaping pulmonary immune responses: Communication between innate and adaptive immune systems. *PLoS One* **7**, (2012).

120. Wickremasinghe, M. I., Thomas, L. H. & Friedland, J. S. Pulmonary epithelial cells are a source of IL-8 in the response to Mycobacterium tuberculosis: essential role of IL-1 from infected monocytes in a NF-kappa B-dependent network. *J. Immunol.* **163**, 3936–47 (1999).

121. Li, Y., Wang, Y. & Liu, X. The Role of Airway Epithelial Cells in Response to Mycobacteria Infection. *Clin. Dev. Immunol.* **2012**, 11 (2012).

122. Scordo, J. M., Knoell, D. L. & Torrelles, J. B. Alveolar Epithelial Cells in Mycobacterium tuberculosis Infection: Active Players or Innocent Bystanders? *J. Innate Immun.* **8**, 3–14 (2016).

123. McDonough, K. A. & Kress, Y. Cytotoxicity for lung epithelial cells is a virulence-associated phenotype of Mycobacterium tuberculosis. *Infect. Immun.* **63**, 4802–4811 (1995).

124. Dobos, K. M., Spotts, E. A., Quinn, F. D. & King, C. H. Necrosis of lung epithelial cells during infection with Mycobacterium tuberculosis is preceded by cell permeation. *Infect. Immun.* **68**, 6300–6310 (2000).

125. Castro-Garza, J., King, C. H., Swords, W. E. & Quinn, F. D. Demonstration of spread by *Mycobacterium tuberculosis* bacilli in A549 epithelial cell monolayers. *FEMS Microbiol. Lett.* **212**, 145–149 (2002).

126. Birkness, K. A. *et al.* An in vitro tissue culture bilayer model to examine early events in Mycobacterium tuberculosis infection. *Infect. Immun.* **67**, 653–658 (1999).

127. van Leeuwen, L. M. *et al.* Mycobacteria employ two different mechanisms to cross the blood-brain barrier. *Cell. Microbiol.* **20**, e12858 (2018).

128. Bermudez, L. E. & Goodman, J. Mycobacterium tuberculosis invades and replicates within type II alveolar cells. *Infect. Immun.* **64**, 1400–1406 (1996).

129. Kohama, H. *et al.* Mucosal immunization with recombinant heparin-binding haemagglutinin adhesin suppresses extrapulmonary dissemination of Mycobacterium bovis bacillus Calmette-Guérin (BCG) in infected mice. *Vaccine* **26**, 924–932 (2008).

130. Stylianou, E. *et al.* Mucosal delivery of antigen-coated nanoparticles to lungs confers protective immunity against tuberculosis infection in mice. *Eur. J. Immunol.* **44**, 440–449 (2014).

131. Nebenzahl, Y. M. *et al.* Streptococcus pneumoniae cell-wall-localized phosphoenolpyruvate protein phosphotransferase can function as an adhesin: Identification of its host target molecules and evaluation of its potential as a vaccine. *PLoS One* **11**, (2016).

132. Upadhyay, S., Mittal, E. & Philips, J. A. Tuberculosis and the art of macrophage manipulation. *Pathog. Dis.* **76**, (2018).

133. Neyrolles, O., Wolschendorf, F., Mitra, A. & Niederweis, M. Mycobacteria, metals, and the macrophage. *Immunol. Rev.* **264**, 249–263 (2015).

134. Pauwels, A. M., Trost, M., Beyaert, R. & Hoffmann, E. Patterns, Receptors, and Signals: Regulation of Phagosome Maturation. *Trends in Immunology* vol. 38 407–422 (2017).

135. Law, F. *et al.* The VPS34 PI3K negatively regulates RAB-5 during endosome maturation. *J. Cell Sci.* **130**, 2007–2017 (2017).

136. Simonsen, A. *et al.* EEA1 links PI(3)K function to Rab5 regulation of endosome fusion. *Nature* **394**, 494–498 (1998).

137. Harrison, R. E., Bucci, C., Vieira, O. V., Schroer, T. A. & Grinstein, S. Phagosomes Fuse with Late Endosomes and/or Lysosomes by Extension of Membrane Protrusions along Microtubules: Role of Rab7 and RILP. *Mol. Cell. Biol.* **23**, 6494–6506 (2003).

138. Yates, R. M., Hermetter, A. & Russell, D. G. The kinetics of phagosome maturation as a function of phagosome/lysosome fusion and acquisition of hydrolytic activity. *Traffic* **6**, 413–420 (2005).

139. Segal, A. W. The function of the NADPH oxidase of phagocytes and its relationship to other NOXs in plants, invertebrates, and mammals. *International Journal of Biochemistry and Cell Biology* vol. 40 604–618 (2008).

140. Uribe-Quero, E. & Rosales, C. Control of phagocytosis by microbial pathogens. *Frontiers in Immunology* vol. 8 1368 (2017).

141. Crowle, A. J., Dahl, R., Ross, E. & May, M. H. Evidence that vesicles containing living, virulent Mycobacterium tuberculosis or Mycobacterium avium in cultured human macrophages are not acidic. *Infect. Immun.* **59**, 1823–1831 (1991).

142. Clemens, D. L. & Horwitz, M. A. Characterization of the Mycobacterium tuberctdosis phagosome and evidence that phagosomal maturation is inhibited. *J. Exp. Med.* **181**, 257–270 (1995).

143. Via, L. E. & Alfons Huber, L. Arrest of Mycobacterial Phagosome Maturation Is Caused by a Block in Vesicle Fusion between Stages Controlled by rab5 and rab7 Skin dendritic cells View project Characterization of the alternative sigma factor AlgU View project. *Artic. J. Biol. Chem.* (1997) doi:10.1074/jbc.272.20.13326.

144. Fratti, R. A., Backer, J. M., Gruenberg, J., Corvera, S. & Deretic, V. Role of phosphatidylinositol 3-kinase and Rab5 effectors in phagosomal biogenesis and mycobacterial phagosome maturation arrest. *J. Cell Biol.* **154**, 631–644 (2001).

145. Ferrari, G., Langen, H., Naito, M. & Pieters, J. A coat protein on phagosomes involved in the intracellular survival of mycobacteria. *Cell* **97**, 435–447 (1999).

146. Jayachandran, R. *et al.* Survival of Mycobacteria in Macrophages Is Mediated by Coronin 1-Dependent Activation of Calcineurin. *Cell* **130**, 37–50 (2007).

147. Malik, Z. A., Denning, G. M. & Kusner, D. J. Inhibition of Ca2+ signaling by

Mycobacterium tuberculosis is associated with reduced phagosome-lysosome fusion and increased survival within human macrophages. *J. Exp. Med.* **191**, 287–302 (2000).

148. Malik, Z. A., Iyer, S. S. & Kusner, D. J. Mycobacterium tuberculosis Phagosomes Exhibit Altered Calmodulin-Dependent Signal Transduction: Contribution to Inhibition of Phagosome-Lysosome Fusion and Intracellular Survival in Human Macrophages . *J. Immunol.* **166**, 3392–3401 (2001).

149. Vergne, I., Chua, J. & Deretic, V. Mycobacterium tuberculosis Phagosome Maturation Arrest: Selective Targeting of PI3P-Dependent Membrane Trafficking. *Traffic* **4**, 600–606 (2003).

150. Kang, P. B. *et al.* The human macrophage mannose receptor directs Mycobacterium tuberculosis lipoarabinomannan-mediated phagosome biogenesis. *J. Exp. Med.* **202**, 987–999 (2005).

151. Hmama, Z. *et al.* Quantitative analysis of phagolysosome fusion in intact cells: Inhibition by mycobacterial lipoarabinomannan and rescue by an 1α,25-dihydroxyvitamin D3-phosphoinositide 3-kinase pathway. *J. Cell Sci.* **117**, 2131–2139 (2004).

152. Welin, A. *et al.* Incorporation of Mycobacterium tuberculosis lipoarabinomannan into macrophage membrane rafts is a prerequisite for the phagosomal maturation block. *Infect. Immun.* **76**, 2882–2887 (2008).

153. Hayakawa, E. *et al.* A Mycobacterium tuberculosis-derived lipid inhibits membrane fusion by modulating lipid membrane domains. *Biophys. J.* **93**, 4018–4030 (2007).

154. Wong, D., Bach, H., Sun, J., Hmama, Z. & Av-Gay, Y. Mycobacterium tuberculosis protein tyrosine phosphatase (PtpA) excludes host vacuolar-H +-ATPase to inhibit phagosome acidification. *Proc. Natl. Acad. Sci. U. S. A.* **108**, 19371–19376 (2011).

155. Wong, D. *et al.* Protein tyrosine kinase, PtkA, is required for Mycobacterium tuberculosis growth in macrophages. *Sci. Rep.* **8**, (2018).

156. Sturgill-Koszycki, S. *et al.* Lack of acidification in Mycobacterium phagosomes produced by exclusion of the vesicular proton-ATPase. *Science (80-.).* **263**, 678–681 (1994).

157. McDonough, K. A., Kress, Y. & Bloom, B. R. Pathogenesis of tuberculosis: Interaction of Mycobacterium tuberculosis with macrophages. *Infect. Immun.* **61**, 2763–2773 (1993).

158. Myrvik, Q. N., Leake, E. S. & Wright, M. J. Disruption of phagosomal membranes of normal alveolar macrophages by the H37Rv strain of Mycobacterium tuberculosis. A correlate of virulence. *Am. Rev. Respir. Dis.* **129**, 322–328 (1984).

159. Leake, E. S., Myrvik, Q. N. & Wright, M. J. *Phagosomal Membranes of Mycobacterium bovis BCG-Immune Alveolar Macrophages Are Resistant to Disruption by Mycobacterium tuberculosis H37Rv Downloaded from*. *INFECTION AND IMMUNITY* vol. 45 http://iai.asm.org/ (1984).

160. van der Wel, N. *et al.* M. tuberculosis and M. leprae Translocate from the Phagolysosome to the Cytosol in Myeloid Cells. *Cell* **129**, 1287–1298 (2007).

161. Conrad, W. H. *et al.* Mycobacterial ESX-1 secretion system mediates host cell lysis through bacterium contact-dependent gross membrane disruptions. *Proc. Natl. Acad. Sci. U. S. A.* **114**, 1371–1376 (2017).

162. Refai, A. *et al.* Two distinct conformational states of Mycobacterium tuberculosis virulent factor early secreted antigenic target 6 kDa are behind the discrepancy around its biological functions. *FEBS J.* **282**, 4114–4129 (2015).

163. Simeone, R. *et al.* Cytosolic Access of Mycobacterium tuberculosis: Critical Impact of Phagosomal Acidification Control and Demonstration of Occurrence In Vivo. *PLoS*

Pathog. **11**, (2015).

164. Simons, K. & Toomre, D. Lipid rafts and signal transduction. *Nature Reviews Molecular Cell Biology* vol. 1 31–39 (2000).

165. Shin, J. S., Gao, Z. & Abraham, S. N. Involvement of cellular caveolae in bacterial entry into mast cells. *Science (80-.).* **289**, 785–788 (2000).

166. Malaviya, R., Gao, Z., Thankavel, K., Van der Merwe, P. A. & Abraham, S. N. The mast cell tumor necrosis factor a response to FimH-expressing Escherichia coli is mediated by the glycosylphosphatidylinositol-anchored molecule CD48. *Proc. Natl. Acad. Sci. U. S. A.* **96**, 8110–8115 (1999).

167. Baorto, D. M. *et al.* Survival of FimH-expressing enterobacteria in macrophages relies on glycolipid traffic. *Nature* **389**, 636–639 (1997).

168. Martín-Martín, A. I., Vizcaíno, N. & Fernández-Lago, L. Cholesterol, ganglioside GM1 and class A scavenger receptor contribute to infection by Brucella ovis and Brucella canis in murine macrophages. *Microbes Infect.* **12**, 246–251 (2010).

169. Roop, R. M., Bellaire, B. H., Valderas, M. W. & Cardelli, J. A. Adaptation of the brucellae to their intracellular niche. *Mol. Microbiol.* **52**, 621–630 (2004).

170. Grassmé, H. *et al.* Host defense against Pseudomonas aeruginosa requires ceramide-rich membrane rafts. *Nat. Med.* **9**, 322–330 (2003).

171. Hartlova, A., Cerveny, L., Hubalek, M., Krocova, Z. & Stulik, J. Membrane rafts: a potential gateway for bacterial entry into host cells. *Microbiol. Immunol.* **54**, 237–245 (2009).

172. Zaas, D. W., Duncan, M., Rae Wright, J. & Abraham, S. N. The role of lipid rafts in the pathogenesis of bacterial infections. *Biochimica et Biophysica Acta - Molecular Cell*

Research vol. 1746 305–313 (2005).

173. Maldonado-Garcia, G., Chico-Ortiz, M., Lopez-Marin, L. M. & Sánchez-Garcia, F. J. High-polarity Mycobacterium avium-derived lipids interact with murine macrophage lipid rafts. *Scand. J. Immunol.* **60**, 463–470 (2004).

174. Gatfield, J. & Pieters, J. Essential role for cholesterol in entry of mycobacteria into macrophages. *Science (80-.).* **288**, 1647–1650 (2000).

175. Shin, D. M. *et al.* Mycobacterium tuberculosis lipoprotein-induced association of TLR2 with protein kinase C ζ in lipid rafts contributes to reactive oxygen species-dependent inflammatory signalling in macrophages. *Cell. Microbiol.* **10**, 1893–1905 (2008).

176. Fine-Coulson, K., Reaves, B. J., Karls, R. K. & Quinn, F. D. The Role of Lipid Raft Aggregation in the Infection of Type II Pneumocytes by Mycobacterium tuberculosis. *PLoS One* **7**, e45028 (2012).

177. Amer, A. O., Byrne, B. G. & Swanson, M. S. Macrophages rapidly transfer pathogens from lipid raft vacuoles to autophagosomes. *Autophagy* **1**, 53–58 (2005).

178. Glick, D., Barth, S. & Macleod, K. F. Autophagy: Cellular and molecular mechanisms. *Journal of Pathology* vol. 221 3–12 (2010).

179. Reggiori, F. & Ungermann, C. Autophagosome Maturation and Fusion. *Journal of Molecular Biology* vol. 429 486–496 (2017).

180. Lee, Y. K. & Lee, J. A. Role of the mammalian ATG8/LC3 family in autophagy: Differential and compensatory roles in the spatiotemporal regulation of autophagy. *BMB Reports* vol. 49 424–430 (2016).

181. Wileman, T. Autophagy as a defence against intracellular pathogens. *Essays Biochem.* **55**, 153–163 (2013).

182. Pickart, C. M. Back to the Future with Ubiquitin. *Cell* vol. 116 181–190 (2004).

183. Gutierrez, M. G. *et al.* Autophagy is a defense mechanism inhibiting BCG and Mycobacterium tuberculosis survival in infected macrophages. *Cell* **119**, 753–766 (2004).

184. Watson, R. O., Manzanillo, P. S. & Cox, J. S. Extracellular M. tuberculosis DNA targets bacteria for autophagy by activating the host DNA-sensing pathway. *Cell* **150**, 803–815 (2012).

185. Shin, D. M. *et al.* Mycobacterium tuberculosis eis regulates autophagy, inflammation, and cell death through redox-dependent signaling. *PLoS Pathog.* **6**, (2010).

186. Romagnoli, A. *et al.* ESX-1 dependent impairment of autophagic flux by Mycobacterium tuberculosis in human dendritic cells. *Autophagy* **8**, 1357–1370 (2012).

187. Chandra, P. *et al.* Mycobacterium tuberculosis Inhibits RAB7 Recruitment to Selectively Modulate Autophagy Flux in Macrophages. *Sci. Rep.* **5**, (2015).

188. McEwan, D. G. Host-pathogen interactions and subversion of autophagy. *Essays in Biochemistry* vol. 61 687–697 (2017).

189. Bah, A., Lacarrière, C. & Vergne, I. Autophagy-related proteins target ubiquitin-free mycobacterial compartment to promote killing in macrophages. *Front. Cell. Infect. Microbiol.* **6**, (2016).

190. Schille, S. *et al.* LC3-associated phagocytosis in microbial pathogenesis. *International Journal of Medical Microbiology* vol. 308 228–236 (2018).

191. Heckmann, B. L. & Green, D. R. LC3-associated phagocytosis at a glance. *Journal of cell science* vol. 132 (2019).

192. Heckmann, B. L., Boada-Romero, E., Cunha, L. D., Magne, J. & Green, D. R. LC3-Associated Phagocytosis and Inflammation. *Journal of Molecular Biology* vol. 429 3561–

3576 (2017).

193. Proikas-Cezanne, T., Takacs, Z., Dönnes, P. & Kohlbacher, O. WIPI proteins: Essential PtdIns3P effectors at the nascent autophagosome. *Journal of Cell Science* vol. 128 207–217 (2015).

194. Deretic, V. Autophagy in tuberculosis. *Cold Spring Harb. Perspect. Med.* **4**, (2014).

195. Lerena, M. C. & Colombo, M. I. Mycobacterium marinum induces a marked LC3 recruitment to its containing phagosome that depends on a functional ESX-1 secretion system. *Cell. Microbiol.* **13**, 814–835 (2011).

196. Köster, S. *et al.* Mycobacterium tuberculosis is protected from NADPH oxidase and LC3-associated phagocytosis by the LCP protein CpsA. *Proceedings of the National Academy of Sciences of the United States of America* vol. 114 E8711–E8720 (2017).

197. Birmingham, C. L. *et al.* Listeria monocytogenes evades killing by autophagy during colonization of host cells. *Autophagy* **3**, 442–451 (2007).

198. Lam, G. Y., Cemma, M., Muise, A. M., Higgins, D. E. & Brumell, J. H. Host and bacterial factors that regulate LC3 recruitment to Listeria monocytogenes during the early stages of macrophage infection. *Autophagy* **9**, 985–995 (2013).

199. Stewart, E., Triccas, J. A. & Petrovsky, N. Adjuvant strategies for more effective tuberculosis vaccine immunity. *Microorganisms* vol. 7 (2019).

200. Sallusto, F., Geginat, J. & Lanzavecchia, A. C entral M emory and E ffector M emory T C ell S ubsets : Function, Generation, and Maintenance . *Annu. Rev. Immunol.* **22**, 745–763 (2004).

201. Lin, P. L. & Flynn, J. A. L. CD8 T cells and Mycobacterium tuberculosis infection. *Seminars in Immunopathology* vol. 37 239–249 (2015).

202. Lindenstrøm, T., Knudsen, N. P. H., Agger, E. M. & Andersen, P. Control of Chronic Mycobacterium tuberculosis Infection by CD4 KLRG1 − IL-2–Secreting Central Memory Cells . *J. Immunol.* **190**, 6311–6319 (2013).

203. Perdomo, C. *et al.* Mucosal BCG vaccination induces protective lung-resident memory T cell populations against tuberculosis. *MBio* **7**, (2016).

204. Darrah, P. A. *et al.* Prevention of tuberculosis in macaques after intravenous BCG immunization. *Nature* **577**, 95–102 (2020).

205. Barclay, W. R. *et al.* Protection of monkeys against airborne tuberculosis by aerosol vaccination with bacillus Calmette-Guerin. *Am. Rev. Respir. Dis.* **107**, 351–358 (1973).

206. E. Ribi, R. L. Anacker, W. R. Barclay, W. Brehmer, S. C. Harris, W. R. L. & Simmons, and J. Efficacy of Mycobacterial Cell Walls as a Vaccine against Airborne Tuberculosis in the Rhesus Monkey. *J. Infect. Dis.* , **123**, 527–538 (1971).

207. Stylianou, E. *et al.* Identification and evaluation of novel protective antigens for the development of a candidate tuberculosis subunit vaccine. *Infect. Immun.* **86**, (2018).

208. Steingart, K. R. *et al.* Performance of purified antigens for serodiagnosis of pulmonary tuberculosis: A meta-analysis. *Clin. Vaccine Immunol.* **16**, 260–276 (2009).

209. Achkar, J. M. *et al.* Host Protein Biomarkers Identify Active Tuberculosis in HIV Uninfected and Co-infected Individuals. *EBioMedicine* **2**, 1160–1168 (2015).

210. Beyazova, U., Rota, S., Cevheroğlu, C. & Karsligil, T. Humoral immune response in infants after BCG vaccination. *Tuber. Lung Dis.* **76**, 248–253 (1995).

211. Brown, R. M. *et al.* Lipoarabinomannan-Reactive Human Secretory Immunoglobulin A Responses Induced by Mucosal Bacille Calmette-Guérin Vaccination. *J. Infect. Dis.* **187**, 513–517 (2003).

212. De Vallière, S., Abate, G., Blazevic, A., Heuertz, R. M. & Hoft, D. F. Enhancement of innate and cell-mediated immunity by antimycobacterial antibodies. *Infect. Immun.* **73**, 6711–6720 (2005).

213. Niki, M. *et al.* Evaluation of Humoral Immunity to Mycobacterium tuberculosis-Specific Antigens for Correlation with Clinical Status and Effective Vaccine Development. (2015) doi:10.1155/2015/527395.

214. Hauck, F., Neese, B. H., Panchal, A. S. & El-Amin, W. Identification and Management of Latent Tuberculosis Infection. *Am. Fam. Physician* **79**, 879–886 (2009).

215. Maertzdorf, J. *et al.* Mycobacterium tuberculosis Invasion of the Human lung: First contact. *Front. Immunol.* **9**, (2018).

216. Reuschl, A.-K. *et al.* Innate activation of human primary epithelial cells broadens the host response to Mycobacterium tuberculosis in the airways. *PLOS Pathog.* **13**, e1006577 (2017).

217. Mehta, P. K., King, C. H., White, E. H., Murtagh, J. J. & Quinn, F. D. Comparison of in vitro models for the study of Mycobacterium tuberculosis invasion and intracellular replication. *Infect. Immun.* **64**, 2673–2679 (1996).

218. Pethe, K. *et al.* The heparin-binding haemagglutinin of M. tuberculosis is required for extrapulmonary dissemination. *Nature* **412**, 190–194 (2001).

219. Chitale, S. *et al.* Recombinant Mycobacterium tuberculosis protein associated with mammalian cell entry. *Cell. Microbiol.* **3**, 247–254 (2001).

220. Racanelli, A. C., Kikkers, S. A., Choi, A. M. K. & Cloonan, S. M. Autophagy and inflammation in chronic respiratory disease. *Autophagy* vol. 14 221–232 (2018).

221. Guo, X. G., Ji, T. X., Xia, Y. & Ma, Y. Y. Autophagy protects type II alveolar epithelial

cells from Mycobacterium tuberculosis infection. *Biochem. Biophys. Res. Commun.* **432**, 308–313 (2013).

222. Danelishvili, L., McGarvey, J., Li, Y. J. & Bermudez, L. E. Mycobacterium tuberculosis infection causes different levels of apoptosis and necrosis in human macrophages and alveolar epithelial cells. *Cellular Microbiology* vol. 5 649–660 (2003).

223. Keane, J., Remold, H. G. & Kornfeld, H. Virulent Mycobacterium tuberculosis Strains Evade Apoptosis of Infected Alveolar Macrophages . *J. Immunol.* **164**, 2016–2020 (2000).

224. Fine-Coulson, K., Reaves, B. J., Karls, R. K. & Quinn, F. D. The Role of Lipid Raft Aggregation in the Infection of Type II Pneumocytes by Mycobacterium tuberculosis. *PLoS One* **7**, (2012).

225. García-Pérez, B. E., Mondragón-Flores, R. & Luna-Herrera, J. Internalization of Mycobacterium tuberculosis by macropinocytosis in non-phagocytic cells. *Microb. Pathog.* **35**, 49–55 (2003).

226. Muñoz, S., Rivas-Santiago, B. & Enciso, J. A. Mycobacterium tuberculosis entry into mast cells through cholesterol-rich membrane microdomains. *Scand. J. Immunol.* **70**, 256–263 (2009).

227. Carlsson, S. R. & Simonsen, A. Membrane dynamics in autophagosome biogenesis. *Journal of Cell Science* vol. 128 193–205 (2015).

228. Schleimer, R. P., Kato, A., Kern, R., Kuperman, D. & Avila, P. C. Epithelium: At the interface of innate and adaptive immune responses. *Journal of Allergy and Clinical Immunology* vol. 120 1279–1284 (2007).

229. Olsen, A. *et al.* Targeting Mycobacterium tuberculosis tumor necrosis factor alpha-downregulating genes for the development of antituberculous vaccines. *MBio* **7**, (2016).

230. Shin, A. R. *et al.* Mycobacterium tuberculosis HBHA protein reacts strongly with the serum immunoglobulin M of tuberculosis patients. *Clin. Vaccine Immunol.* **13**, 869–875 (2006).

231. Stylianou, E. *et al.* Mucosal delivery of antigen-coated nanoparticles to lungs confers protective immunity against tuberculosis infection in mice. *Eur. J. Immunol.* **44**, 440–449 (2014).

232. Castro-Garza, J. *et al.* Detection of anti-HspX antibodies and HspX protein in patient sera for the identification of recent latent infection by Mycobacterium tuberculosis. *PLoS One* **12**, (2017).

233. Mycobrowser. https://mycobrowser.epfl.ch/genes/Rv0097.

234. Thomas, R. & Brooks, T. Attachment of Yersinia pestis to human respiratory cell lines is inhibited by certain oligosaccharides. *J. Med. Microbiol.* **55**, 309–315 (2006).

235. Thomas, R. J. & Brooks, T. J. Oligosaccharide receptor mimics inhibit Legionella pneumophila attachment to human respiratory epithelial cells. *Microb. Pathog.* **36**, 83–92 (2004).

236. Debbabi, H. *et al.* Primary type II alveolar epithelial cells present microbial antigens to antigen-specific CD4 + T cells. *Am. J. Physiol. Cell. Mol. Physiol.* **289**, L274–L279 (2005).

237. Manabe, Y. C. *et al.* Different strains of Mycobacterium tuberculosis cause various spectrums of disease in the rabbit model of tuberculosis. *Infect. Immun.* **71**, 6004–6011 (2003).

238. Sanjuan, M. A. *et al.* Toll-like receptor signalling in macrophages links the autophagy pathway to phagocytosis. *Nature* **450**, 1253–1257 (2007).

239. Kong, D. & Kunimoto, D. Y. Secretion of human interleukin 2 by recombinant Mycobacterium bovis BCG. *Infect. Immun.* **63**, 799–803 (1995).

240. Wagner, D., Sangari, F. J., Kim, S., Petrofsky, M. & Bermudez, L. E. Mycobacterium avium infection of macrophages results in progressive suppression of interleukin-12 production in vitro and in vivo. *J. Leukoc. Biol.* **71**, 80–8 (2002).

241. Braunstein, M., Bardarov, S. S. & Jacobs, W. R. Genetic methods for deciphering virulence determinants of Mycobacterium tuberculosis. *Methods Enzymol.* **358**, 67–99 (2002).

242. MOLLENHAUER, H. H. PLASTIC EMBEDDING MIXTURES FOR USE IN ELECTRON MICROSCOPY. *Stain Technol.* **39**, 111–4 (1964).

243. Goldsmith, C. S., Elliott, L. H., Peters, C. J. & Zaki, S. R. Ultrastructural characteristics of Sin Nombre virus, causative agent of hantavirus pulmonary syndrome. *Arch. Virol.* **140**, 2107–2122 (1995).

244. JM, G. *et al.* Phage Display Analysis of Monoclonal Antibody Binding to Anthrax Toxin Lethal Factor. *Toxins (Basel).* **9**, (2017).

245. Rodrigue, S. *et al.* Identification of mycobacterial ?? factor binding sites by chromatin immunoprecipitation assays. *J. Bacteriol.* **189**, 1505–1513 (2007).

246. Chen, Z. *et al.* Efficacy of parainfluenza virus 5 (PIV5)-based tuberculosis vaccines in mice. *Vaccine* **33**, 7217–7224 (2015).

247. Glaziou, P., Floyd, K. & Raviglione, M. Trends in tuberculosis in the UK. doi:10.1136/thoraxjnl-2018-211537.

248. Uthayakumar, D. *et al.* Non-specific Effects of Vaccines Illustrated Through the BCG Example: From Observations to Demonstrations. *Front. Immunol.* **9**, 2869 (2018).

249. Aaby, P. & Benn, C. S. Saving lives by training innate immunity with bacille Calmette-Guérin vaccine. *Proceedings of the National Academy of Sciences of the United States of America* vol. 109 17317–17318 (2012).

250. Brennan, M. J. *et al.* Preclinical evidence for implementing a prime-boost vaccine strategy for tuberculosis. *Vaccine* vol. 30 2811–2823 (2012).

251. Rouanet, C., Debrie, A. S., Lecher, S. & Locht, C. Subcutaneous boosting with heparin binding haemagglutinin increases BCG-induced protection against tuberculosis. *Microbes Infect.* **11**, 995–1001 (2009).

252. Parra, M. *et al.* The mycobacterial heparin-binding hemagglutinin is a protective antigen in the mouse aerosol challenge model of tuberculosis. *Infect. Immun.* **72**, 6799–6805 (2004).

253. Masungi, C. *et al.* Differential T and B Cell Responses against Mycobacterium tuberculosis Heparin-Binding Hemagglutinin Adhesin in Infected Healthy Individuals and Patients with Tuberculosis . *J. Infect. Dis.* **185**, 513–520 (2002).

254. Verwaerde, C. *et al.* HBHA vaccination may require both Th1 and Th17 immune responses to protect mice against tuberculosis. *Vaccine* **32**, 6240–6250 (2014).

255. Shollenberger, L., Grenfell, R., Samli, E. F. & Harn, D. Vaccine self-assembling immune matrix (VacSIM) is a non-viral delivery platform that augments responses to recombinant protein vaccines (VAC6P.940). *J. Immunol.* **192**, (2014).

256. Wilkinson, K. A. & Wilkinson, R. J. Polyfunctional T cells in human tuberculosis. *European Journal of Immunology* vol. 40 2139–2142 (2010).

257. Lewinsohn, D. M. *et al.* Clinical Infectious Diseases Prevention Clinical Practice Guidelines: Diagnosis of Tuberculosis in Adults and Children. (2016)

doi:10.1093/cid/ciw694.

258. Hoft, D. F. *et al.* Investigation of the Relationships between Immune-Mediated Inhibition of Mycobacterial Growth and Other Potential Surrogate Markers of Protective Mycobacterium tuberculosis Immunity . *J. Infect. Dis.* **186**, 1448–1457 (2002).

259. Cowley, S. C. & Elkins, K. L. CD4 + T Cells Mediate IFN-γ-Independent Control of Mycobacterium tuberculosis Infection Both In Vitro and In Vivo . *J. Immunol.* **171**, 4689–4699 (2003).

260. Abebe, F. Is interferon-gamma the right marker for bacille Calmette-Guérin-induced immune protection? The missing link in our understanding of tuberculosis immunology. *Clin. Exp. Immunol.* **169**, 213–219 (2012).

261. Khader, S. A. *et al.* IL-23 and IL-17 in the establishment of protective pulmonary CD4+ T cell responses after vaccination and during Mycobacterium tuberculosis challenge. *Nat. Immunol.* **8**, 369–377 (2007).

262. Wozniak, T. M., Saunders, B. M., Ryan, A. A. & Britton, W. J. Mycobacterium bovis BCG-specific Th17 cells confer partial protection against Mycobacterium tuberculosis infection in the absence of gamma interferon. *Infect. Immun.* **78**, 4187–4194 (2010).

263. Lin, P. L. & Flynn, J. L. Understanding Latent Tuberculosis: A Moving Target. *J. Immunol.* **185**, 15–22 (2010).

264. Okamoto Yoshida, Y. *et al.* Essential Role of IL-17A in the Formation of a Mycobacterial Infection-Induced Granuloma in the Lung. *J. Immunol.* **184**, 4414–4422 (2010).

265. Fine, K. L. *et al.* Involvement of the autophagy pathway in trafficking of *Mycobacterium tuberculosis* bacilli through cultured human type II epithelial cells. *Cell. Microbiol.* **14**, 1402–1414 (2012).

266. Naroeni, A. & Porte, F. Role of cholesterol and the ganglioside GM1 in entry and short-term survival of Brucella suis in murine macrophages. *Infect. Immun.* **70**, 1640–1644 (2002).